

STRUCTURE AND REACTIVITY OF CYCLE AND CRYPTOCHROME: TWO
KEY COMPONENTS OF THE *DROSOPHILA* CIRCADIAN CLOCK

A Dissertation

Presented to the Faculty of the Graduate School
of Cornell University

In Partial Fulfillment of the Requirements for the Degree of
Doctor of Philosophy

by

Craig Chiu Manahan

February 2016

© 2016 Craig Chiu Manahan

LINKING STRUCTURE TO FUNCTION IN THE CIRCADIAN CLOCK OF
DROSOPHILA MELANOGASTER

Craig Chiu Manahan Ph. D.

Cornell University 2016

The circadian clock is necessary throughout almost all life forms in order to control physiological changes throughout the ~24 hour day. At the molecular level, a transcription-translation feedback loop is the foundation for eukaryotic clocks, and this loop is entrained by external cues to the change in environment. In this study, both the positive arm of the loop and the method of entrainment by light have been investigated for proteins involved in the circadian clock of the fruit fly *Drosophila melanogaster*.

Cycle (CYC) is a transcription factor that dimerizes with its partner Clock (dCLK) through two tandem Per-ARNT-Sim domains to activate clock controlled genes. In this study, the structure of the PAS B domain of Cycle was investigated by crystallography, and the behavior of this domain was investigated. We reveal by comparing the solved structure with that of homologous mammalian protein mBMAL1 what structural changes occur upon binding of partner CLK, and we point out differences in the structure between CYC and mBMAL1. We show the importance of a tryptophan residue in mediating homodimerization of CYC and heterodimerization of CYC with CLK and Period (PER). We also discover a novel glycerol binding mode in CYC, and discuss possible roles for this binding.

Cryptochrome (CRY) provides the major light entrainment mechanism in *Drosophila* by using light to alter conformation, bind partners Timeless (TIM) and Jetlag (JET), and lead to their degradation. In this study we investigate how CRY

senses light mechanistically by reducing its FAD cofactor, whether this reduction is sufficient to lead to partner binding, and why FAD reduction causes conformational changes.

BIOGRAPHICAL SKETCH

Craig Chiu Manahan was born in 1988 to Ted Manahan and Chuchang Chiu in Colorado Springs, CO. He has one older brother, Clifton Manahan. Craig spent time as a child living in Albany, OR, and Singapore, before attending high school in Fort Collins, CO. Here he developed an interest in the sciences under the tutelage of teachers such as Glenn Gainley, and decided to attend the University of Colorado: Boulder, and study Biochemistry.

At CU: Boulder, he researched cancer drugs and P27 ubiquitination under the supervision of Prof. Xuedong Liu. In addition, he spent a summer researching membrane protein movement in the lab of Prof. George Barisas at Colorado State University: Fort Collins. After graduation, he continued his education in biochemistry at Cornell University under Prof. Brian Crane studying the circadian clock.

For my Wife and Parents

ACKNOWLEDGMENTS

Thanks to my PI Brian Crane, for constant support and patience. Thanks to my fellow lab members for their help with ideas and experiments. Thank you for my committee members Prof. Rick Cerione and Prof. Hening Lin for their critiques and help with instruments and materials.

This work is based upon research conducted at the Cornell High Energy Synchrotron Source (CHESS), which is supported by the National Science Foundation and the National Institutes of Health/National Institute of General Medical Sciences under NSF award DMR-1332208, using the Macromolecular Diffraction at CHESS (MacCHESS) facility, which is supported by award GM-103485 from the National Institute of General Medical Sciences, National Institutes of Health.

The project described was supported by Award Number T32GM008500 from the National Institute of General Medical Sciences. The content is solely the responsibility of the authors and does not necessarily represent the official views of the National Institute of General Medical Sciences or the National Institutes of Health.

Research reported in this publication was supported by the National Institute of General Medical Sciences of the National Institutes of Health under Award Number P41GM103521.

TABLE OF CONTENTS

Biographical Sketch	v
Dedication	vi
Acknowledgments	vii
Table of Contents	viii
Chapter 1: Molecular basis of the <i>Drosophila melanogaster</i> Circadian Clock	1
Chapter 2: Crystal Structure of <i>Drosophila melanogaster</i> Cycle PAS domain shows conformational change associated with Clock interaction and reveals new ligand binding	34
Chapter 3: Mutational Studies of <i>Drosophila melanogaster</i> Cryptochrome mutants show role for Histidine residue and emphasize importance of Tryptophans for electron transport.	60
Chapter 4: Conclusions and Further Studies	89
Appendix 1: Spectra of Cryptochrome Mutants	95

CHAPTER 1

MOLECULAR BASIS OF THE *DROSOPHILA MELANOGASTER* CIRCADIAN CLOCK

Introduction

Control of biological function with respect to time is essential to survival for almost all higher organisms, from cyanobacteria to humans. Some examples of functions under circadian control are photosynthesis and growth in plants, activity and body temperature in insects, and a wide variety of functions in humans including sleep cycle, plasma level, blood pressure, and heart rate. Among others, disruption of the correct circadian clock is associated with obesity, diabetes, and cancer^{1,2}.

Temporal control is regulated by an organism's circadian clock. Circadian rhythms are the means by which an organism can adapt to changes in their environment that occur on a day to day basis. Organisms have many molecular changes that occur over time, but in order to respond to the hourly changes in environment, oscillations in activity must occur on about a 24 hour cycle without any external input. However a true circadian clock must also be set to the correct day-night timeframe, and be able to correct itself to match with the 24 hour clock, so it must have some way of getting entrained by the environment.

Molecular Basis of Circadian Rhythms

On a molecular level, this means that all known circadian clocks contain an oscillator which contains both positive and negative elements in order to provide autoregulatory feedback loops. Positive elements increase activity whereas negative

elements reduce activity, and the interaction between these two elements creates a 24 hour cycle.

Circadian clocks are found mostly in higher order organisms. Cyanobacteria, however, are one of the only single-celled organisms which contain a clock. In Cyanobacteria, circadian rhythms are controlled by a post-translational feedback loop (PTFL) in which post-translational modifications of proteins occur under circadian control. Under this system, the protein KaiC controls circadian output, and its activity is regulated by the positive element KaiA and the negative element KaiB. KaiA phosphorylates KaiC, while KaiB dephosphorylates KaiC, and the interplay between these two processes occurs on a ~24 hour cycle. In fact, it has been shown that with only these three proteins and ATP, KaiC undergoes phosphorylation cycles in a circadian rhythm. PTFLs of different types have also been seen in mammalian blood cells and algae, leaving an open question as to whether PTFLs are more widespread in higher organisms. ^{3,4}

In eukaryotes, the clock is controlled at the translational level using a mechanism called the transcription translation feedback loop (TTFL). The specific mechanisms of this loop differ in many organisms, but the underlying architecture remains the same. Positive elements activate the clock by activating transcription of certain clock controlled genes (ccgs), which in turn are translated into proteins. These proteins then go on signal other proteins to change their activity, causing a signaling cascade that eventually leads to changes in the cell which cause an increase in circadian activity. However, some ccgs are used to control the circadian clock. When these proteins are translated, they go on to interact and block the positive elements

from activating ccgs, including their own gene, and reduce circadian activity (Fig. 1). Once the negative elements are degraded, the positive elements are once again free to activate circadian genes, and the loop starts again.⁵⁻⁷ The interplay between these two processes occurs on a 24 hour cycle, causing circadian rhythms.

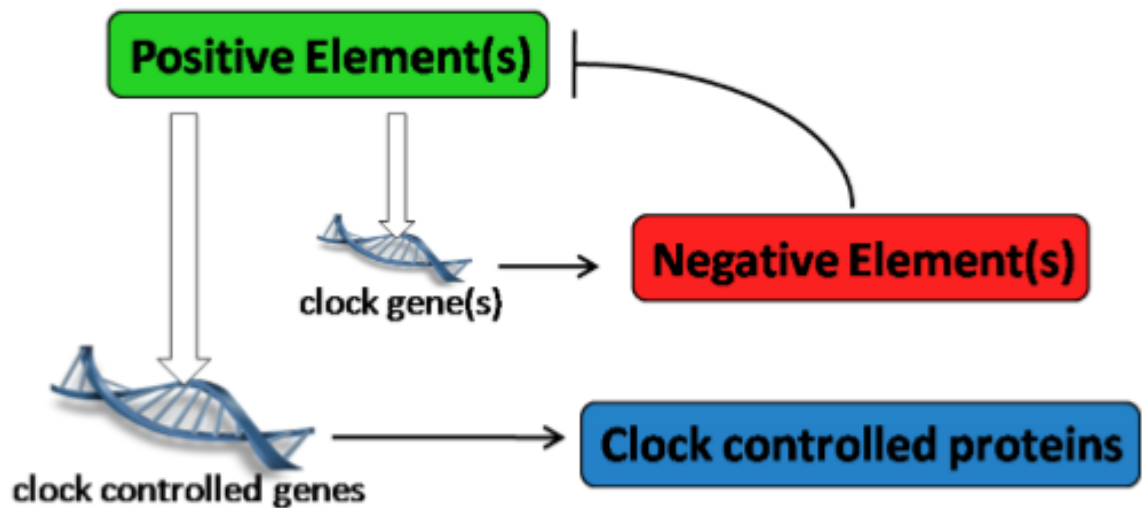


Fig. 1: Transcription-translation feedback loop (TTFL). Positive elements (transcription factors) promote the translation of clock controlled genes (ccgs), which lead to the production of clock controlled proteins, the basis of circadian output. A subset of ccgs are clock genes, which control the circadian clock. These genes lead to the translation of negative elements, which inhibit the positive elements on a ~24 hour cycle.

In order to entrain the circadian clock to the day-night cycle, an organism must be able to sense its environment. The two main ways that this has been shown to occur are by temperature and light. Light has been shown to play many different mechanistic roles in the clock, depending on the organism. Light can affect either the positive or negative elements. By performing its role at the same time every day, light can act as a cue to “set” the clock at the same activity on a day-to-day cycle.

Drosophila melanogaster, a fruit fly, is used as a model organism to study the circadian clock. The molecular basis for the *Drosophila* clock has a lot in common to that of humans, however using *Drosophila* as a model organism allows researchers to perform genetic studies and in some cases provides for more tractable proteins to study. *Drosophila* has a short life cycle and relatively easy maintenance of cultures, allowing fly geneticists quick access to results.

Architecture of the Drosophila Circadian Clock

The first circadian clock gene to be discovered was the *Drosophila* gene *period*(PER) in 1971 by Konopka and Benzer⁸. This was done by mutating flies and looking for changes in the rhythm of eclosion or locomotor activity of the flies. The next fly gene to be discovered was of Period's partner, called *timeless*(TIM), in 1994 by Michael Young's lab,⁹ where mutants of TIM also had defects in eclosion and locomotor activity, and also affected levels of PER mRNA. It was then confirmed that the proteins PER and TIM interact in the cytosol, leading to nuclear entry¹⁰. In 1998 Michael Rosbash's lab discovered two partner transcription factors involved in the circadian clock called *clock*(CLK)¹¹ and *cycle*(CYC)¹². The mutant forms of this genes caused low levels of PER and TIM mRNA and protein, and it was proposed that these were the positive element of *Drosophila*'s clock, binding the E box of *per* and *tim* DNA and promoting their transcription. Since then, this hypothesis has been confirmed and it has been discovered that after entering the nucleus, PER and TIM bind CLK and CYC, inhibiting their own transcription. Thus, the transcription factors

CLK and CYC are generally considered the main positive elements of the *Drosophila* clock, whereas PER and TIM are considered the primary negative elements ^{5,7}.

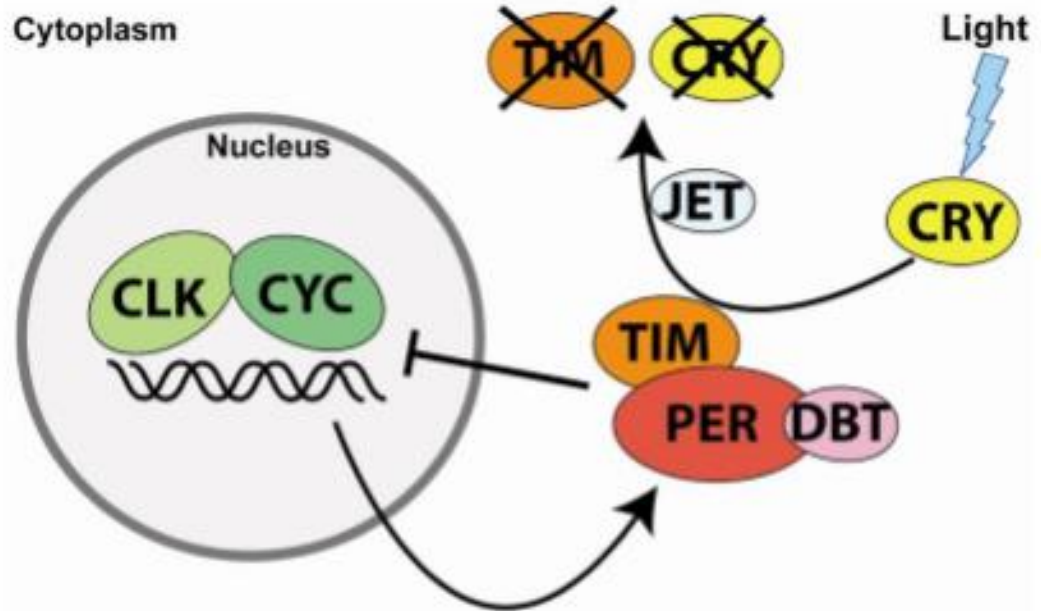


Fig. 2: Architecture of the *Drosophila melanogaster* circadian clock. Transcription factors Clock (CLK) and Cycle (CYC) promote the production of proteins Timeless (TIM) and Period (PER), which dimerize and enter the nucleus, inhibiting their own translation. Phosphorylation of PER by the kinase Doubletime (DBT) regulates dimerization and nuclear entry. The clock is entrained by the protein Cryptochrome (CRY), which, upon light exposure, binds to TIM and leads to its ubiquitination by the F-box protein Jetlag (JET) an E3 ubiquitin ligase. Both TIM and CRY are then degraded by the proteasome.

How *Drosophila* entrained its clock was an open question until the discovery of the fruit fly version of the protein Cryptochrome (CRY) by the Rosbash lab, of which the mutant had poor light synchronization and a defective clock ^{13,14}. The *Arabidopsis thaliana* versions of CRY had previously been discovered and characterized to some extent, so a light sensing role in *Drosophila* was not a surprise ¹⁵. It was then discovered in 2004 that CRY carries out its role of entraining the

circadian clock by binding TIM in a light dependent manner and committing it to ubiquitination and degradation by the proteasome¹⁶.

Timeless

Timeless (TIM) is a large protein of ~1350 amino acids that, due to difficulties with expression and purification, has not been studied much *in vitro*. PER is stabilized by interaction with TIM, and this interaction is required for movement of the proteins from the cytosol to the nucleus where they can inhibit CLK/CYC. TIM is predicted to be a largely unstructured protein with repeating armadillo alpha helical motifs¹⁷. Light regulates the amount of TIM, and thus the stability of PER, by changing TIM's interaction with dCRY. In the presence of light, CRY recruits the E3 ubiquitin ligase JETLAG (JET) to a complex containing TIM which leads to the ubiquitination and degradation of TIM by the proteasome⁵.

Period

Period is the first circadian clock gene to have been discovered, and thus it is probably the most widely studied. *Drosophila* period is 1,224 amino acids in size contains two Per/Arnt/Sim (PAS) domains, labeled PASA and PASB which span from amino acids ~240-500. Mammals have three versions of PER, called PER1-3, which are about 30% identical in the PAS domains to dPER, but contain little other homology (Fig. 3)¹⁸.

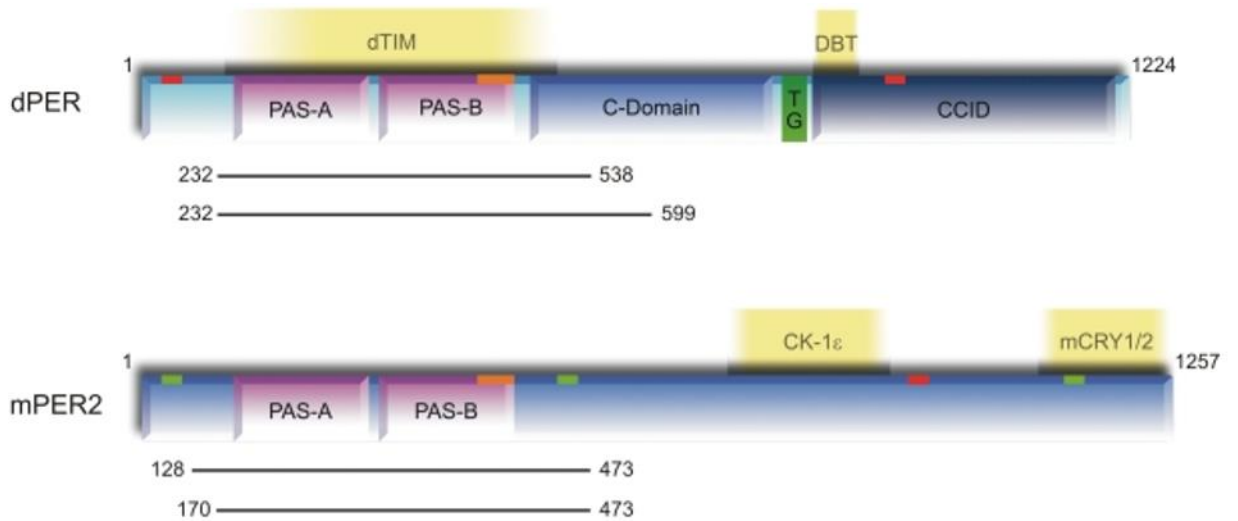


Fig. 3: Domain architecture of dPER and mouse Period2 (mPER2). The two PAS domains (PAS-A and PAS-B); the cytoplasmic localization domain (CLD, orange bar); nuclear localization signals (NLS, red bars); nuclear export signal (NES, green bars); the conserved C-domain; the threonine-glycine (TG) repeat region; and the dCLK:CYC inhibition domain (CCID) of dPER and/or mPER2 are shown schematically. Binding sites of CK-1 ϵ , dTIM, DBT, and mCRY1/2 are depicted. Fragments of dPER and mPER2 that have been crystallized are shown by black bars. (PLoS Biol. 2009 Apr; 7(4): e1000094)

Transcription of dPER and its partner TIM is activated by dCLK and CYC, and after translation dPER and TIM reenter the nucleus and inhibit their own transcription, acting as negative elements of the circadian clock⁵. Time dependent changes in dPER and TIM levels, localization and activity are influenced by post translational modifications and interactions with the kinase Doubletime (DBT) and casein kinase II (CKII)¹⁹. In mammals, instead of TIM, mPER1-3 directly binds to mCRY1/2 to act as negative elements of the clock¹⁹.

The highest homology between PER proteins is found in their PAS domains, which mediate both homo and hetero-dimerization²⁰. In mammals, CRY binds the C-terminus of PER and stabilizes PER, preventing ubiquitination and degradation^{20,21}. In

drosophila, dPER instead binds TIM, stabilizing both from degradation and promoting nuclear localization⁵. The interaction between dPER/TIM as well as nuclear localization and activity have been found to be affected by a number of post translational modifications. A key player in these modifications is the kinase Doubletime (DBT or CK1), which phosphorylates dPER, leading to ubiquitination by the f-box protein Slimb and degradation. dTIM can block this phosphorylation, stabilizing dPER²². In mammals the CK1 homolog similarly interacts with mPER, regulating the circadian clock by modulating mPER's interaction with mCRY²³.

In addition to dimerization with TIM, a series of phosphorylations by other kinases may be needed for nuclear localization of the PER/TIM dimer. Some kinases that are suggested to mediate this localization are glycogen synthase kinase 3 (GSK-3)^{24,25} and casein kinase 2 α (CK2 α)²⁶⁻²⁸. Furthermore, glycosylation in the form of O-linked N-acetyl glucosamine modifications (O-GlcNAcylation) of dPER by O-GlcNAc transferase (OGT) can modulate PER nuclear accumulation^{29,30}. Intriguingly, O-GlcNAcylation and phosphorylation by DBT may compete for the same sites on dPER. OGT knockout mice have altered circadian rhythms and mPER2 has been shown to be glycosylated and the same sites as CK1 phosphorylation suggesting a similar role for mOGT in mammals²⁹.

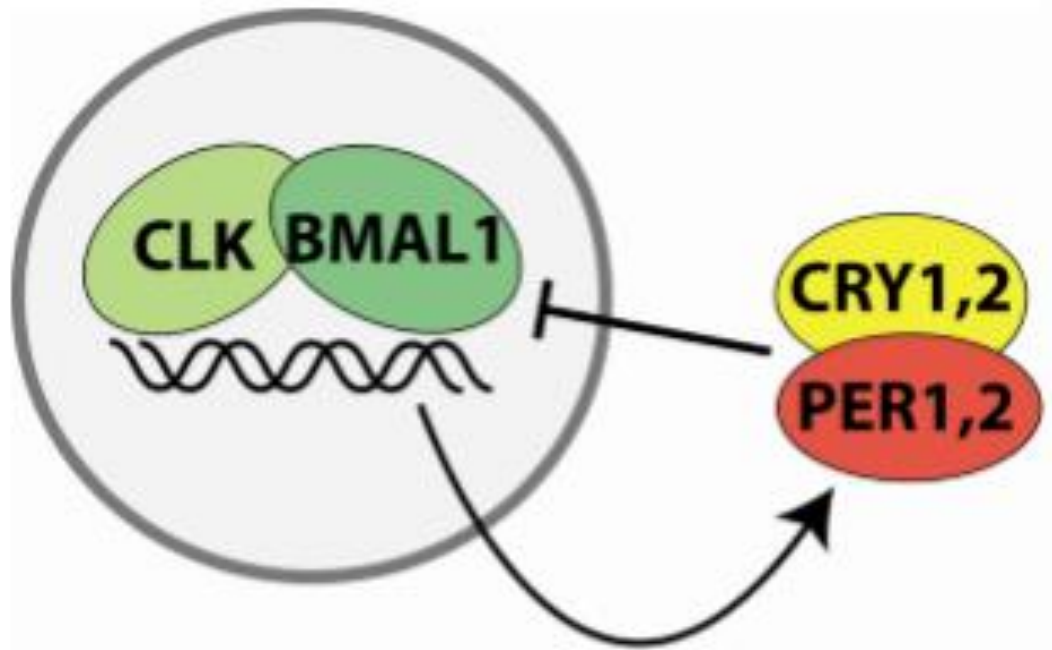


Fig. 4: Molecular architecture of the mammalian circadian clock. Transcription factors Clock (CLK) and brain-muscle ARNT-like 1 (BMAL1) promote production of proteins Period (PER) 1/2 and Cryptochrome 1/2 (CRY) which dimerize and reenter the nucleus to inhibit their own transcription.

PAS Domains

Per/Arnt/Sim (PAS) domains were first identified in 1991 as being found in three proteins: period, single-minded, and aryl hydrocarbon receptor nuclear translocator. Then, in 1993 PAS domains were characterized as being dimerization domains found in many different transcription factors and other signaling proteins in all different types of life³¹. PAS domains are ~100-120 residues long, and although they have a common fold, they often exhibit low sequence identity with other PAS domains. PAS domains have been shown to bind cofactors including small molecules/metabolites, hemes, and flavins, but many PAS domains are thought to

have no ligand binding. PAS domains are often used to mediate interactions between proteins by dimerizing³².

PAS domains can bind cofactors either covalently or non-covalently, and the function of the cofactor can vary depending on the signal that the protein needs to carry. Some PAS domains use their cofactor directly detect a signal, for example oxygen sensing PAS domains which bind heme or light sensing domains which bind flavins. Other PAS domains receive a signal in the form of ligand binding, which then is used to change its function, such as the CitA citrate sensor binding citrate, DcuS binding malate, or DctB binding succinate³³. A study of PAS domain ligand binding found that most are bound in the same place in the protein, a conserved cleft formed by a beta sheet and two alpha helices³².

PAS domains can be found as either single or paired (PAS-A/PAS-B) domains, and are often linked with signal transduction proteins. They can function as signal sensors as described above or can function in signal transmission and protein interaction for other domains³³. Thus PAS domains have been found linked to kinases, ion channels, transcription factors, and phosphodiesterases³⁴. Transcription factors with linked PAS domains include the clock proteins CLK and CYC in *Drosophila* along with their mammalian homologs white-collar proteins and vivid in *Neurospora*, and phototropin in *Arabidopsis*. In these systems PAS domains with Flavin cofactors act as light receptors, but those without ligands also have an important role by mediating formation of oligomers through variable PAS packings- with changes in PAS interactions often triggered by signal transduction³⁵.

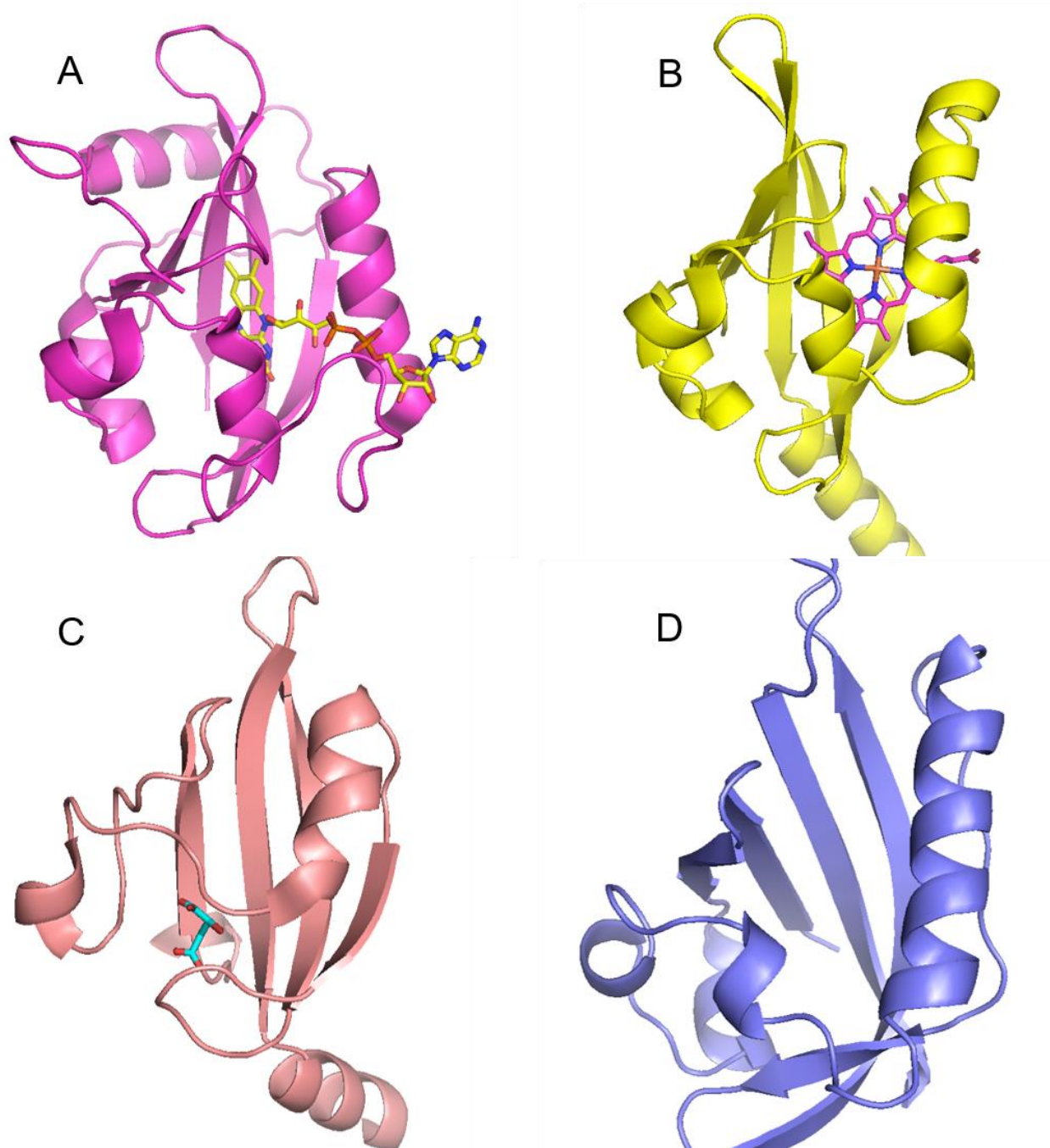


Fig. 5: Structural diversity of PAS domains-a selection of structure of PAS domains and their ligands taken from the protein data bank. (A) Vivid from *Neurospora crassa* in magenta with FAD cofactor in yellow (2PD7). (B) FixL PAS B from *Bradyrhizobium japonicum* in yellow with heme cofactor in magenta (1XJ3). (C) DcuS PAS A from *E. coli* in salmon with C4-dicarboxylate ligand in cyan (3BY8). Period from *Drosophila melanogaster* in light blue with no ligand bound (1WA9).

Table 1: List of some of the available PAS domain structures and the cofactors found in these structures. (Structure, 2009, 17 October)³⁵

PAS Domain Structures

protein	organism	PDB ^a	cofactor ^b	reference ^{c,d}
PYP	<i>Rhodospirillum centenum</i>	1MZU	<i>p</i> -coumaric acid	(Rajagopal and Moffat, 2003)
PYP	<i>Halorhodospira halophila</i>	1NWZ	<i>p</i> -coumaric acid	(Borgstahl et al., 1995; Getzoff et al., 2003)
neochrome PAS B	<i>Adiantum capillus-veneris</i>	1G28	FMN	(Crosson and Moffat, 2001; Crosson and Moffat, 2002)
phot1 PAS A	<i>Chlamydomonas reinhardtii</i>	1N9L	FMN	(Fedorov et al., 2003)
phot1 PAS B	<i>Avena sativa</i>	2V0U	FMN	(Halavaty and Moffat, 2007; Harper et al., 2003)
phot1 PAS A	<i>Arabidopsis thaliana</i>	2Z6C	FMN	(Nakasako et al., 2008)
phot2 PAS A	<i>Arabidopsis thaliana</i>	2Z6D	FMN	(Nakasako et al., 2008)
YtvA	<i>Bacillus subtilis</i>	2PR5	FMN	(Möglich and Moffat, 2007)
Vivid	<i>Neurospora crassa</i>	2PD7	FAD	(Zoltowski et al., 2007)
NifL PAS A	<i>Azotobacter vinelandii</i>	2GJ3	FAD	(Key et al., 2007)
MmoS PAS A, B	<i>Methylococcus capsulatus</i>	3EWK	FAD	(Ukaegbu and Rosenzweig, 2009)
FixL PAS B	<i>Bradyrhizobium japonicum</i>	1XJ3	heme	(Gong et al., 1998; Key and Moffat, 2005)
FixL	<i>Sinorhizobium meliloti</i>	1D06	heme	(Miyatake et al., 2000)
DOS PAS A	<i>Escherichia coli</i>	1V9Z	heme	(Kurokawa et al., 2004; Park et al., 2004)
GSU0935	<i>Geobacter sulfurreducens</i>	3B42	heme	(Pokkuluri et al., 2008)
GSU0582	<i>Geobacter sulfurreducens</i>	3B47	heme	(Pokkuluri et al., 2008)
DetB PAS A, B	<i>Sinorhizobium meliloti</i>	3E4O	C ₃ , C ₄ sugars	(Zhou et al., 2008)
DeuS PAS A	<i>Escherichia coli</i>	3BY8	C ₄ sugars	(Cheung and Hendrickson, 2008; Pappalardo et al., 2003)
CitA PAS A	<i>Klebsiella pneumoniae</i>	2J80	citrate	(Reinelt et al., 2003; Sevvana et al., 2008)
Q87T87	<i>Vibrio parahaemolyticus</i>	2QHK	glycerol ^e	-
Q5V5P7 PAS C	<i>Haloarcula marismortui</i>	3BWL	1H-indole-3-carbaldehyde ^e	-
RHA05790 PAS B	<i>Rhodococcus jostii</i>	3FG8	3-phosphonoxy-butanoic acid ^e	-
PhoQ	<i>Escherichia coli</i>	3BQ8	metal ²⁺	(Cheung et al., 2008)
PhoQ	<i>Salmonella typhimurium</i>	1YAX	metal ²⁺	(Cho et al., 2006)
HIF2α PAS B	<i>Homo sapiens</i>	1P97, 3F1O	N-[2-nitro-4-(trifluoromethyl)phenyl]morpholin-4-amine ^e	(Erbel et al., 2003; Scheuermann et al., 2009)
ARNT PAS B	<i>Homo sapiens</i>	1X0O	-	(Card et al., 2005; Scheuermann et al., 2009)
PAS kinase PAS A	<i>Homo sapiens</i>	1LL8	-	(Amezcuca et al., 2002)
NCoA-1/SRC-1 PAS B	<i>Homo sapiens</i>	1OJ5	-	(Razeto et al., 2004)
Per PAS A, B	<i>Drosophila melanogaster</i>	1WA9	-	(Yildiz et al., 2005)
HERG	<i>Homo sapiens</i>	1BYW	-	(Morais Cabral et al., 1998)
LuxQ PAS A, B	<i>Vibrio harveyi</i>	2HJE	-	(Neiditch et al., 2006)
BphP	<i>Deinococcus radiodurans</i>	2O9C	-	(Wagner et al., 2005; Wagner et al., 2007)
BphP3	<i>Rhodospseudomonas palustris</i>	2OOL	-	(Yang et al., 2007)
BphP	<i>Pseudomonas aeruginosa</i>	3C2W	-	(Yang et al., 2008)

Clock and Cycle

Drosophila Clock (dCLK) and Cycle (CYC) are transcription factors homologous to the mammalian proteins Clock (mCLK) and BMAL1. These proteins each have helix-loop-helix (HLH) domains which bind the E-box promoter of DNA and two PAS domains which dimerize making a CLK/CYC heterodimer. In addition, both dCLK and mCLK have a long extension on the c-terminus which includes a glutamine-rich and poly-glutamine region. This region has been shown to have histone acetyl transferase activity in mCLK, though this activity has not been confirmed in dCLK as of yet.

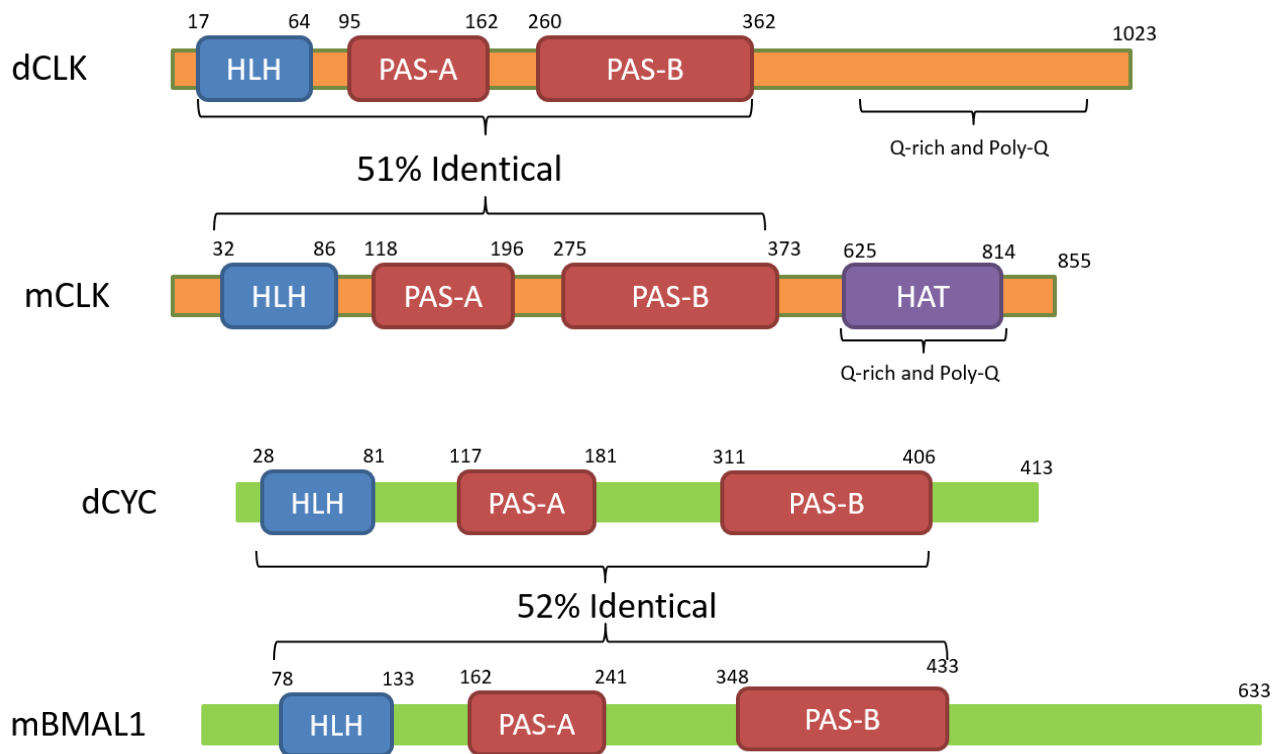


Fig. 6: Architecture of positive transcription factors in *Drosophila* and mammals. Helix-loop-helix domain (HLH) in blue. Per-ARNT-Sim (PAS) in red. Histone-acetyltransferase (HAT) in purple.

Metabolism/Metabolites and the Circadian Clock

Among the genes controlled by the clock are a number of genes involved in metabolism, and organisms with defective clock genes are also susceptible to defects in metabolism^{36,37}. In addition there is evidence that changes in metabolism can also influence the circadian clock, For example changing the feeding schedule can change the phase of the circadian clock in the Suprachiasmatic nucleus (SCN)³⁸. Proposed methods for entraining the clock by feeding include through glucose levels or hormones promoted by feeding^{39,40}.

In addition, the metabolic state of the cell can affect the redox equilibrium in the form of NAD⁺/NADH ratio. This ratio has been found to affect the DNA binding of CLK/BMAL1, perhaps through the action of the NAD⁺ histone deacetylase SIRT1, which interacts with CLK and deacetylates BMAL1 and PER, decreasing CLK/BMAL1 transcriptional activity⁴¹⁻⁴³. SIRT1 also interacts with proteins involved in gluconeogenesis⁴⁴, and SIRT1 activity has been shown to fluctuate with a circadian rhythm⁴².

Cryptochrome

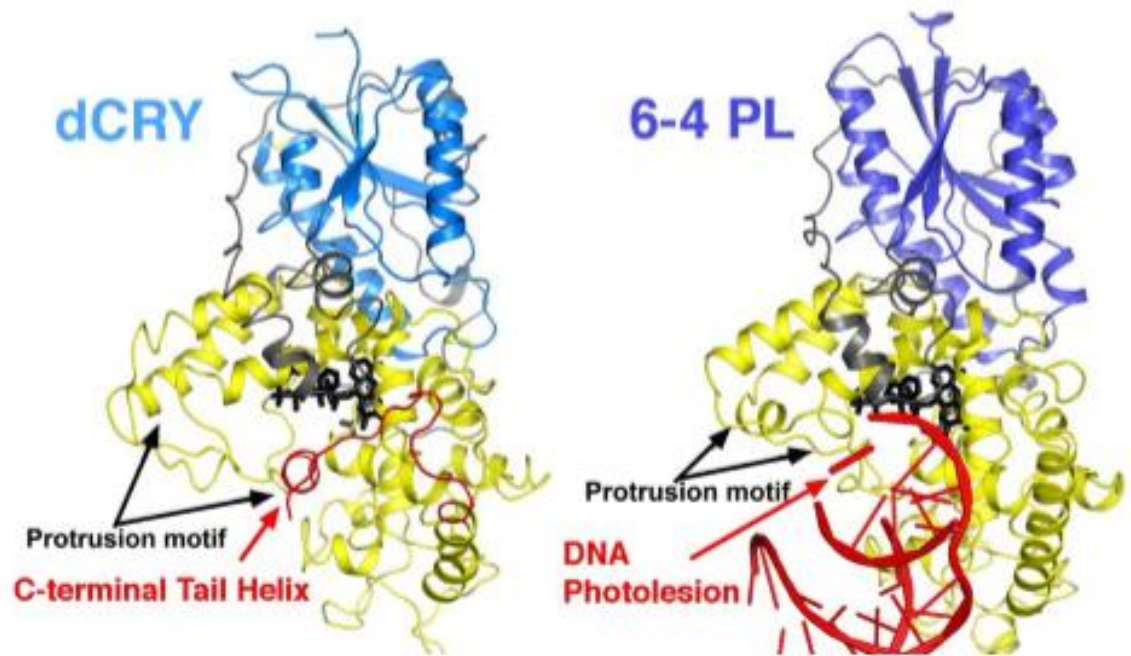


Fig. 7 Structural similarities between cryptochrome and photolyase. *dCry* (left) and *Dm*(6-4) photolyase (right) have similar 3-D structure and the C-terminal tail in CRY occupies the same groove as the DNA in photolyase (Nature, 2011, **480**(7377), 396-399)

Cryptochromes are proteins closely related to photolyase (PL) DNA repair enzymes. Photolyase binds an FAD cofactor that carries out DNA repair by donating an electron through cyclic electron transfer and breaking a DNA linkage. In addition, PLs can bind a second pterin cofactor (usually methenyl-trihydrofolate (MTHF)) that appears to act as an antenna cofactor which helps absorb light. CRYs contain a domain very similar to PLs, termed the photolyase homology domain (PHD), and an additional extension on the c-terminus called the c-terminal tail/extension (CTT or CTE). The CTT forms a helix that binds in the active center groove alongside the flavin, in analogy to where substrate DNA lesions bind in PLs (Fig. 7). It is not

thought that CRYs bind an antenna cofactor, as the binding pocket is not fully conserved and no structures have included any cofactors there.

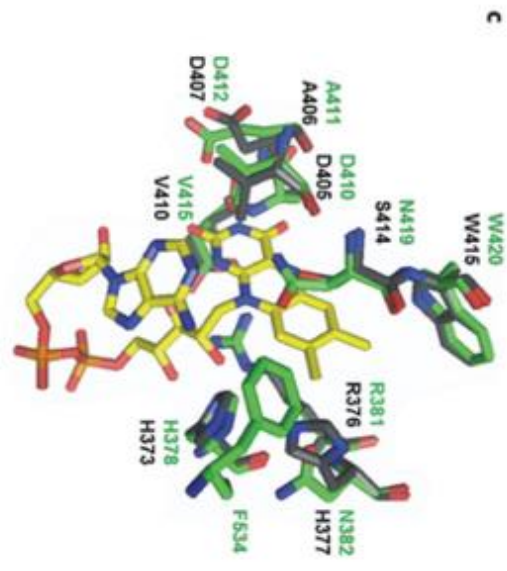
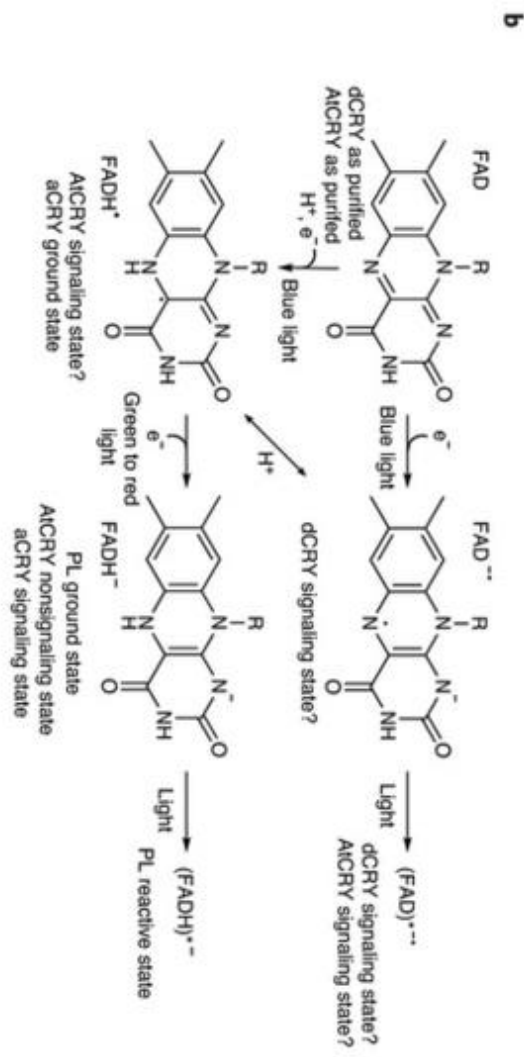
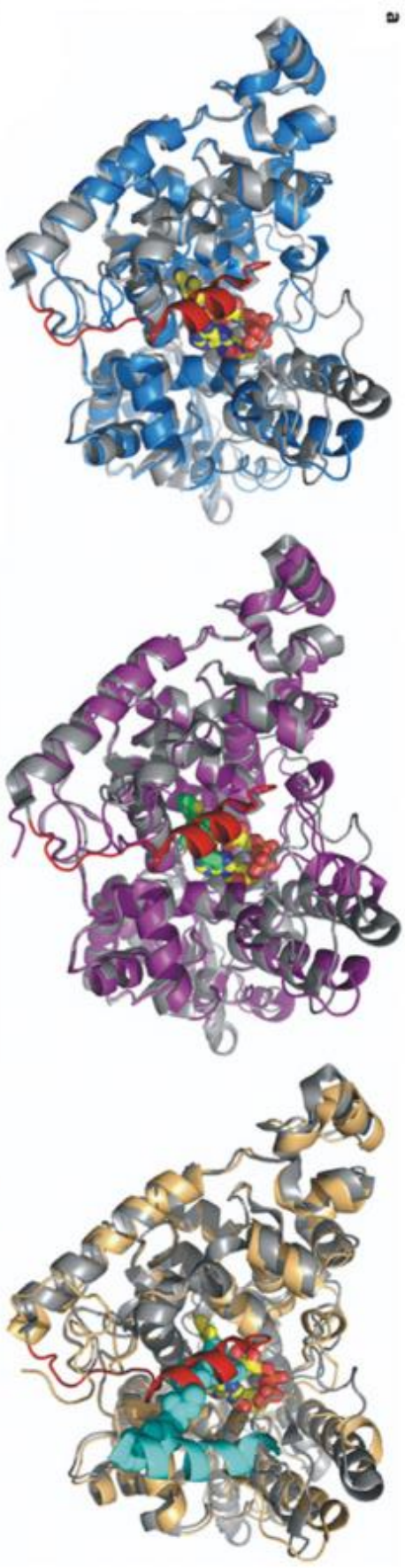
CRY/PL type proteins are usually divided into classes, depending on their function and presence of a CTE. These classes include 6-4 PLs, cyclobutane pyrimidine dimer (CPD) PLs, CRY-DASH proteins, which have a CTE but also some DNA repair activity, and CRYs. Cryptochromes can further be divided into type I CRYs, such as *Drosophila* CRY and *Arabidopsis thaliana* CRYs (AtCRYs), which have some light-sensing activity, and mammalian, or type II CRYs, which do not.

The difference between type I CRYs and type II CRYs can be seen with *Drosophila* CRY (dCRY) and mouse CRY mCRY1. In *Drosophila*, dCRY light-dependently binds to TIM and targets it for degradation through recruitment of the E3 ubiquitin ligase JET^{45,16,46-48}, after which dCRY itself is degraded by the ubiquitin ligase BRWD3⁴⁹. The light-dependent signaling mechanism is sent by dCRY via a reduction in the redox state of its FAD cofactor accompanied by conformational changes in its CTE^{48,50-52}.

In mammals, mCRY1 carries out a different function, where instead of a light sensor it is a member of the core TTFL, entering the nucleus and interacting directly with CLOCK/BMAL1 as a gene repressor^{5,53}. mCRY1 is not thought to have any light sensing activity of its own, and it is not even clear that it binds FAD *in vivo*, though FAD binding can be reconstituted in purified proteins with a very similar binding mode to dCRY. Human CRY, which purifies without FAD bound, has been able to rescue light sensing to some extent in dCRY defective flies^{54,55}. In addition, the same FAD binding pocket is also targeted by mCRY's E3 ubiquitin ligase SCFFbx¹³, and

recent high-throughput screening identified a compound that also targets the same FAD binding pocket of mCRY2 and disrupts the circadian rhythms in cultured cells (Fig. 8A). Thus, it seems possible that flavin competes with protein and small-molecule ligands for binding within this pocket and such interactions may depend on the flavin redox state^{39,54,56}.

Fig. 8: (a) The flavin pocket in various CRY and PL structures is used to recognize cofactors, substrates, regulatory elements, targets and small-molecule inhibitors, thereby providing mechanisms to couple molecular recognition to flavin chemistry. Superposition of dCRY (gray with red CTT and yellow FAD, PDB code [4GU5](#)), mouse mCRY2 PL domain with FAD (residues 1–512, blue with dark blue FAD, PDB code [4I6G](#)), mouse mCRY2 PL domain with a small molecule bound (purple with green small molecule, PDB code [4MLP](#)) and mouse mCRY2 PL domain with the C terminus of FBXL3 bound in the FAD pocket (gold with teal FBXL3 residues 400–428, PDB code [4I6J](#)). **(b)** Changes in FAD redox states driven by light in dCRY, AtCRY and aCRY; both the ASQ and a light-excited ASQ may be signaling states of dCRY. Similarly, the NSQ and light-excited ASQ could be AtCRY signaling states (see text), and aCRY signals from a ground NSQ state. **(c)** dCRY and mCRY2 residues that lie near FAD are strongly conserved.



Photoreduction mechanism of PLs and CRYs

In PLs, the active state of FAD is the fully reduced state, which is then excited by light to start cyclic electron transfer. However, PLs are purified in the oxidized state which must then be reduced by light before PL can carry out its DNA repair activity. In 1990 it was observed that a tryptophan residue acted as an electron donor for this process⁵⁷, then in 1991 residue W306 was identified in *E. coli* PL as essential for this process⁵⁸. However upon publication of the first structure of PL in 1995⁵⁹ it was found that W306 was located too far from the FAD cofactor to be an efficient electron donor, and an electron tunneling/hopping mechanism was proposed using two other conserved tryptophan residues to lead from the FAD to W306⁶⁰. This hypothesis has been supported by subsequent experiments⁶¹⁻⁶⁴, and the generally accepted method for PL reduction is that W306 donates an electron through this TRP triad, and then W306 is reduced by an external reductant to stabilize the fully reduced FAD⁻.

Since type I CRYs, such as dCRY and AtCRY are purified with FAD fully oxidized and FAD is reduced by light, it was thought that they might use a homologous TRP triad to transfer electrons⁶⁵. For the most part, this has been born out *in vitro*, but has conflicting results *in vivo*.

In 2002 it was found that mutating the TRP closest to FAD (sometimes called the proximal TRP) in dCRY, W420, to alanine allowed cells to retain light-responsive activity in S2 cells, while mutation of the other two tryptophans to alanine, W397 and W342 (called the middle and terminal TRP respectively), abolished light response. Mutations of W397 and W342 to tyrosine or phenylalanine, which are structurally

different from tryptophan but potentially could carry out the same electron transport function, allowed CRY to impart some light-responsive activity ⁶⁶.

Mutational Studies of CRY Homologs

Mutational studies have also been carried out on Cryptochromes from other species, which may inform on the reduction mechanism in *Drosophila*. In 2005 studies were made in *Arabidopsis thaliana* AtCRY1, which showed that blocking reduction by mutating TRP triad residues impaired function both *in vitro* and *in vivo* ⁶⁷. However, in 2007 and 2008, two studies of butterfly cryptochrome 1 (DpCRY1) showed that mutating the terminal electron donor W328 to phenylalanine blocked photoreduction *in vitro* but had no effect *in vivo*, and that blocking photoreduction *in vitro* did not necessarily correlate with blocking light-induced degradation *in vivo* for dCRY W342F as well as DpCRY1 proximal and terminal TRP mutations. In dCRY W342F and proximal and terminal tryptophan mutations in DpCRY1, the FAD is not reduced *in vitro*, though after long exposure dCRY W342F had some reduction, perhaps suggesting an alternate electron transfer pathway ^{68,69}. In 2013 additional *in vitro* studies showed W397F abolishes radical formation and inhibits trypsin digest, but doesn't abolish it ⁷⁰, and two studies have shown that W420F abolishes the formation of a radical^{69,71}. In 2011 an AtCRY2 study showed that mutating any of the TRP triad residues to alanine halted photoreduction *in vitro*, but had full activity or constitutive activity *in vivo*⁷².

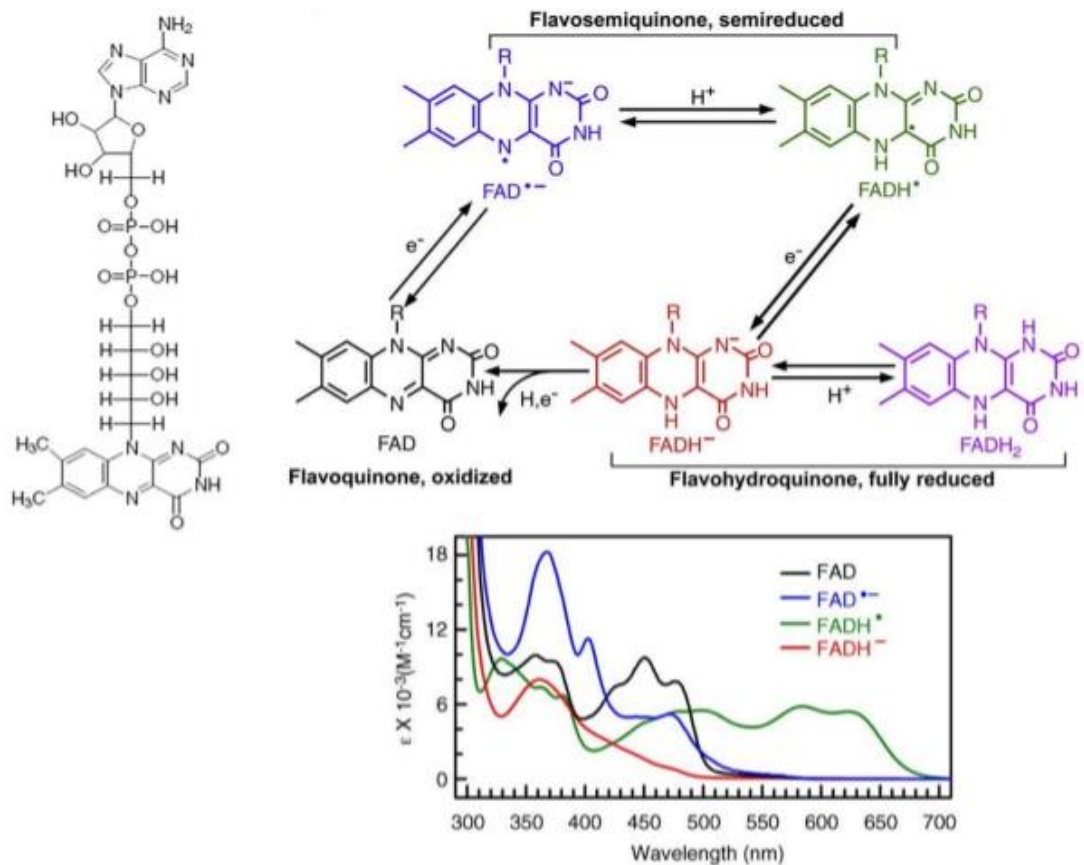


Fig. 9 Redox states of FAD and their absorption spectra. FAD (Left), its redox states (top right) and the absorption spectrum of the redox states (bottom). (Current opinion in plant biology, 2010. **13**(5): 578-586)

CRY Photoreduction Mechanism is in Question

Evidence against TRP triads being the method of reduction *in vivo* led to suggestions that CRYs having a fully oxidized FAD cofactor *in vitro* is merely an artifact of purification, and that *in vivo* CRY would contain a reduced semiquinone FAD, and that the active state upon light exposure would be an excited semiquinone state^{68,69}. This theory is supported by the fact that some light-induced conformational change can be seen *in vivo* even when no reduction is seen by UV-visible spectroscopy^{48,70}. In addition, there is some evidence^{48,70} that if oxidized CRY is

chemically reduced in the absence of light, no conformational change is seen^{48,73}. It was proposed that instead of electron transport through the TRP triad, internal ET in the FAD would lead to reduction. Recent data on PLs indicate that internal ET reactions between adenine and isoalloxazine moieties of FAD could transiently (<100 ps) generate changes in the flavin redox state that may contribute to CRY signaling⁷⁴. However, another study contradicted these results, showing that chemical reduction did result in conformational change, and that this change was correlated with a change in binding of CRY's partners. In addition, it was shown that conformational change was directly correlated with FAD redox state temporally-which would not necessarily be true if an excited FAD was the active state⁷⁵. In addition, EPR was used to detect the light-induced formation and degradation of the semiquinone state of AtCRY1 both *in vitro* and *in vivo*⁷⁶.

In *Arabidopsis*, both AtCRY1 and AtCRY2 purify from insect cell expression with oxidized FAD, which is then reduced to a NSQ by blue light and fully reduced to a HQ by green light. (Fig. 8B) One theory for light activation in AtCRYs holds that light excitation of an AtCRY ASQ causes rapid photoreduction, which is responsible for sending a signal. What would AtCRY then reduce? Notably, AtCRY1 binds ATP near the FAD cavity, and AtCRY1 catalyzes autophosphorylation in a light-dependent manner⁷⁷. Thus, cyclic electron transfer between FAD and ATP may lead to conformational changes that promote autophosphorylation activity.

Other Key Residues May Play Role In Stabilizing FAD Radical of CRY

Deprotonation may also be involved in stabilizing the FAD radical formed in CRYs. In 2006 it was shown by FTIR that AtCRY1 D396 is likely deprotonated in the process of reduction of FAD to a neutral radical⁷⁸. This position is occupied by cysteine in dCRY, perhaps why an anionic radical is formed instead. However this cysteine has been mutated to Ala in AgCRY1 or ApCRY1 and no change was seen in the redox state, suggesting AtCRY1 takes up proton from water. In addition, mutation of this cysteine to asparagine led to formation of neutral semiquinone-but this did not affect activity *in vivo*⁶⁹. This residue has also been mutated to cysteine in CrCPH1 and it is shown that this prevents proton transfer to the FAD, shortening the lifetime of the radical and producing no conformational change. However, when ATP is added, the FAD is stably reduced to an anionic radical, which is sufficient to induce conformational change⁷⁹.

It has also been proposed that a histidine may play a role as a proton acceptor. In 2012 a study on CrCPH1 showed that a TRP cation radical is formed in the FAD pocket by donating an electron to the FAD. At the same time it is potentially deprotonated to stabilize the radical, and it is suggested that a histidine would become protonated because of this⁸⁰. Some evidence to support a protonation event being involved in the reduction of FAD is that the rate of recovery in aCRY was determined to be pH dependent. Thus it was suggested that a histidine residue may be responsible for catalyzing the deprotonation of an FADH radical at high pH, in turn inducing decay of the radical⁸¹.

Cysteine residues may also play a role in electron transport by acting as an electron sink to help change potentials of nearby tryptophans. It has been shown that mutating cysteines next to members of the TRP triad can change reduction kinetics⁷⁰. In dCRY C416A, next to W420 accelerates the decay of the anionic radical whereas C416D slows it down⁶⁹, and mutating C337 next to W397 accelerates formation and decay of a radical species. C523A also accelerates formation and decay of a radical, perhaps by acting through M421 which is located near W397 and C337⁷⁰.

One theory as to why blocking reduction *in vitro* can still lead to reduction *in vivo* is that there may be alternate reduction pathways that are only accessible *in vivo*. For example, in 2011 EPR spectroscopy was used to show that frog XICRY can use an alternative terminal electron donor if the original one is mutated⁸². This was followed up in 2013 by an article showing that if the TRP triad is mutated then XICRY can use alternate tyrosines and tryptophans to carry out FAD reduction⁸³. It was also proposed from the structure of dCRY that there are three additional tryptophans that could perhaps function as an electron transfer pathway if the original TRP triad was blocked⁸⁴. Additionally, small metabolites such as NADPH and ATP were found to promote photoreduction in AtCRY2, even in TRP triad mutants⁸⁵. However, this has been disputed by another study, which found that ATP did not rescue photoreduction in AtCRY1 TRP triad mutants *in vitro*, and that these mutants were still active *in vivo*⁸⁶. In 2015 a fourth tryptophan was found to be essential for reduction in XI(6-4)PL, and it was proposed that this additional residue, which was homologous to tryptophans present in only animal CRYs and PLs, was part of a TRP tetrad as the terminal electron donor.

Magnetosensing

One role of CRY currently being explored is its role in light-dependent magnetosensing. CRY mutants were found to be defective in the response of *Drosophila* to magnetic fields, and this behavior can be rescued by the introduction of dCRY and mCRYs^{87–89}. In birds, mCRY activation correlates with behavioral sensitivity to magnetic fields, and the wavelength sensitivity of the behavioral effect suggests involvement of the HQ state⁹⁰. In plants, AtCRY responses are influenced by magnetic fields⁹¹. Although the underlying mechanism of magnetosensing is largely unknown, the ability of flavin to produce magnetic dipoles in the form of radical pair states may be the key chemical feature. In this mechanism, the conversion between the triplet and singlet states of a correlated spin pair is influenced by the geomagnetic field, and a spin state–selective chemical reaction generates signals. However, the difference in triplet and singlet state energies must be small, and the nuclear hyperfine coupling that mediates the spin conversion must be of similar strength as the field effect⁹². This implies separation of the radical pairs within the protein to weaken their coupling as well as anisotropic hyperfine interactions to give directionality, and radical pairs composed of anionic flavin radicals and radical cation tryptophans in CRYs satisfy the distance constraint⁹³. Time-resolved EPR has established such a spin-correlated radical pair between FAD and tryptophan upon blue-light illumination of frog CRY⁹⁴. Additionally, magnetic fields (albeit those considerably stronger than earth's field) affect photoreduced flavin yields in purified CRY⁹⁵. How the protein conformation reads out the spin-pair interaction remains to be determined, but it may involve modulating the rate of return to the oxidized flavin ground state⁹².

Structure and Reactivity of Drosophila Cycle and Cryptochrome

In this dissertation, I will discuss my recent findings concerning the structure and reactivity of the proteins Cycle and Cryptochrome involved in the circadian clock of *Drosophila melanogaster*.

I will show the structure of the PAS B domain of the transcription factor Cycle, and our findings that confirm a key tryptophan in dimerization of this protein. In addition, we have shown that this domain binds a novel ligand for PAS domains, glycerol, which has the potential to interact with fatty acid metabolism.

I also use mutational studies to look at the role of key residues involved in the light absorption and conformational change of the light sensing protein Cryptochrome. I confirm the importance of the tryptophan triad in electron transport, and also of a fourth tryptophan in this transport chain as well-the first study of this residue in *Drosophila* Cryptochrome. In addition, we show how a cysteine residue near Cryptochrome's FAD cofactor is responsible for the redox state of the FAD after light exposure. This redox change leads to conformational change of the protein, which is gated by protonation of a nearby histidine residue.

These findings provide insight into the mechanism of action for key components of the circadian clock of both *Drosophila* and mammals, and inform on further areas for study.

REFERENCES

1. Karatsoreos, I. N. Effects of circadian disruption on mental and physical health. *Curr. Neurol. Neurosci. Rep.* **12**, 218–225 (2012).
2. Bersten, D. C., Sullivan, A. E., Peet, D. J. & Whitelaw, M. L. bHLH–PAS proteins in cancer. *Nat. Rev. Cancer* **13**, 827–841 (2013).
3. Mackey, S. R. & Golden, S. S. Winding up the cyanobacterial circadian clock. *Trends Microbiol.* **15**, 381–388 (2007).
4. Brown, S. a., Kowalska, E. & Dallmann, R. (Re)inventing the Circadian Feedback Loop. *Dev. Cell* **22**, 477–487 (2012).
5. Crane, B. R. & Young, M. W. Interactive Features of Proteins Composing Eukaryotic Circadian Clocks. *Annu. Rev. Biochem.* **83**, 191–219 (2014).
6. Partch, C. L., Green, C. B. & Takahashi, J. S. Molecular architecture of the mammalian circadian clock. *Trends Cell Biol.* **24**, 90–9 (2014).
7. Peschel, N. & Helfrich-Forster, C. Setting the clock--by nature: circadian rhythm in the fruitfly *Drosophila melanogaster*. *FEBS Lett* **585**, 1435–1442 (2011).
8. Konopka, R. J. & Benzer, S. Clock Mutants of *Drosophila melanogaster*. **68**, 2112–2116 (1971).
9. Sehgal, Amita, et al. Loss of circadian behavioral rhythms and per RNA oscillations in the *Drosophila* mutant 'timeless'. (1994). at <<http://www.ncbi.nlm.nih.gov/pubmed/8128246>>
10. Gekakis, N. *et al.* Isolation of timeless by PER protein interaction: defective interaction between timeless protein and long-period mutant PERL. *Science (80-.)*. **270**, 811–815 (1995).
11. Allada, R., White, N. E., So, W. V., Hall, J. C. & Rosbash, M. A Mutant *Drosophila* Homolog of Mammalian Clock Disrupts Circadian Rhythms and Transcription of period and timeless. **93**, 791–804 (1998).
12. Rutila, J. E. *et al.* CYCLE Is a Second bHLH-PAS Clock Protein Essential for Circadian Rhythmicity and Transcription of *Drosophila* period and timeless. *Cell* **93**, 805–814 (1998).
13. Emery, P., So, W. V, Kaneko, M., Hall, J. C. & Rosbash, M. CRY, a *Drosophila* clock and light-regulated cryptochrome, is a major contributor to circadian rhythm resetting and photosensitivity. *Cell* **95**, 669–679 (1998).
14. Stanewsky, R. *et al.* The cryb mutation identifies cryptochrome as a circadian photoreceptor in *Drosophila*. *Cell* **95**, 681–692 (1998).
15. Cashmore, A. R. The Cryptochrome Family of Blue / UV-A Photoreceptors ". *J. Plant Res.* 267–270 (1998).

16. Busza, A., Emery-Le, M., Rosbash, M. & Emery, P. Roles of the two *Drosophila* CRYPTOCHROME structural domains in circadian photoreception. *Science* (80-.). **304**, 1503–1506 (2004).
17. Rosato, E., Tauber, E. & Kyriacou, C. P. Molecular genetics of the fruit-fly circadian clock. *Eur. J. Hum. Genet.* 729–738 (2006). doi:10.1038/sj.ejhg.5201547
18. Hennig, S. *et al.* Structural and functional analyses of PAS domain interactions of the clock proteins *Drosophila* PERIOD and mouse PERIOD2. *PLoS Biol* **7**, e94 (2009).
19. King, H. A., Hoelz, A., Crane, B. R. & Young, M. W. Structure of an Enclosed Dimer Formed by the *Drosophila* Period Protein. *J. Mol. Biol.* **413**, 561–572 (2011).
20. Yagita, K. *et al.* Dimerization and nuclear entry of mPER proteins in mammalian cells. *Genes Dev.* **14**, 1353–1363 (2000).
21. Lee, C., Etchegaray, J. P., Cagampang, F. R., Loudon, a S. & Reppert, S. M. Posttranslational mechanisms regulate the mammalian circadian clock. *Cell* **107**, 855–867 (2001).
22. Kim, E. Y., Ko, H. W., Yu, W. J., Hardin, P. E. & Edery, I. A DOUBLETIME kinase binding domain on the *Drosophila* PERIOD protein is essential for its hyperphosphorylation, transcriptional repression, and circadian clock function. *Mol. Cell. Biol.* **27**, 5014–5028 (2007).
23. Vanselow, K. *et al.* Differential effects of PER2 phosphorylation: molecular basis for the human familial advanced sleep phase syndrome (FASPS). *Genes Dev* **20**, 2660–2672 (2006).
24. Hara, T., Koh, K., Combs, D. J. & Sehgal, A. Post-translational regulation and nuclear entry of TIMELESS and PERIOD are affected in new timeless mutant. *J. Neurosci.* **31**, 9982–9990 (2011).
25. Martinek, S., Inonog, S., Manoukian, A. S. & Young, M. W. A role for the segment polarity gene shaggy/GSK-3 in the *Drosophila* circadian clock. *Cell* **105**, 769–779 (2001).
26. Lin, J. M., Kilman, V. ., Keegan, K., Paddock, B. & Emerey-Le, M. A role for casein kinase 2a in the *Drosophila* circadian clock. *Nature* **420**, 816–820 (2002).
27. Akten, B. *et al.* A role for CK2 in the *Drosophila* circadian oscillator. *Nat. Neurosci.* **6**, 251–257 (2003).
28. Nawathean, P. & Rosbash, M. The Doubletime and CKII Kinases Collaborate to Potentiate *Drosophila* PER Transcriptional Repressor Activity. *Mol. Cell* **13**, 213–223 (2004).
29. Kim, E. Y., Jeong, E. H., Park, S., Jeong, H. & Edery, I. A role for O - GlcNAcylation in setting circadian clock speed. *Genes Dev* **26**, 490–502 (2012).

30. Kaasik, K. *et al.* Glucose Sensor O-GlcNAcylation Coordinates with Phosphorylation to Regulate Circadian Clock. *Cell Metab.* **17**, 291–302 (2013).
31. Huang, Z. J., Edery, I. & Rosbash, M. PAS IS A DIMERIZATION DOMAIN COMMON TO DROSOPHILA PERIOD AND SEVERAL TRANSCRIPTION FACTORS. *Nature* **364**, 259–262 (1993).
32. Ayers, R. A. & Moffat, K. Review Structure and Signaling Mechanism of Per-ARNT-Sim Domains. 1282–1294 (2009). doi:10.1016/j.str.2009.08.011
33. Henry, J. T. & Crosson, S. Ligand-Binding PAS Domains in a Genomic , Cellular , and Structural Context. (2011). doi:10.1146/annurev-micro-121809-151631
34. Diensthuber, R. P., Bommer, M., Gleichmann, T. & Moglich, A. Full-Length Structure of a Sensor Histidine Kinase Pinpoints Coaxial Coiled Coils as Signal Transducers and Modulators. *Structure* **21**, 1127–1136 (2013).
35. Moglich, A., Ayers, R. A. & Moffat, K. Structure and Signaling Mechanism of Per-ARNT-Sim Domains. *Structure* **17**, 1282–1294 (2009).
36. Panda, S. *et al.* Coordinated transcription of key pathways in the mouse by the circadian clock. *Cell* **109**, 307–320 (2002).
37. De Bacquer, D. *et al.* Rotating shift work and the metabolic syndrome: a prospective study. *Int. J. Epidemiol.* **38**, 848–854 (2009).
38. Damiola, F. *et al.* Restricted feeding uncouples circadian oscillators in peripheral tissues from the central pacemaker in the suprachiasmatic nucleus. *Genes Dev.* **14**, 2950–2961 (2000).
39. Hirota, T. *et al.* Identification of small molecule activators of cryptochrome. *Science (80-.)*. **337**, 1094–1097 (2012).
40. LeSauter, J., Hoque, N., Weintraub, M., Pfaff, D. W. & Silver, R. Stomach ghrelin-secreting cells and food-entrainable circadian clocks. *Proc. Natl. Acad. Sci.* **106**, 13582–13587 (2009).
41. Rutter, J. Regulation of Clock and NPAS2 DNA Binding by the Redox State of NAD Cofactors. *Science (80-.)*. **293**, 510–514 (2001).
42. Nakahata, Y. *et al.* The NAD(+)-dependent deacetylase SIRT1 modulates CLOCK-mediated chromatin remodeling and circadian control. *Cell* **134**, 329–340 (2008).
43. Asher, G. *et al.* SIRT1 regulates circadian clock gene expression through PER2 deacetylation. *Cell* **134**, 317–28 (2008).
44. Rodgers, J. T. *et al.* Nutrient control of glucose homeostasis through a complex of PGC-1 α and SIRT1. *Nature* **434**, 113–118 (2005).
45. Naidoo, N., Song, W., Hunter-Ensor, M. & Sehgal, A. A role for the proteasome in the light response of the timeless clock protein. *Science (80-.)*. **285**,

1737–1741 (1999).

46. Koh, K., Zheng, X. Z. & Sehgal, A. JETLAG resets the *Drosophila* circadian clock by promoting light-induced degradation of TIMELESS. *Science* (80-.). **312**, 1809–1812 (2006).
47. Peschel, N., Chen, K. F., Szabo, G. & Stanewsky, R. Light-dependent interactions between the *Drosophila* circadian clock factors cryptochrome, jetlag, and timeless. *Curr Biol* **19**, 241–247 (2009).
48. Ozturk Selby, C.P., Annayev, Y., Zhong, D., Sancar, A., N. Reaction Mechanism of *Drosophila* cryptochrome. *Proc Natl Acad Sci U S A* **108**, 516–521 (2011).
49. Ozturk, N., VanVickle-Chavez, S. J., Akileswaran, L., Van Gelderb, R. N. & Sancar, A. Ramshackle (Brwd3) promotes light-induced ubiquitylation of *Drosophila* Cryptochrome by DDB1-CUL4-ROC1 E3 ligase complex. *Proc. Natl. Acad. Sci. U. S. A.* **110**, 4980–4985 (2013).
50. Vaidya, A. T. *et al.* Flavin reduction activates *Drosophila* cryptochrome. *Proc Natl Acad Sci U S A* **110**, 20455–20460 (2013).
51. Dissel, S. *et al.* A constitutively active cryptochrome in *Drosophila melanogaster*. *Nat Neurosci* **7**, 834–840 (2004).
52. Yang, H. Q. *et al.* The C termini of *Arabidopsis* cryptochromes mediate a constitutive light response. *Cell* **103**, 815–827 (2000).
53. Chaves, I. *et al.* The cryptochromes: blue light photoreceptors in plants and animals. *Annu Rev Plant Biol* **62**, 335–364 (2011).
54. Xing, W. *et al.* SCF(FBXL3) ubiquitin ligase targets cryptochromes at their cofactor pocket. *Nature* **496**, 64–68 (2013).
55. Vieira, J. *et al.* Human Cryptochrome-1 Confers Light Independent Biological Activity in Transgenic *Drosophila* Correlated with Flavin Radical Stability. *PLoS One* **7**, (2012).
56. Nangle, S., Xing, W. M. & Zheng, N. Crystal structure of mammalian cryptochrome in complex with a small molecule competitor of its ubiquitin ligase. *Cell Res.* **23**, 1417–1419 (2013).
57. Heelis, P. F., Okamura, T. & Sancar, A. Excited-State Properties of *Escherichia coli* DNA Photolyase in the Picosecond to Millisecond Time Scale. *Biochemistry* **29**, 5694–5698 (1990).
58. Li, Y. F., Heelis, P. F. & Sancar, A. Active Site of DNA Photolyase: Tryptophan-306 Is the Intrinsic Hydrogen Atom Donor Essential for Flavin Radical Photoreduction and DNA Repair in Vitro. *Biochemistry* **30**, 6322–6329 (1991).
59. Park, H. W., Kim, S. T., Sancar, A. & Deisenhofer, J. Crystal structure of

- DNA photolyase from *Escherichia coli*. *Science* (80-.). **268**, 1866–1872 (1995).
60. Cheung, M. S., Daizadeh, I., Stuchebrukhov, A. A. & Heelis, P. F. Pathways of Electron Transfer in *Escherichia coli* DNA Photolyase : *Biophys. J.* **76**, 1241–1249 (1999).
 61. Aubert, C., Vos, M. H., Mathis, P. & Brettel, K. Intraprotein radical transfer during photoactivation of DNA photolyase. *Nature* **405**, 586–590 (2000).
 62. Saxena, C., Sancar, A. & Zhong, D. Femtosecond Dynamics of DNA Photolyase : Energy Transfer of Antenna Initiation and Electron Transfer of Cofactor Reduction. *J. Phys. Chem. B* **108**, 18026–18033 (2004).
 63. Byrdin, M. *et al.* Quantum Yield Measurements of Short-Lived Photoactivation Intermediates in DNA Photolyase : Toward a Detailed Understanding of the Triple Tryptophan Electron Transfer Chain †. *J. Phys. Chem. A* **114**, 3207–3214 (2010).
 64. Liu, Z. *et al.* Determining complete electron flow in the cofactor photoreduction of oxidized photolyase. *Proc Natl Acad Sci U S A* **110**, 12966–12971 (2013).
 65. Berndt, A. *et al.* A novel photoreaction mechanism for the circadian blue light photoreceptor *Drosophila* cryptochrome. *J Biol Chem* **282**, 13011–13021 (2007).
 66. Froy, O., Chang, D. C. & Reppert, S. M. Redox potential: differential roles in dCRY and mCRY1 functions. *Curr Biol* **12**, 147–152 (2002).
 67. Zeugner, A. *et al.* Light-induced Electron Transfer in Arabidopsis Cryptochrome-1 Correlates with in Vivo Function *. *J. Biol. Chem.* **280**, 19437–19440 (2005).
 68. Song, S.-H. *et al.* Formation and function of flavin anion radical in cryptochrome 1 blue-light photoreceptor of monarch butterfly. *J Biol Chem* **282**, 17608–17612 (2007).
 69. Ozturk, N., Song, S. H., Selby, C. P. & Sancar, A. Animal type 1 cryptochromes. Analysis of the redox state of the flavin cofactor by site-directed mutagenesis. *J Biol Chem* **283**, 3256–3263 (2008).
 70. Czarna, A. *et al.* Structures of *Drosophila* cryptochrome and mouse cryptochrome1 provide insight into circadian function. *Cell* **153**, 1394–1405 (2013).
 71. Berndt, A. *et al.* Structures of *Drosophila* Cryptochrome and Mouse Cryptochrome1 Provide Insight into Circadian Function. *Cell* **153**, 1394–1405 (2013).
 72. Li, X. *et al.* Arabidopsis cryptochrome 2 (CRY2) functions by the photoactivation mechanism distinct from the tryptophan (trp) triad-dependent photoreduction. *Proc Natl Acad Sci U S A* **108**, 20844–20849 (2011).
 73. Ozturk, N., Selby, C. P., Zhong, D. & Sancar, A. Mechanism of

- Photosignaling by Drosophila Cryptochrome. *J. Biol. Chem.* **289**, 4634–4642 (2014).
74. Liu, Z. Y. *et al.* Dynamic determination of the functional state in photolyase and the implication for cryptochrome. *Proc. Natl. Acad. Sci. U. S. A.* **110**, 12972–12977 (2013).
75. Vaidya, A. T. *et al.* Flavin reduction activates Drosophila cryptochrome. *Proc. Natl. Acad. Sci. U. S. A.* **110**, 20455–60 (2013).
76. Herbel, V. *et al.* Lifetimes of Arabidopsis cryptochrome signaling states in vivo. *Plant J.* **74**, 583–592 (2013).
77. Liu, H., Liu, B., Zhao, C., Pepper, M. & Lin, C. The action mechanisms of plant cryptochromes. *Trends Plant Sci* **16**, 684–691 (2011).
78. Kottke, T., Batschauer, A., Ahmad, M. & Heberle, J. Blue-light-induced changes in *Arabidopsis* cryptochrome 1 probed by FTIR difference spectroscopy. *Biochemistry* **45**, 2472–2479 (2006).
79. Hense, A., Herman, E., Oldemeyer, S. & Kottke, T. Proton Transfer to Flavin Stabilizes the Signaling State of the Blue Light Receptor Plant Cryptochrome. *J. Biol. Chem.* **290**, 1743–1751 (2015).
80. Immeln, D., Weigel, A., Kottke, T. & Pérez Lustres, J. L. Primary events in the blue light sensor plant cryptochrome: Intraprotein electron and proton transfer revealed by femtosecond spectroscopy. *J. Am. Chem. Soc.* **134**, 12536–12546 (2012).
81. Spexard, M., Thöing, C., Beel, B., Mittag, M. & Kottke, T. Response of the sensory animal-like cryptochrome aCRY to blue and red light as revealed by infrared difference spectroscopy. *Biochemistry* **53**, 1041–1050 (2014).
82. Biskup, T. *et al.* Time-resolved EPR identifies unexpected electron transfer in cryptochrome. *Angew* **50**, 12647–12651 (2011).
83. Biskup, T. *et al.* Variable Electron Transfer Pathways in an Amphibian. *J. Biol. Chem.* **288**, 9249–9260 (2013).
84. Zoltowski, B. D. *et al.* Structure of full-length Drosophila cryptochrome. *Nature* **480**, 396–399 (2011).
85. Engelhard, C. *et al.* Cellular Metabolites Enhance the Light Sensitivity of Arabidopsis Cryptochrome through Alternate Electron Transfer Pathways. *Plant Cell* **26**, 4519–31 (2014).
86. Gao, J. *et al.* Trp triad-dependent rapid photoreduction is not required for the function of *Arabidopsis* CRY1. *Proc. Natl. Acad. Sci.* **112**, 9135–9140 (2015).
87. Gegear, R. J., Foley, L. E., Casselman, A. & Reppert, S. M. Animal cryptochromes mediate magnetoreception by an unconventional photochemical mechanism. *Nature* **463**, 804–807 (2010).
88. Foley, L. E., Gegear, R. J. & Reppert, S. M. Human cryptochrome exhibits

- light-dependent magnetosensitivity. *Nat Commun* **2**, 356 (2011).
89. Gear, R. J., Casselman, A., Waddell, S. & Reppert, S. M. Cryptochrome mediates light-dependent magnetosensitivity in *Drosophila*. *Nature* **454**, 1014–1018 (2008).
90. Niessner, C. *et al.* Magnetoreception: activated cryptochrome 1a concurs with magnetic orientation in birds. *J. R. Soc. Interface* **10**, 20130638 (2013).
91. Ahmad, M., Galland, P., Ritz, T., Wiltschko, R. & Wiltschko, W. Magnetic intensity affects cryptochrome-dependent responses in *Arabidopsis thaliana*. *Planta* **225**, 615–624 (2007).
92. Dodson, C. A., Hore, P. J. & Wallace, M. I. A radical sense of direction: signalling and mechanism in cryptochrome magnetoreception. *Trends Biochem Sci* **38**, 435–446 (2013).
93. Solov'yov, I. A., Domratcheva, T. & Schulten, K. Separation of photo-induced radical pair in cryptochrome to a functionally critical distance. *Sci Rep* **4**, 3845 (2014).
94. Biskup, T. Time-resolved electron paramagnetic resonance of radical pair intermediates in cryptochromes. *Mol. Phys.* **111**, 3698–3703 (2013).
95. Maeda, K. *et al.* Magnetically sensitive light-induced reactions in cryptochrome are consistent with its proposed role as a magnetoreceptor. *Proc. Natl. Acad. Sci.* **109**, 4774–4779 (2012).

CHAPTER 2

CRYSTAL STRUCTURE OF *DROSOPHILA MELANOGASTER* CYCLE PAS DOMAIN SHOWS A CONFORMATIONAL CHANGE ASSOCIATED WITH CLOCK INTERACTION AND REVEALS NEW LIGAND BINDING

Introduction

The circadian clock controls temporal changes of activity that occur on a 24 hour cycle. Outputs of the circadian clock include the sleep cycle, metabolism, cell growth, and blood pressure. Defects in the circadian clock have been shown to be correlated with a variety of diseases including sleep disorders, metabolic disorders, and cancer^{1,2}.

On a molecular level, the circadian clock is composed of a transcription-translation feedback loop, where in mammals the transcription factors Clock (CLK) and BMAL1 promote the transcription of a variety of proteins including PERIOD (PER) and Cryptochrome (CRY), which re-enter the nucleus and inhibit their own transcription on a 24hr cycle³. In the fruit fly *Drosophila melanogaster* the roles of these transcription factors are taken by their homologs dCLK and dBMAL1, also called Cycle (CYC). These factors instead promote the transcription of dPER and Timeless (TIM)⁴. CYC, BMAL1, and both dCLK and mCLK are composed of a Helix-Loop-Helix domain which binds DNA, and two tandem Per-Arnt-Sim (PAS) domains (Fig. 1).

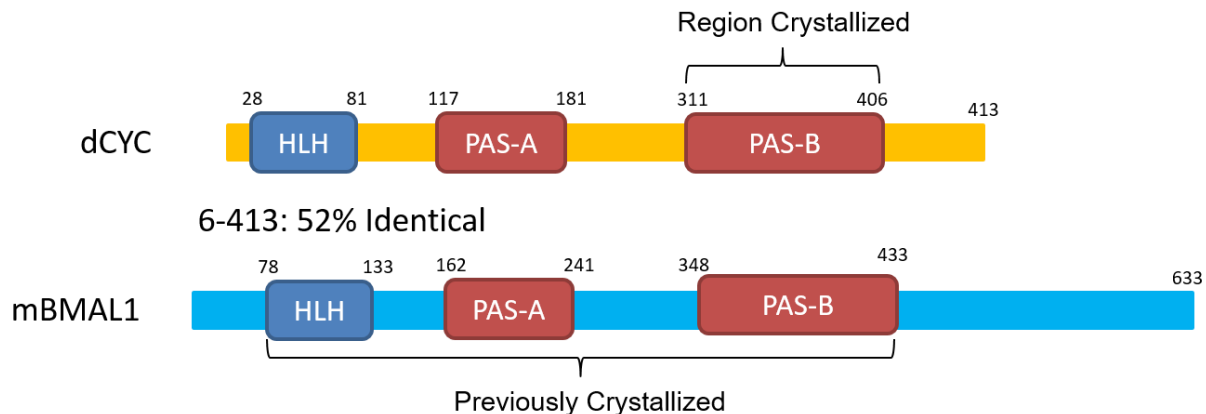


Fig. 1- Schematic of dCYC and mBMAL1 showing regions previously crystallized in mBMAL1 and the region of dCYC crystallized and studied in this paper.

PAS domains can be found as both single and paired (PAS-A/PAS-B) domains, and are often linked with signal transduction proteins. They can function as signal sensors as described above or can function in signal transmission and protein interaction for other domains⁵. Thus PAS domains have been found linked to kinases, ion channels, transcription factors, and phosphodiesterases⁶. Transcription factors with linked PAS domains include the clock proteins CLK and CYC in *Drosophila* along with their mammalian homologs, white-collar proteins and vivid in *Neurospora*, and phototropin in *Arabidopsis*. In both *Arabidopsis* and *Neurospora*, PAS domains with flavin cofactors act as light receptors, but PAS domains without ligands also have an important role by mediating formation of oligomers through variable PAS packings- with changes in PAS interactions often triggered by signal transduction⁷.

dCLK/CYC have different interactions with dPER/TIM than mCLK/mBMAL1 do with their partners mPER/CRY, and no structures of dCLK/CYC have been published. In order to compare the structure of *Drosophila* cycle to the published structure of mCLK/mBMAL1⁸ we have crystallized the PAS-B domain of

Cycle and a tryptophan mutant to 1.23 Å and performed a variety of biochemical assays in order to probe it's behavior.

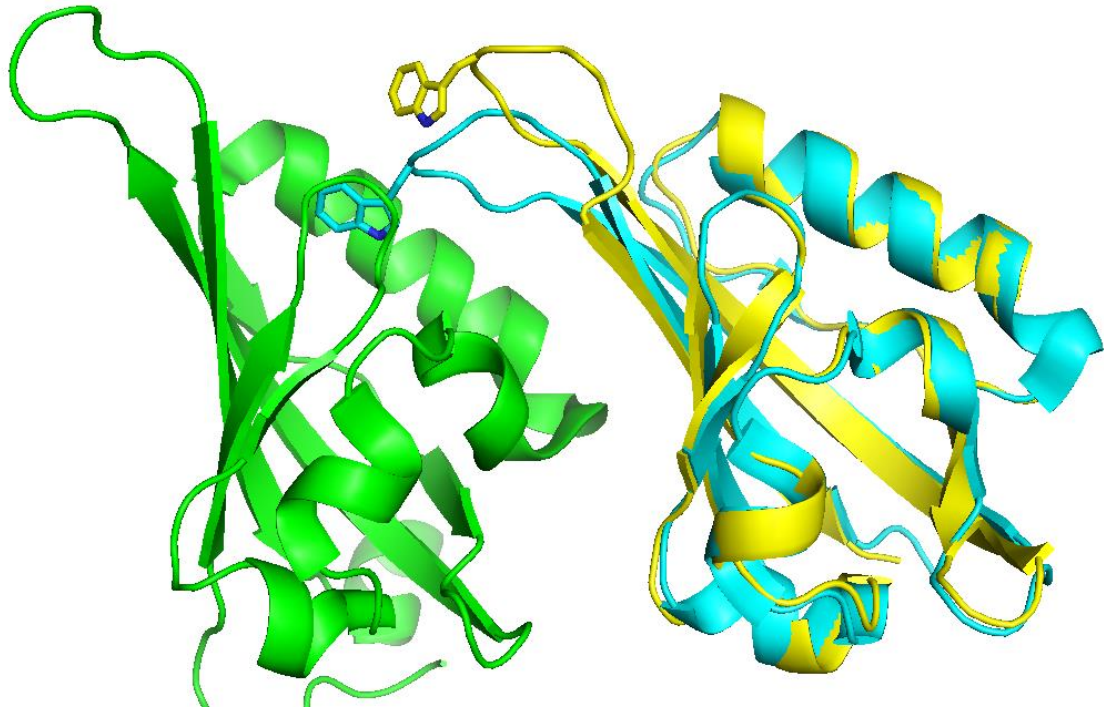


Fig. 2: Alignment of Cycle PAS B with BMAL1 in BMAL1/mCLOCK heterodimer. mCLOCK in Green, BMAL1 in Cyan, Cycle in Yellow.

Structure of dCYC PAS B compared to mBMAL1 PAS B

Overall, the global structure of dCYC is very similar to that of BMAL1. The only main difference is in the loop between $\beta 4$ and $\beta 5$, which in BMAL1 is curved down towards mCLK to slot into a hydrophobic groove, whereas in dCYC it is straight up in line with the β sheets. This change in loop conformation also propagates into the β sheets, causing a small curvature that is not present in dCYC (Fig. 2). There are several changes on dCYC from the published mBMAL1 structure in residues that may interact with CLK. One of the hydrophobic phenylalanine residues on BMAL1

which appears to slot into a hydrophobic “groove” in mCLK, F421, is instead a charged arginine in dCYC, potentially destabilizing this interaction with dCLK. In addition, T437 of BMAL1, which in the BMAL mCLK structure appears to be too far away from mCLK to interact to any significant degree, is instead a lysine residue in dCYC, providing charge and length that may be needed to “reach” over to dCLK and interact.

dCYC	311	f isr h sge g k f l f idq r at l v i g f l p q e il g t s f y e y f h n e d i a a l m e s h	360
mBMAL1	340	y v s r h a i d g k f v f v d q r a t a i l a y l p q e l l g t s c y e y f h q d d i g h l a e c h	389
dCYC	361	k m v m q v p e k v t t q v y r f r e c k d n s y i q l q s e w r a f k n p w t s e i d y i i a k n s	410
mBMAL1	390	r q v l q t r e k i t t n c y k f k i k d g s f i t l r s r w f s f m n p w t k e v e y i v s t n t	439
dCYC	411	v f l	413
		.	
mBMAL1	440	v v l	443

Fig. 2-Alignment of dCYC and mBMAL1 PAS B using EMBOSS Water. Key mCLK interacting residues mentioned in the text highlighted in blue. Key pocket residues mentioned highlighted in red.

In addition to these differences in sequence, there are several sidechains that appear to be in different conformations in this dCYC structure compared to the published mBMAL1 structure, potentially showing how the sidechains move to stabilize interactions with CLK compared to when CYC/BMAL1 is alone. One of these residues is F423 of BMAL1, which appears to reach out into the groove in mCLK in the dimer structure, but in dCYC is instead at a 90 degree angle. Some other residues that may change conformation to interact with CLK include K398 and D432 (both are glutamic acid residues in CYC) (Fig. 2 and 3).

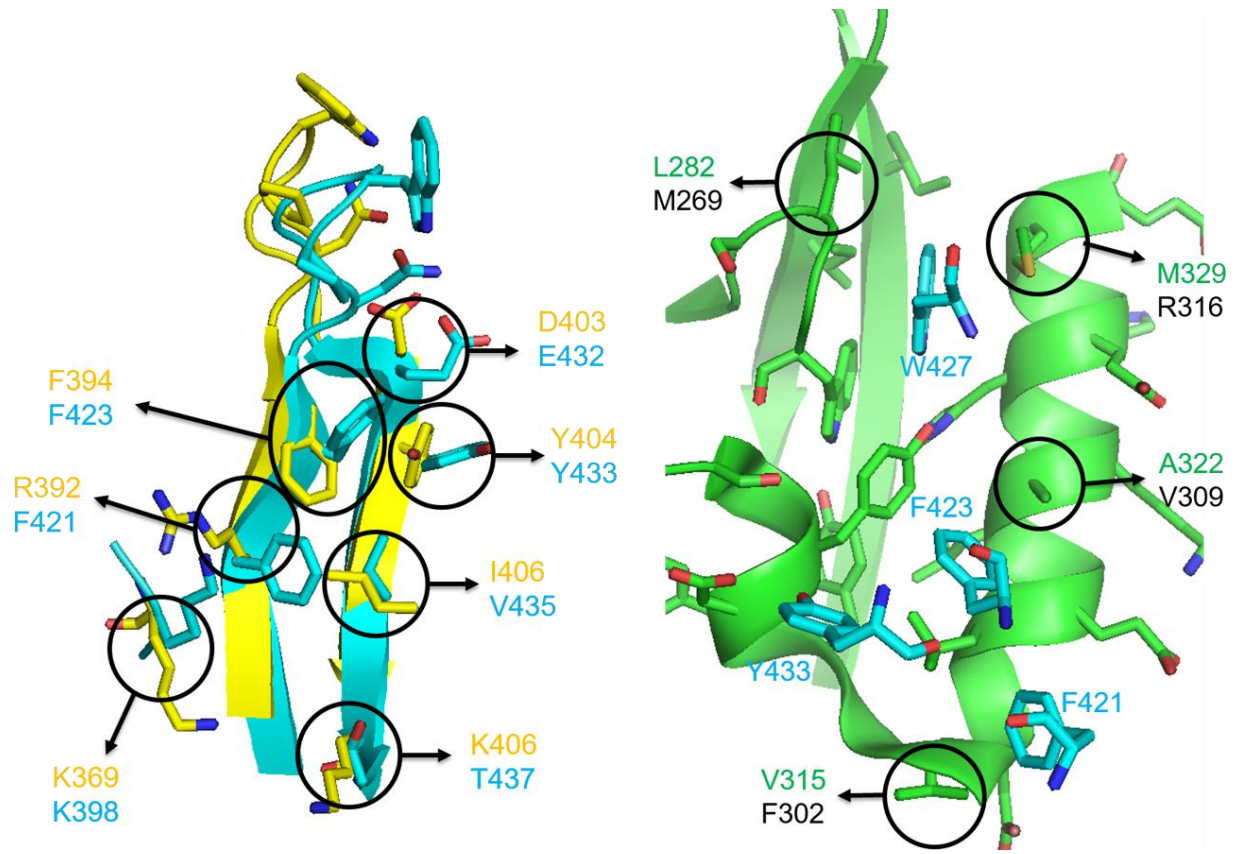


Fig. 3-Alignment of CYC with BMAL1 showing residues that may interact with clock and possible changes. (a) Shows CYC in Yellow, BMAL1 in Cyan. (b) Shows mCLOCK in green and BMAL1 residues in cyan for orientation with residues that are altered in dCLK in black.

Some of these changes in conformation and sequence may manifest in a slight difference in the charged surface calculated for these structures. The mCLK interacting face of BMAL1 appears to have a larger positive surface area compared to that of dCYC. In addition, there is a small “pocket” of neutral/negative surface on this face that is not present in the dCYC structure. This could be a significant difference given that the face of mCLK that binds BMAL1 is highly negative (Fig. 4).

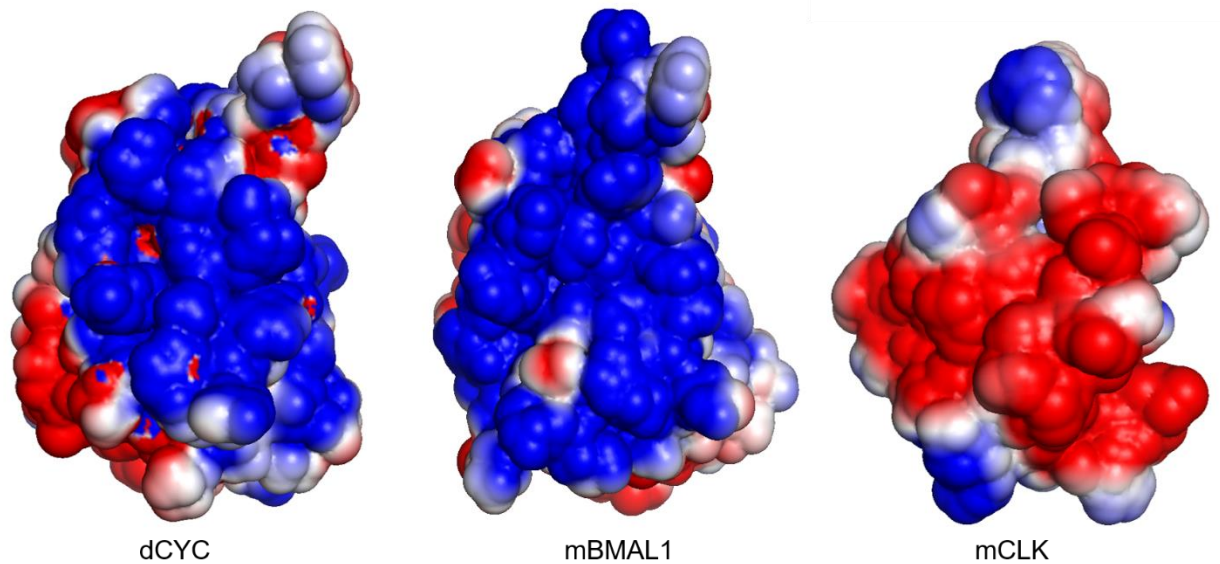


Fig. 4-Electrostatic potentials of dCYC, mBMAL1, and mCLK PAS B domains. dCYC and mBMAL1 show the side interacting w/mCLK. mCLK shows the side interacting w/ mBMAL1. The colors are ramped from red negative potential ($-5kT/e$) to blue positive potential ($5kT/e$).

Mutations in dCLK vs. mCLK

dCLK has several key interacting residues mutated from the homologous amino acids in the mCLK BMAL1 structure that may contribute to changes in dCLK/CYC interaction compared to mCLK/mBMAL1 in addition to structural differences explained above. The “groove” in mCLK which seems to be key for interaction with BMAL1 is the site of three differences between the mCLK and dCLK amino acid sequences. In mCLK two residues next to the key loop W427 on mBMAL, M329 and L282, have been mutated to an arginine and leucine respectively in dCLK. These changes potentially make the insertion of a tryptophan residue as in the mBMAL1/mCLK less favorable when looking at dCYC/dCLK. The change of V315 to a phenylalanine in dCLK has the potential to introduce some pi stacking interactions with the phenylalanine residues on dCYC. A small change of A322 in

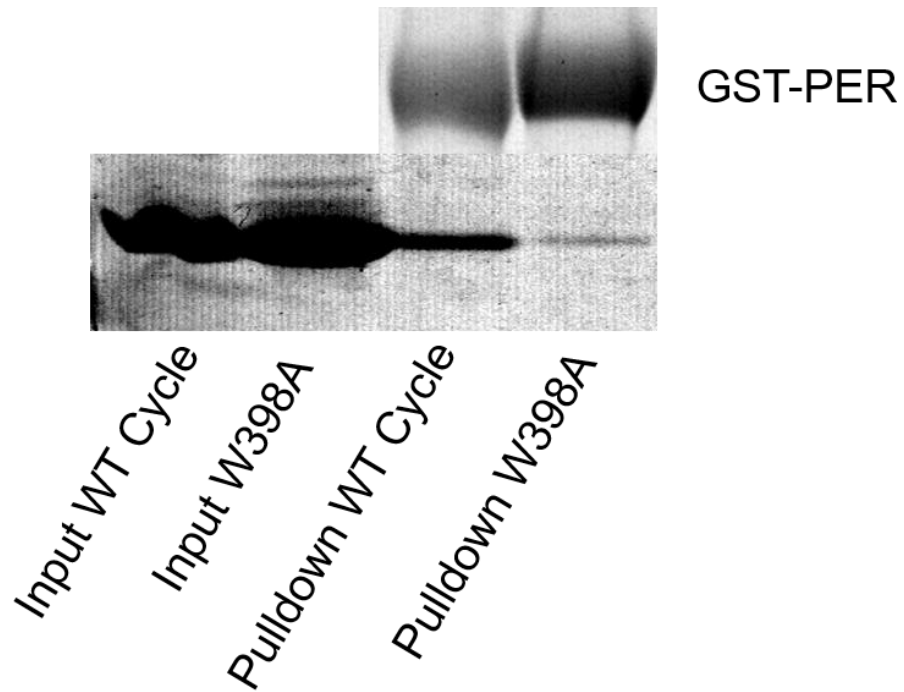


Fig. 6-Pulldown of WT CYC PAS B and W398A mutant by GST-PER (PAS AB)

In order to test the behavior of the WT and W398A proteins, pull-downs were performed with GST-dPeriod (PAS-AB). In this assay, binding of Cycle PASB was observed with dPER to a greater extent with the WT than with W398A, suggesting that this residue not only plays a role in binding to dCLK, but also may play a role in dCLK/CYC binding to PER/TIM.

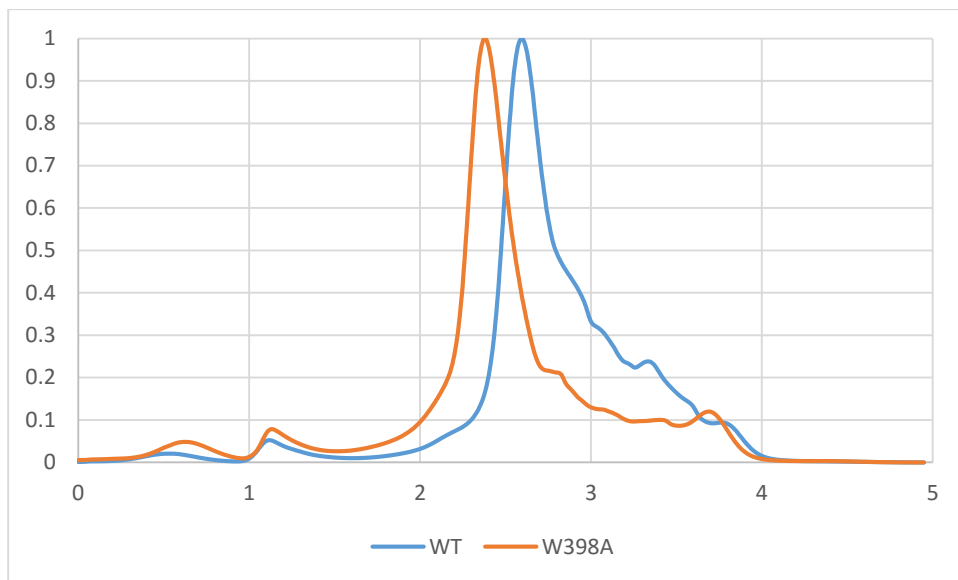


Fig.7-Analytical SEC Chromatography of WT Cycle PAS B (blue) and W398A (Orange) nickel column elutions.

W398A Mutant Changes Homodimer Conformation

During purification, the W398A mutant eluted earlier than the WT on size exclusion chromatography (Fig. 7), suggesting a different conformation or larger oligomeric state of the mutant compared to the WT. In order to elucidate the cause of this shift, pulsed dipolar electron spin resonance (ESR) spectroscopy (PDS) was performed after labeling the proteins using a native cysteine residue C379 (there is only one cysteine in Cycle PAS B) and MTSL nitroxide spin label. By using double electron-electron resonance (DEER), distances between labels can be obtained by observing the strength of the dipolar coupling between the unpaired spins. Both WT and W398A showed a dipolar coupling signal, suggesting that both proteins were dimerizing to some extent. However, the distances measured differed between the two, indicating a change in the mode of dimerization.

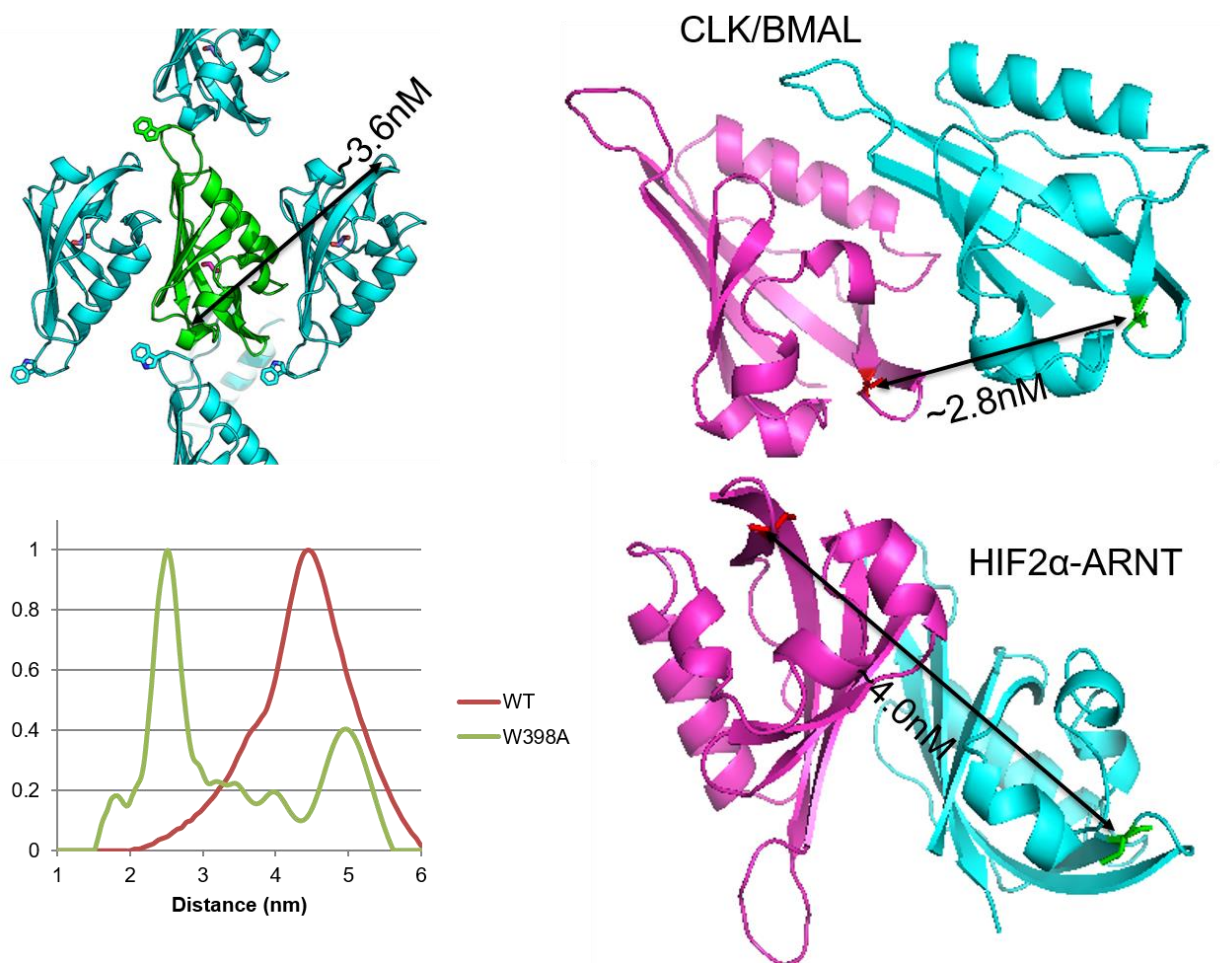


Fig.8 Distance distribution in Cycle PAS B dimer. (a)Arrangement of Cycle PAS B in the crystal. (b) Distance distributions calculated from PDS of MTSL-labeled Cycle PAS B. WT in Blue, W398A in Purple. Curves normalized for comparison. (c), (d) Orientation of Cycle Pas B if aligned with the PAS B domains of mCLK/mBMAL1 as in PDB 4F3L (c) or Hif-2 α /ARNT as in 3F1N and the calculated distance between C379 residues.

The WT distance distribution is centered at around 4.5nm, while W398A had a peak distance of ~2.7nm. Neither distance matched the ~3.6nm distance seen in crystal packing, so alternate conformations were sought that could explain the distances measured. By modeling our structure of Cycle Pas-B using other solved PAS dimers as a guide, we found that the W398A distance matches well with a dimerization motif

similar to the PAS-B domains of mCLK/BMAL1 (“face-to back”)(PDB 4F3L)⁸ whereas the WT distance matches well with a dimerization similar to that similar to the Hif2 α -ARNT heterodimer (inverted back to back) (PDB 3F1N)¹⁰. Overall these results suggest that as well as mediating CLK/CYC interactions and possible CYC/PER interactions, the conserved tryptophan residue corresponding to W398 on CYC can also mediate homodimerization (Fig. 8).

Table 1. Data collection and refinement statistics for crystal structures described in this study.

	WT Cycle PAS B w/Ethylene Glycol	Cycle PAS B W398A w/Ethylene Glycol	Cycle PAS B W398A w/Glycerol	Cycle PAS B W398A w/Water
PDB ID	5F5Y	5F68	5F69	5F6A
Data Collection				
Space Group	C 1 2 1	C 1 2 1	C 1 2 1	C 1 2 1
Cell dimensions-				
a,b,c (Å)	72.71,44.52,38.44	73.31,44.17,38.57	73.30,44.40,38.50	73.00,44.52,38.19
α,β,γ (°)	90.00,116.36,90	90.00,115.16,90	90.00,114.75,90	90.00,115.32,90
Resolution (Å)	36.76-2.20	36.77-1.23	36.94-1.37	34.52-1.93
Rmerge	0.07	0.1	0.09	0.1
$\langle I/\sigma I \rangle$	5.7 (at 2.20Å)	1.81 (at 1.23Å)	1.29 (at 1.37Å)	1.19 (at 1.92Å)
Completeness (%)	97.2	92.9	98.2	78.2
Refinement				
R _{Free}	.198,.245	.180,.196	.170,.198	0.223,.250
Rfree test set	557 reflections (11.68%)	2000 reflections (7.73%)	1856 reflections (8.61%)	612 reflections (10.06%)
Wilson B-Factor (Å ²)	26.4	8.1	13.3	22.3
Anisotropy	0.573	0.221	0.28	0.589
Total number of atoms	903	963	1000	881
Average B, all atoms (Å ²)	33	14	20	32
Ramachandran outliers	0%	0%	0%	0%
Sidechain outliers	2.10%	1.10%	1.10%	1.10%

dCYC PAS B Has an Internal Pocket That Can Be Occupied by Ethylene Glycol or Glycerol

Upon investigation of the electron density of dCYC, it was discovered that there was significant unassigned density in the internal pocket of the PAS-B domain of both WT and W398A proteins. This density was assigned as ethylene glycol, which was used as the cryoprotectant for both proteins (Fig. 9a). This assignment was further supported by a significant growth in this electron density when glycerol instead was used as a cryoprotectant for W398A crystals-suggesting that glycerol was taking the place of the ethylene glycol in the pocket (Fig. 9b). Crystallization of a protein without anything in the pocket was complicated by the fact that Cycle PasB was unstable without the presence of glycerol. However, by using glucose as a cryoprotectant and letting the crystals soak for ~15 minutes before exposure to x-rays, a structure was solved with much smaller density in the pocket, which could be assigned to water (Fig. 9c). This finding confirms our assignment of the density as ethylene glycol when EG is used as a cryoprotectant and glycerol when glycerol is used as a cryoprotectant.

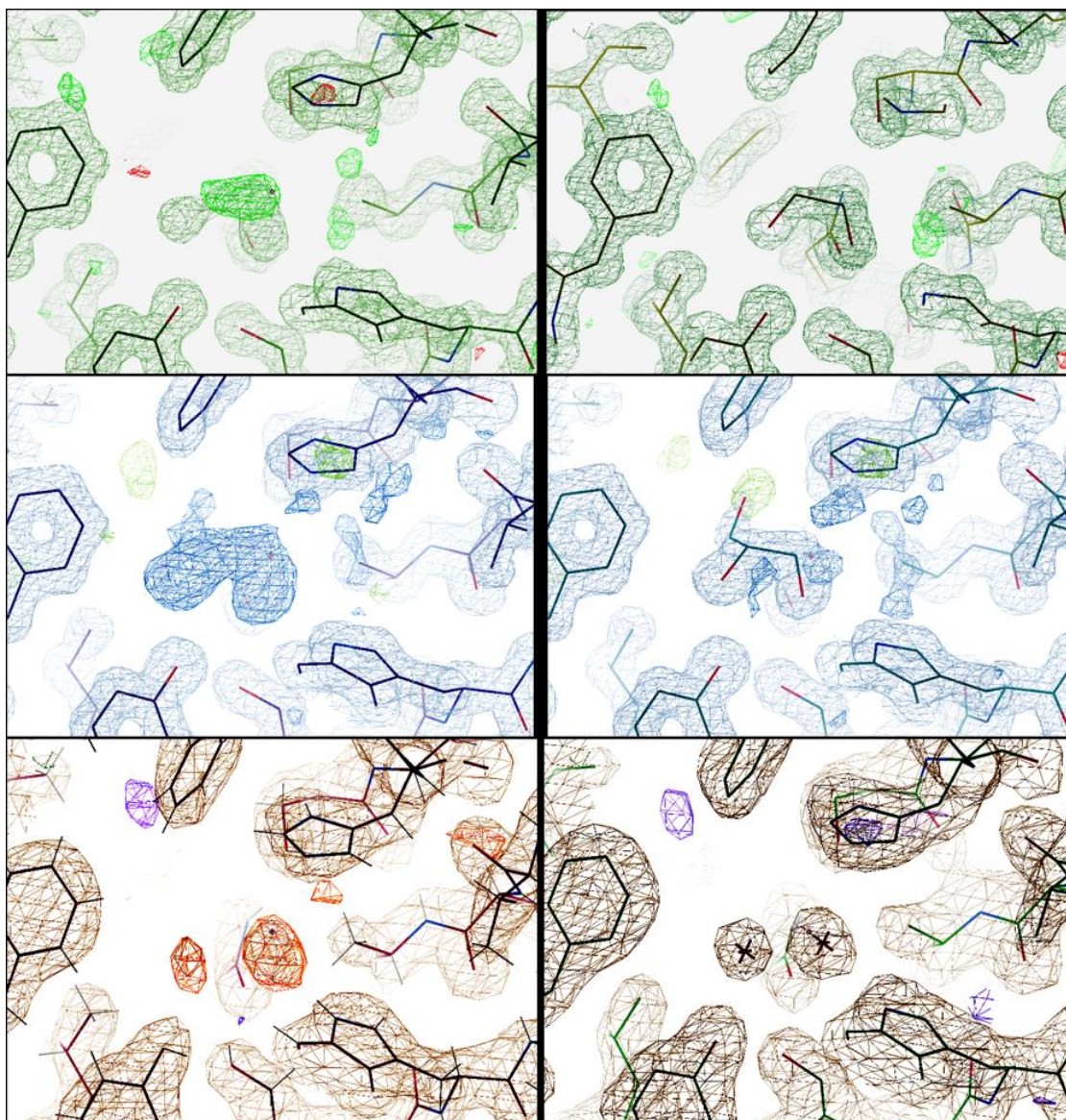


Fig. 9-Electron density of the pocket without (1) and with (2) ligand modeled for structures of Cycle PAS B binding ethylene glycol (a), glycerol (b), and water (c).

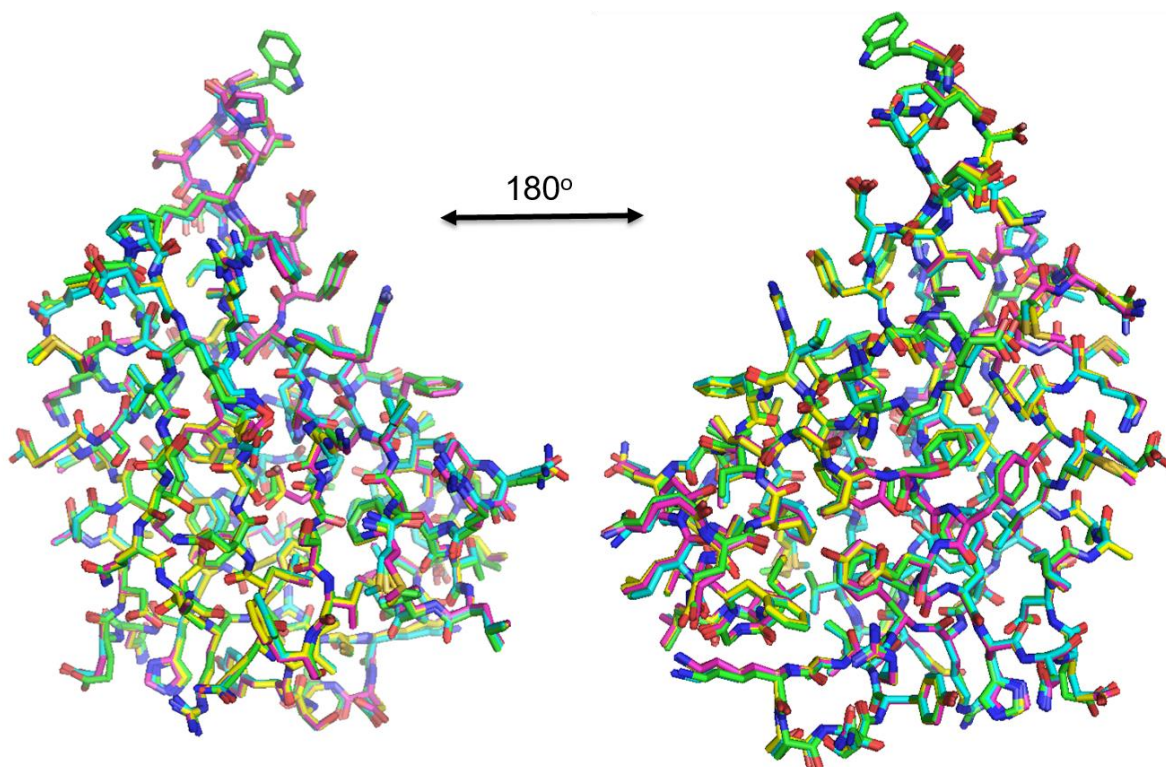


Fig. 10 Alignment of four Cycle PAS B structures: WT w/ Ethylene Glycol in Green, W398A with EG in Magenta, W398A w/ Glycerol in Yellow, W398A w/ Water in Cyan.

Although the difference in density in the pocket of Cycle PAS B is clearly visible in the different structures, no other significant changes were found (Fig. 10). The pocket that glycerol/EG binds in can generally be described as having a hydrophobic side (Fig. 11b), consisting of residues F348, F344, F311, and F321, and a hydrophilic side, (Fig. 11a), consisting of residues Y375, S389, S313, H315, and N409. The EG molecule seems to have the –OH groups pointed towards the hydrophilic side, while the carbon backbone is more situated near the hydrophobic side. In glycerol, the additional carbon and –OH groups are pointed towards S313. In addition, intermediate residues A407 and W391 are located off to the side of the ligands (Fig. 11a).

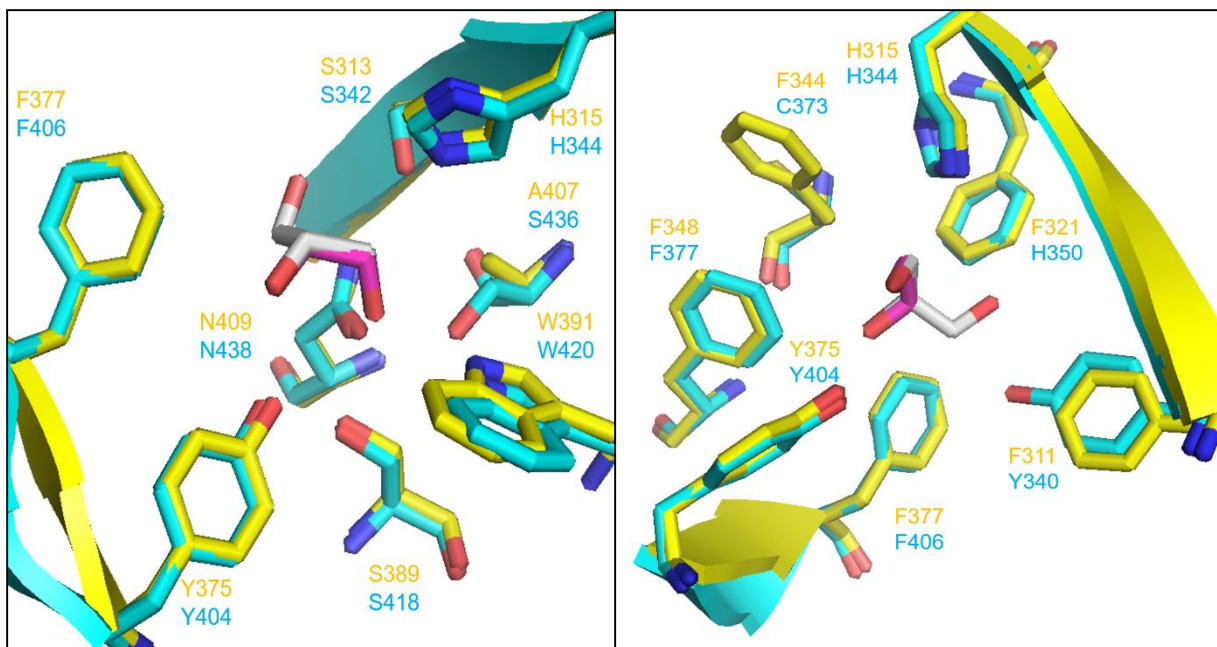


Fig. 11-Overlay of residues surrounding Ethylene Glycol (Magenta) and Glycerol (Grey) in Cycle PAS B (Yellow) and alignment with BMAL1. (a) Shows one side with more hydrophilic residues and (b) shows the opposite orientation with more hydrophobic residues.

Discussion of Pocket and Ligand Binding

In an attempt to determine if any other molecules could bind in the pocket, perhaps suggesting a physiological role for binding, thermal melt experiments were carried out with a variety of common metabolites and ligands that are found *in vivo*, using Sypro orange as a reporter fluorophore and Biolog metabolite plates to screen a total of 495 small molecules. None of these provided significant stabilization of cycle melting temperature, though both glycerol and ethylene glycol did (data not shown). Of note is the fact that high concentrations of glycerol and ethylene glycol were needed to see this stabilization, perhaps suggesting that the stabilization seen is from global solvation effects and not binding in the pocket-and that binding of a ligand in the pocket of Cycle PAS B does not provide sufficient stabilization effects to register

using this assay. In addition, crystals were soaked with a variety of small molecules, including ribose, arabinose, pyruvate, and $\text{Zn}(\text{SO}_4)_2$, with no change in electron density in the crystal structures.

PAS domains can bind cofactors either covalently or non-covalently, and the function of the cofactor can vary depending on the signal that the protein needs to carry. Some PAS domains use their cofactor directly detect a signal; for example, oxygen sensing PAS domains which bind heme or light sensing domains which bind flavin. Other PAS domains receive a signal in the form of ligand binding, which then is used to change its function, such as the CitA citrate sensor binding citrate, DcuS binding malate, or DctB binding succinate⁵. A study of PAS domain ligand binding found that most are bound in the same place in the protein, a conserved cleft formed by a beta sheet and two alpha helices¹¹. This is where glycerol/EG is found in our structure.

Although the heterodimer of mCLK/BMAL1 also contained glycerol in the buffer, and BMAL1 has an almost entirely conserved pocket to CYC, no density was observed in the pocket of BMAL1. It could be that the divergent residues, F311, F344, and A407 in CYC (Y340, C373, and S436 in BMAL1) cause a change in glycerol binding, or that binding to CLK in the dimer structure prevents glycerol from binding in the pocket. However, the authors describe cryoprotecting the protein by stepwise transfer in solutions of PEG 3350 and xylitol, which likely reduced the concentration of glycerol in solution enough to remove the ligand from the crystal.

Of note is the fact that the PAS-B of the Hif-2 α protein (33% identical to CYC pas B) has also been found to bind ethylene glycol molecules¹⁰, although glycerol

binding has not been identified, even in a Hif-1 α structure (35% identical) with 2% glycerol in the buffer¹². In addition, the heterodimer of Hif-2 α in this structure, ARNT, is even more homologous to CYC than Hif-2 α (38% identical), but shows no binding to ethylene glycol. However, there are several key residues surrounding the pocket that are not conserved in these proteins, including a tryptophan residue (W391 in CYC) positioned next to the proposed Ethylene glycol/glycerol binding site. The absence of this residue in Hif-2 α makes the pocket much larger, allowing for the binding of two ethylene glycol molecules, and this pocket has been shown to bind a variety of small molecules found in screens^{10,13}. Of the pocket residues which are divergent between BMAL1 and CYC, Hif2 α is also divergent in CYC residues F344 and A407 (tyrosine and cysteine in Hif2 α).

One other PAS domain in the PDB has been deposited with a glycerol ligand bound, the methyl-accepting chemotaxis protein from *Vibrio parahaemolyticus* (PDB ID 2QHK). However, the electron density surrounding the glycerol molecule has significant unassigned density casting doubt on the validity of the assignment (Fig. 12). In addition, the methyl-accepting chemotaxis protein contains no significant structural or sequence similarity to CYC, so any binding of glycerol seen is likely to be of a different mode. No paper has been published linked to this structure, so it is not known if any further experiments have been done to confirm this assignment.

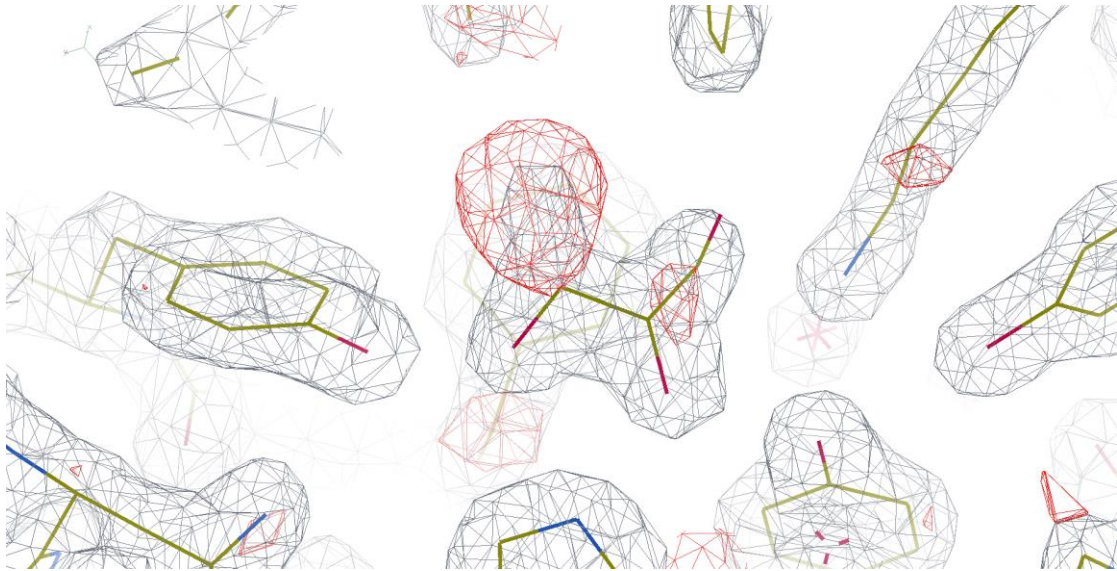


Fig. 12: Structural model and electron density from pocket and glycerol assignment in methyl-accepting chemotaxis protein from *Vibrio parahaemolyticus* (PDB ID 2QHK). 2mFo-DFc density shown in gray mesh. mFo-DFc density shown in red mesh. Electron-density map generated by the Uppsala Electron Density Server.

It seems very unlikely that EG is the physiological ligand of dCYC in the cell, since it has no known metabolic role. However, the presence of glycerol in the pocket of Cycle PAS-B opens up some intriguing possibilities. Interestingly, BMAL1 has been found to play a role in glycerol metabolism and brown adipose tissue formation^{14,15}. During periods of energy shortage, the breakdown of lipids from adipose tissue to free fatty acids (FFAs) and glycerol (lipolysis) becomes an energy source for the cell. This process has been found to be mediated by CLK and BMAL1 in mice, with the timing of glycerol levels severely altered by BMAL1 mutations. This is thought to be the cause of reduced circadian production of adipose triglyceride lipase and hormone-sensitive lipase. However, with the possible discovery of glycerol binding by CYC, the intriguing possibility of feedback from cell glycerol/FFA levels directly to the circadian clock transcription factors CLK and BMAL1 is raised.

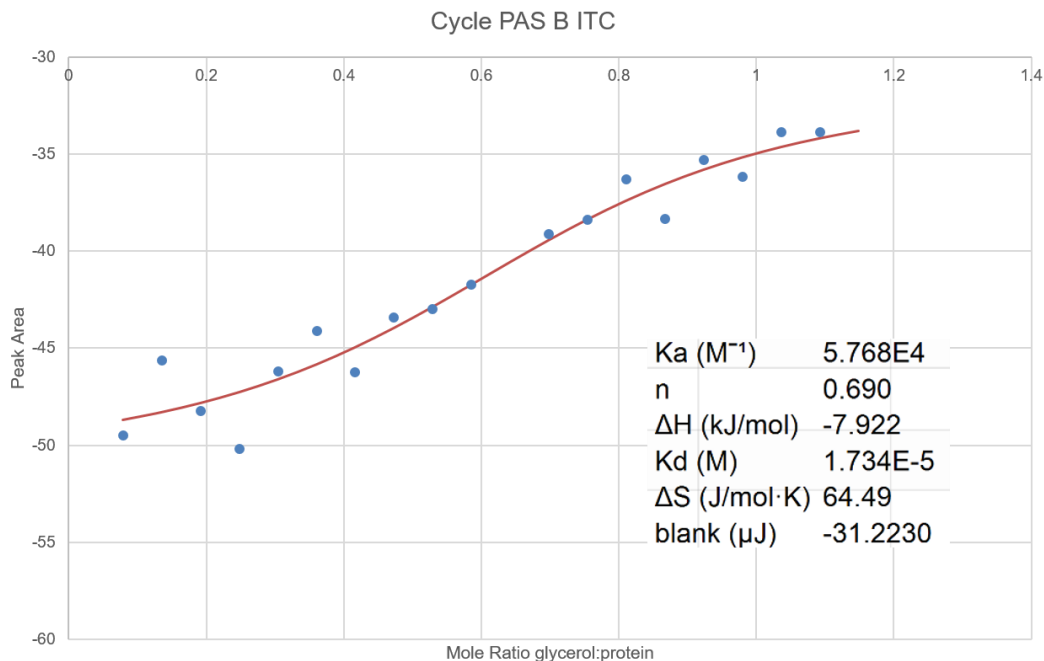


Fig. 13: Iso-thermal-calorimetry data for WT Cycle PAS B and the addition of glycerol, with data shown in blue and model fitted shown in red.

Isothermal titration calorimetry (ITC) was used to calculate the binding constant of glycerol with WT Cycle PAS B, and a K_d was found to be $\sim 17\mu M$ (Fig. 13). Levels of glycerol in mouse serum have been found to be as high as $7mM^{15}$, with similar levels found in fly larvae¹⁶, meaning that binding of glycerol might not have to be extremely tight or specific in order to provide some feedback. This possibility is further supported by the fact that feeding levels of flies has been shown to alter circadian activity¹⁶.

Conclusion

Transcription factors Cycle and Clock are important regulators of the circadian clock in *Drosophila melanogaster*. Our crystal structure of the PAS B domain of

Cycle shows several differences between Cycle and the mammalian homolog mBMAL1 that could be relevant in further assays see a difference in behavior between the two. In addition, SEC chromatography, PDS measurements, and pulldowns by dPER all show a difference between WT and W398A Cycle PAS B, further emphasizing the importance of a conserved tryptophan on the circadian clock by showing that this residue also mediated Cycle homodimerization and binding to dPER in addition to regulating binding with CLK.

Our structure showed a binding of glycerol into the pocket of Cycle PAS B. This is the first evidence of ligand binding by CYC, and glycerol is a novel ligand for PAS domain binding. Physiological relevance of this binding remains to be investigated, perhaps by finding a mutant of CYC which does not bind glycerol and testing its activity *in vivo*.

Methods

Growth and Purification-CYC PAS B cDNA was cloned from a plasmid ordered from the Drosophila Genomics Resource Center. It was cloned into pET28 using the sites NdeI and XhoI. This plasmid was expressed in BL-21(DE3) cells. The cells were grown till density at $A_{600} \sim .8$, induced with .4mM IPTG, and grown overnight at room temperature (~25 degrees). Cells were harvested and frozen at -80 degrees C.

For purification, cells were lysed by sonication in lysis buffer containing 150mM NaCl, 50mM Tris pH 8, and 5mM imidazole. Insoluble cell debris was removed by centrifugation at 48,384g for 35min. The clarified cell lysate was applied

to Nickel NTA Agarose Beads (Gold Biotechnology) equilibrated with lysis buffer and the protein was eluted with elution buffer 150mM NaCl, 50mM Tris pH8, 200mM Imidazole, and 40% glycerol. Protein was further purified using a Superdex75 gel filtration column with gel filtration buffer (GFB) 10% glycerol, 150mM NaCl, 50mM Tris pH8, 5mM DTT. Purified protein was flash frozen in liquid nitrogen and stored at -80 degrees C.

GST-PER (PAS AB) was expressed as previously described⁹. Protein was purified in the same method as CYC PAS B above, except a Superdex300 gel filtration column was used.

Crystallization and Data Collection- Cycle crystals were grown at room temperature in hanging drop vapor diffusion crystal trays (Hampton). The reservoir solution consisted of 75mM Tris pH 7, 100mM (NH₄)₂SO₄ and was mixed with the protein at ~2mg/mL in a 1:1 ratio. Crystals of W398A formed more reliably and larger than those of WT. Crystals formed overnight and reached a size of ~5um. For the WT structure, 40% ethylene glycol was used as a cryoprotectant. For W398A, either 40% ethylene glycol, 40% glycerol, or 500mM glucose was used as a cryoprotectant.

Data was collected at Cornell High Energy Synchrotron Source (CHESS) at Cornell University in Ithaca, NY. The diffraction images were indexed, merged, and scaled using HKL2000, and refined using a mixture of automated refinement from phenix.refine and manual refinement using Coot.

Site-directed Mutagenesis-Site directed mutations were performed as previously described¹⁷ and confirmed by DNA sequencing.

Spin labeling and DEER measurements-Protein samples were labeled using MTSL by incubating on column overnight at 4 degrees before elution. Samples were concentrated and put in 35% glycerol before data collection. PDS was used to determine the distance between dimers as previously described. Protein concentrations of ~100 μ M dimer were prepared and the dipolar evolution at 17.35 Ghz was measured on a home-built 2D Fourier-transform-ESR instrument using four-pulse double-electron electron resonance with a 16-ns pump pulse¹⁷.

Pulldowns By GST-PER PAS AB-500 μ L of GST-PER PAS AB was incubated with 5 μ L of Glutathione Sepharose 4 Fast Flow resin (GE Healthcare) for 20 minutes before washing 3x with 500 μ L of GFB by spinning on a tabletop centrifuge (VWR) before removing excess liquid. 200 μ L of .25mg/mL Cycle PAS B was then added and incubated for 20min before washing 4x with 500 μ L of GFB. 10 μ L of SDS sample buffer was added and bands were visualized by SDS-PAGE and coomassie staining.

Iso-thermal Calorimetry- Nano-ITC LV (TA instruments) was used to run samples of 200 μ L of 300 μ M Cycle PAS B in 1M Sucrose, 50mM HEPES pH 8.0, 150mM NaCl. Heats of injection of 2.5 μ L 1mM Glycerol in the same buffer were recorded and the data was fit by the software provided with the instrument using an independent model and a constant blank. A control experiment of injecting 1mM glycerol into buffer was used as a blank.

Size-exclusion chromatography-Data shown is from running purified Cycle PAS B (WT and W398A) in column Superdex 200 10/300 GL using GFB in an AKTA prime.

Structure modeling-Structure figures for this paper were made using Pymol. Electrostatic potential images were made using the APBS plugin in Pymol. Electron density images were made using COOT.

REFERENCES

1. Karatsoreos, I. N. Effects of circadian disruption on mental and physical health. *Curr. Neurol. Neurosci. Rep.* **12**, 218–225 (2012).
2. Bersten, D. C., Sullivan, A. E., Peet, D. J. & Whitelaw, M. L. bHLH–PAS proteins in cancer. *Nat. Rev. Cancer* **13**, 827–841 (2013).
3. Partch, C. L., Green, C. B. & Takahashi, J. S. Molecular architecture of the mammalian circadian clock. *Trends Cell Biol.* **24**, 90–9 (2014).
4. Crane, B. R. & Young, M. W. Interactive Features of Proteins Composing Eukaryotic Circadian Clocks. *Annu. Rev. Biochem.* **83**, 191–219 (2014).
5. Henry, J. T. & Crosson, S. Ligand-Binding PAS Domains in a Genomic , Cellular , and Structural Context. (2011). doi:10.1146/annurev-micro-121809-151631
6. Diensthuber, R. P., Bommer, M., Gleichmann, T. & Moglich, A. Full-Length Structure of a Sensor Histidine Kinase Pinpoints Coaxial Coiled Coils as Signal Transducers and Modulators. *Structure* **21**, 1127–1136 (2013).
7. Moglich, A., Ayers, R. A. & Moffat, K. Structure and Signaling Mechanism of Per-ARNT-Sim Domains. *Structure* **17**, 1282–1294 (2009).
8. Huang, N. A. *et al.* Crystal Structure of the Heterodimeric CLOCK:BMAL1 Transcriptional Activator Complex. *Science (80-.)*. **337**, 189–194 (2012).
9. King, H. A., Hoelz, A., Crane, B. R. & Young, M. W. Structure of an Enclosed Dimer Formed by the *Drosophila* Period Protein. *J. Mol. Biol.* **413**, 561–572 (2011).
10. Scheuermann, T. H. *et al.* Artificial ligand binding within the HIF2 α PAS-B domain of the HIF2 transcription factor. *Proc. Natl. Acad. Sci. U. S. A.* **106**, 450–5 (2009).
11. Ayers, R. A. & Moffat, K. Review Structure and Signaling Mechanism of Per-ARNT-Sim Domains. 1282–1294 (2009). doi:10.1016/j.str.2009.08.011
12. Cardoso, R. *et al.* Identification of Cys255 in HIF-1 α as a novel site for development of covalent inhibitors of HIF-1 α /ARNT PasB domain protein-protein interaction. *Protein Sci.* **21**, 1885–1896 (2012).
13. Wu, D., Potluri, N., Lu, J., Kim, Y. & Rastinejad, F. Structural integration in hypoxia-inducible factors. *Nature* **524**, 303–308 (2015).

14. Nam, D. *et al.* The adipocyte clock controls brown adipogenesis through the TGF- β and BMP signaling pathways. **16**, 1835–1847 (2015).
15. Shostak, A., Meyer-Kovac, J. & Oster, H. Circadian regulation of lipid mobilization in white adipose tissues. *Diabetes* **62**, 2195–2203 (2013).
16. Lee, G. & Park, J. H. Hemolymph sugar homeostasis and starvation-induced hyperactivity affected by genetic manipulations of the adipokinetic hormone-encoding gene in *Drosophila melanogaster*. *Genetics* **167**, 311–323 (2004).
17. Samanta, D., Borbat, P. P., Dzikovski, B., Freed, J. H. & Crane, B. R. Bacterial chemoreceptor dynamics correlate with activity state and are coupled over long distances. *Proc. Natl. Acad. Sci.* **2**, 2455–2460 (2015).

CHAPTER 3

MUTATIONAL STUDIES OF *DROSOPHILA MELANOGASTER* *CRYPTOCHROME MUTANTS SHOW ROLE FOR HISTIDINE RESIDUE AND* *EMPASIZE IMPORTANCE OF TRYPTOPHANS FOR ELECTRON TRANSPORT*

Introduction

Cryptochromes are proteins closely related to photolyase (PL) DNA repair enzymes, and are involved in the circadian clock of both mammals and insects¹⁻³. Photolyase binds a FAD that carries out DNA repair by donating an electron through cyclic electron transfer and breaking a DNA linkage. CRYs contain a domain very similar to PLs, termed the photolyase homology domain (PHD), and also bind FAD, but they also carry an additional variable length extension on the c-terminus called the c-terminal tail/extension (CTT or CTE). The CTT forms a helix that binds in the active center groove alongside the flavin, analogous to where substrate DNA lesions bind in PLs¹⁻³ (Fig. 1).

CRY/PL type proteins are usually into classes, depending on their function and presence of a CTE. These classes include 6-4 PLs, cyclobutane pyrimidine dimer (CPD) PLs, CRY-DASH proteins, which have a CTE but also some DNA repair activity, and CRYs. Cryptochromes can further be divided into type I CRYs, such as *Drosophila* CRY and *Arabidopsis thaliana* CRYs (AtCRYs) which have some light-sensing activity, and mammalian, or type II CRYs, which do not¹⁻³.

In the fruit fly *Drosophila melanogaster*, *Drosophila* CRY (dCRY) functions as the primary light sensing protein involved in entrainment of the circadian clock. In

Drosophila, the translation of genes encoding proteins Timeless (TIM) and Period (PER) are upregulated by the transcription factors Clock (CLK) and Cycle (CYC). After translation, TIM and PER dimerize, enter the nucleus, and inhibit CLK/CYC, thus downregulating transcription *tim* and *per*. This transcription-translation feedback loop (TTFL) occurs on a ~24 hour cycle, and composes the core clock⁴⁻⁶. dCRY entrains the clock to the day/night cycle by binding to TIM in a light-dependent manner and targeting it for degradation through recruitment of the E3 ubiquitin ligase JET⁷⁻¹¹, while dCRY itself is degraded by the ubiquitin ligase BRWD3¹². The light signal is sent by dCRY through a reduction in the redox state of its FAD cofactor accompanied by conformational changes in its CTE. Changes in this CTE are needed for light-dependent interactions with TIM and JET^{11,13-15}.

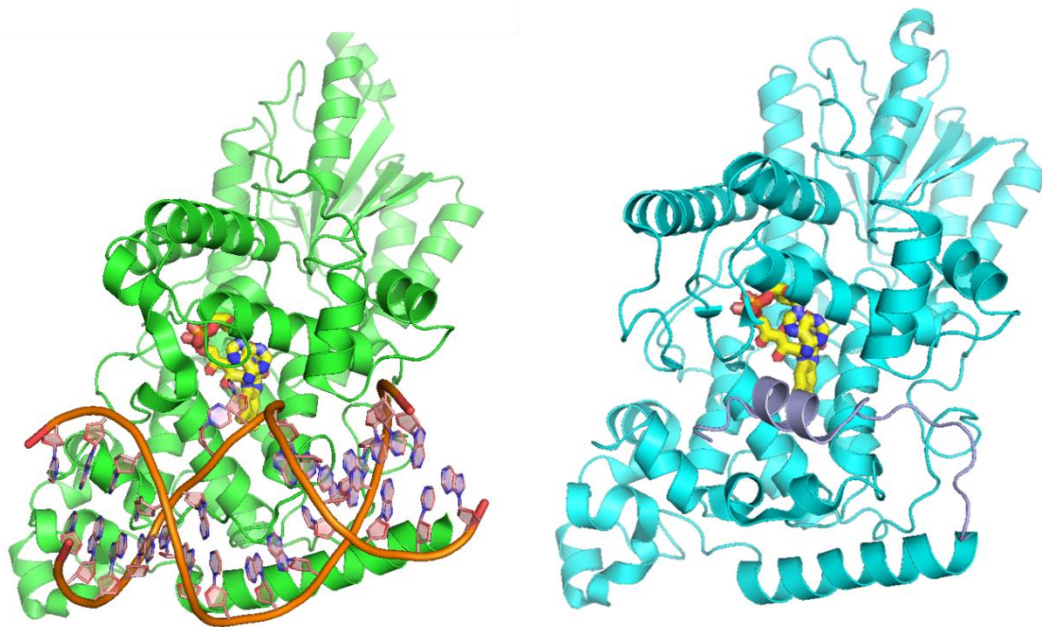


Fig. 1: Structural similarities between cryptochrome and photolyase. *DmCry* (right) and *Dm(6-4)* photolyase (left) have similar 3-D structure and the C-terminal tail in CRY occupies the same groove as the DNA in photolyase. FAD is yellow, DNA is Orange, CTT of dCRY is Light Blue.

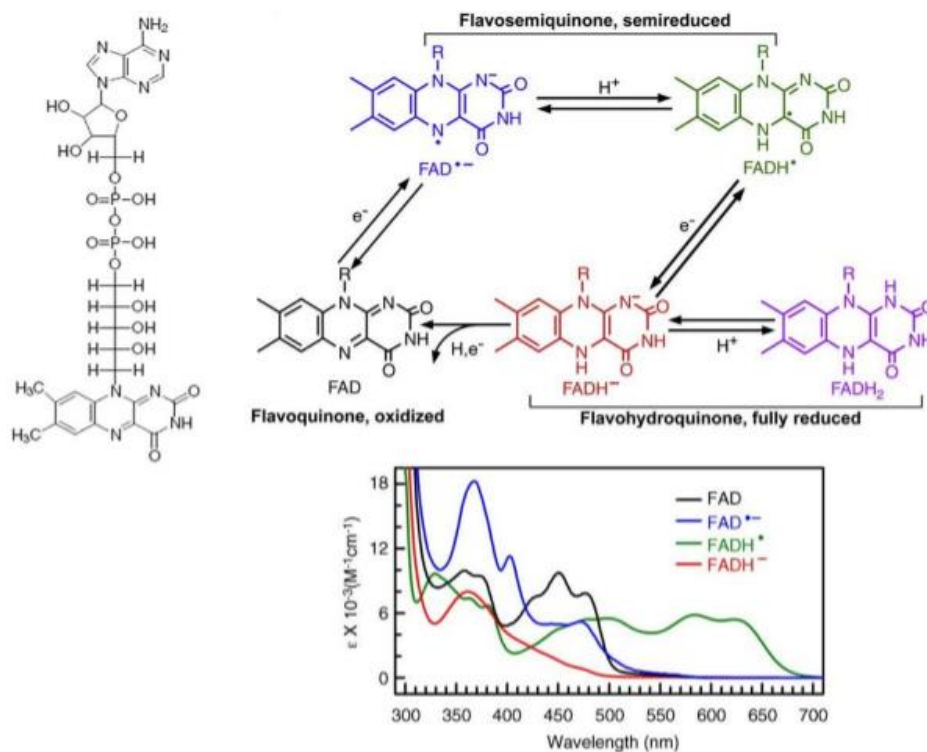


Fig. 2 Redox states of FAD and their absorption spectra. FAD (Left), its redox states (top right) and the absorption spectrum of the redox states (bottom). (Current opinion in plant biology, 2010. **13**(5): 578-586)

The mechanism of light sensing in dCRY is in poorly understood. Although PLs contain an antenna pterin cofactor (usually methenyl-tetrahydrofolate (MTHF)) that appears to help absorb light, it is not thought that CRYs bind an antenna cofactor, as the binding pocket is not fully conserved and no structures have included any cofactors there^{13,16}. It has been shown that upon light exposure, the FAD cofactor of dCRY is reduced from the fully oxidized state (FAD^{OX}) to the anionic semiquinone state (FAD^{*•-}/ASQ)^{1,3,13}(Fig. 2). By studying the UV-visible spectrum of purified dCRY, the redox state of the FAD cofactor can be followed, with reduction to the

ASQ state correlating with an increase in absorbance at 365nm and 403nm, with a decrease in absorbance at 450nm.

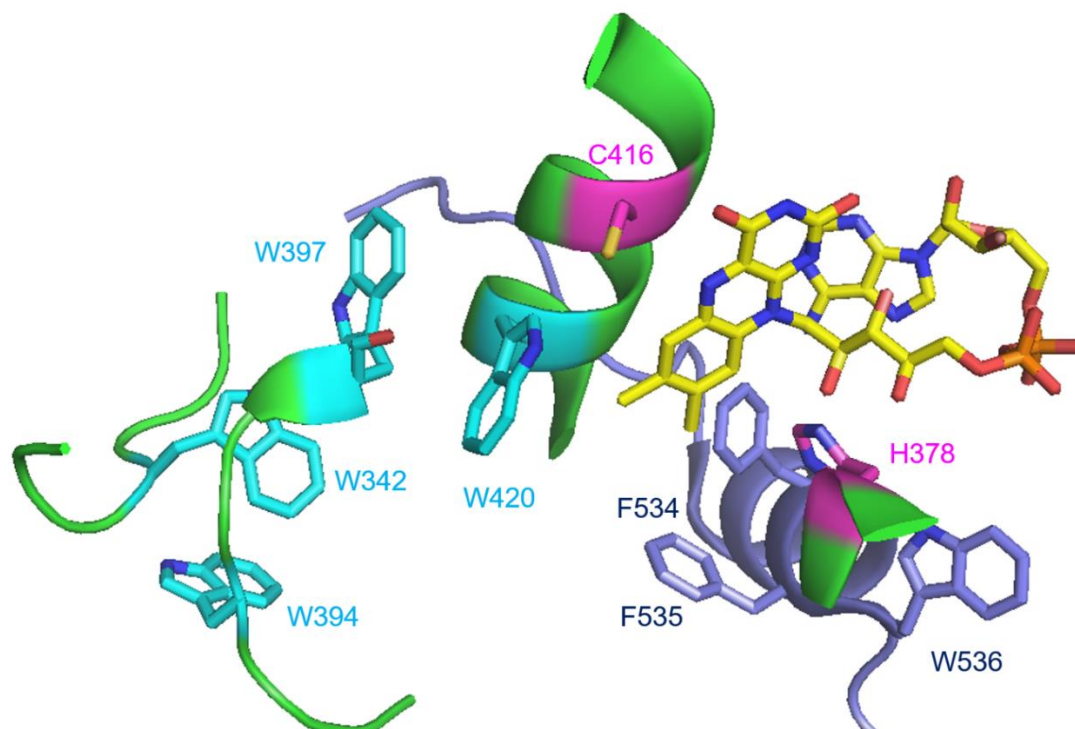


Fig. 3: Schematic of important residues discussed in this paper. Tryptophan “triad” in cyan. CRY CTT and FFW motif in light blue. FAD in yellow. C416 and H378 in magenta.

The source of the electron needed for this reduction has long been thought to be from a series of three tryptophans, called the TRP triad, which would serve as a pathway for tunneling/hopping transport of electrons from an external reductant to the FAD cofactor. This pathway was proposed for CRY because a similar mechanism had been shown to reduce FAD using homologous residues in PL^{1,3,17,18}, and has largely been supported by mutational studies^{19,20}. However, some mutations to the TRP triad which seem to have blocked FAD reduction *in vitro*, still had light sensing activity *in vivo*, casting doubt on to the validity of this mechanism in the environment of the cell^{11,21-24} Recently, a fourth member of the tryptophan triad was proposed as being

important and conserved in animal cryptochromes and photolyases-making a TRP tetrad²⁵(Fig.3).

In addition to the source of electrons for FAD reduction, there has been question as to whether reduction of the FAD cofactor to the ASQ is sufficient to induce conformational change of dCRY, or if additional excitation is needed. One model proposes that dCRY contains oxidized FAD in the ground state (as purified) and light induced photoreduction to the anionic semiquinone is sufficient to send conformational signals and engage targets^{18,26}. In the second model, dCRY contains ASQ in the ground state *in vivo*, and light drives conversion to a short-lived excited state or a further reduced state, which leads to conformational changes^{11,27,28}. Lastly, the mechanism by which reduction/excitation of the FAD cofactor leads to conformational change is unclear.

In an effort to investigate these questions we have undertaken a variety of biochemical studies designed to study the source of electrons needed for FAD reduction in dCRY, how this reduction could cause conformational change, and whether FAD reduction is sufficient to introduce this change and cause binding of dCRY's partners.

Results

In order to assess a wide variety of mutations, it was desirable to express CRY in *E. coli* cells instead of insect cells, as the protein had previously been expressed. In order to do this, CRY was cloned into pET-28 and expressed in C41 cells supplemented with FAD. WT CRY purified from *E. coli* had very similar UV-visible

spectra and reduction/reoxidation kinetics as those of the protein purified from insect cells. From this we concluded that expression in *E. coli* did not cause any major structural changes to CRY and is a valid expression system for this protein (Fig. 4).

Mutations in the TRP Triad of dCRY

In order to determine the importance of TRP triad residues to the photoreduction of CRY's FAD cofactor, mutations were made to these residues and the spectra were recorded both before and after exposure to laser light of wavelength 440nm for 15min. All mutants studied experienced any reduction within the first 5 min., then laser light was kept on the sample for an additional 10min. to ensure that the spectra reached equilibrium.

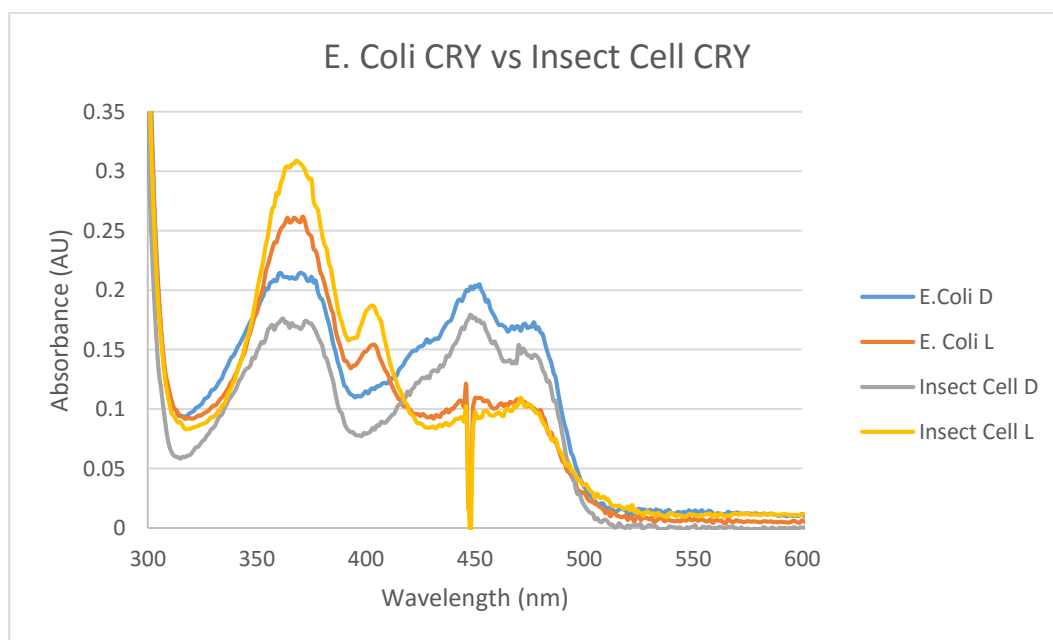


Fig. 4: UV-Vis Spectra of dCRY purified from *E. Coli* in the dark (blue) or after 20min of laser light (orange) compared with dCRY purified from S2 insect cells in the dark (gray) or light (yellow). The dip in absorbance at ~440nm in light spectra is from the laser overexposing the spectrometer.

Overall, we found that mutating any residues in the TRP triad/tetrad had an inhibitory effect on the ability of dCRY to reduce FAD, though the severity of that inhibition varied. All mutants studied appeared to retain at least a small ability to reduce FAD. The results are tabulated in Table 1, with full spectra shown in Appendix 1.

	Reduction t(1/2) (sec)	Recovery t(1/2) (sec)	Δ 450nm	Δ 365nm	Δ 403nm
WT	42	400	8.3E-02	-8.0E-02	-7.0E-02
W420L	80	150	2.6E-02	-6.1E-02	-2.5E-02
W420F	130	360	2.8E-02	-1.5E-02	-9.7E-03
W420Y	110	820	4.7E-02	-4.4E-02	-3.3E-02
W342L	200	250	2.6E-02	-1.5E-02	-7.0E-03
W342Y	400	220	3.7E-02	-2.5E-02	-1.9E-02
W342F			1.0E-02	-9.2E-04	-3.8E-03
W397F	150		5.3E-02	-6.0E-02	-4.1E-02
W397Y	90		2.2E-02	-3.4E-02	-4.0E-02

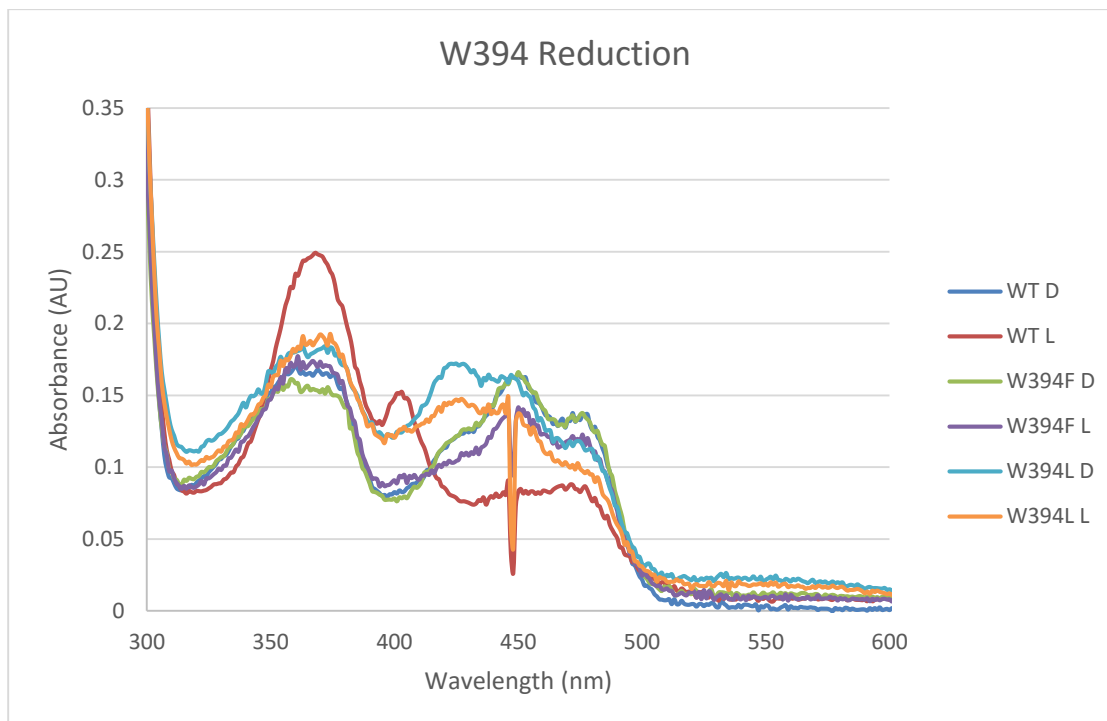
Table 1: Reduction capability of dCRY TRP triad mutants compared to WT. Magnitude of FAD reduction at equilibrium is shown by change in peaks of 450nm, 365nm, and 403 nm of normalized spectra. Kinetics of these changes are represented by t(1/2) of the reduction with light and recovery in the dark.

There are a wide range of reduction capabilities shown, from W342F, which had such a small reduction that kinetics could not be calculated, to W397F, which had a fairly robust reduction of ~65% compared to the WT change of the 450nm peak upon light exposure. In general, the kinetics results seem to correlate well with the

extent of reduction. For example, W342L had a very low magnitude of reduction at equilibrium compared to wild type, which is caused by the fact that it has both much slower reduction kinetics and faster recovery kinetics. However, W420Y, although it had slower reduction kinetics than WT, also had slower recovery kinetics, which resulted in a fairly substantial equilibrium reduction of ~57% yield compared to WT.

Mutations of a Potential Fourth TRP Essential for FAD Reduction

A fourth tryptophan, W394, has been proposed as essential for FAD reduction in cryptochromes. Mutation of this residue caused a drastic decrease in the ability of dCRY to reduce FAD. W394Y did not express with a sufficient yield to enable successful purification, so only W394F and W394L were compared. Both W394F and W394L showed only a very small ability to reduce FAD (Fig. 5). Of note is the fact that the dark state spectrum of W394L had a much larger peak at ~425nm compared to WT, such that it was around the same absorbance as the peak at 450nm. This was attributed to contamination of the sample, since the residue mutated is sufficiently far away from the ligand binding pocket that altering binding in such a way seems unlikely.



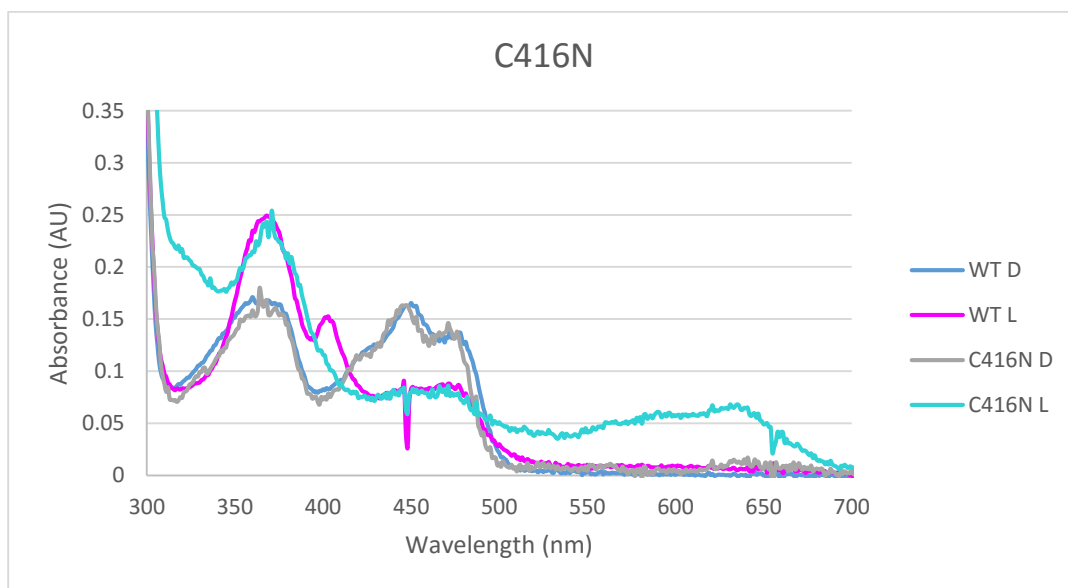
	Reduction t(1/2) (sec)	Recovery t(1/2) (sec)	$\Delta 450\text{nm}$	$\Delta 365\text{nm}$	$\Delta 403\text{nm}$
WT	42	400	8.3E-02	-8.0E-02	-7.0E-02
W394L	300		2.3E-02	-9.1E-03	-1.9E-03
W394F	500	560	2.5E-02	-1.4E-02	-1.4E-02

Fig. 5: (A) Spectra of WT and W394 mutants both before (D) and after (L) 20min of light exposure. (B) Reduction capability of dCRY W394 mutants compared to WT.

Mutation of Cysteine Opposite FAD Affects Active Redox State

One residue that has been shown to be important in cryptochromes is the amino acid located directly across from N5 of the FAD isoalloxazine ring. This nitrogen is thought to hold negative charge when FAD is reduced, and thus it is a prime location for reactions to occur. In some light sensing proteins such as Vivid in *Neurospora*, this takes the form of a covalent bond being formed to an adjacent

cysteine. In plant cryptochromes such as AtCRY1, this position is taken by an aspartic acid, D396, and it is thought that when FAD is reduced in AtCRY1 N5 deprotonates D396 and takes up a proton, which is why the FAD of AtCRY1 is reduced to NSQ instead of ASQ as in dCRY. In dCRY this position is taken by Cysteine 416. In order to study the importance of this residue, we have mutated it to alanine, serine, and asparagine and investigated the results.



	Reduction t(1/2) (sec)	Recovery t(1/2) (sec)	$\Delta 450\text{nm}$	$\Delta 365\text{nm}$	$\Delta 403\text{nm}$
WT	42	400	8.3E-02	-8.0E-02	-7.0E-02
C416S	6	440	7.8E-02	-5.8E-02	-6.5E-02
C416A	22	320	6.4E-02	-2.2E-02	-2.1E-02
C416N	72	300	9.8E-02	2.2E-02	1.3E-02

Fig. 6: (A) UV-Vis Spectra of WT and C416N mutants in the dark and after light exposure. (B) Reduction capability of C416 mutants compared to WT.

All C416 mutations appeared to retain almost full ability to reduce FAD. Alanine and serine mutations reduced more quickly than WT, though they had similar recovery times. However, with C416N, the formation of some neutral semiquinone was seen (Fig. 6). This finding was recently shown in another study as well²⁹.

Role of Histidine Protonation in CRY Conformational Change

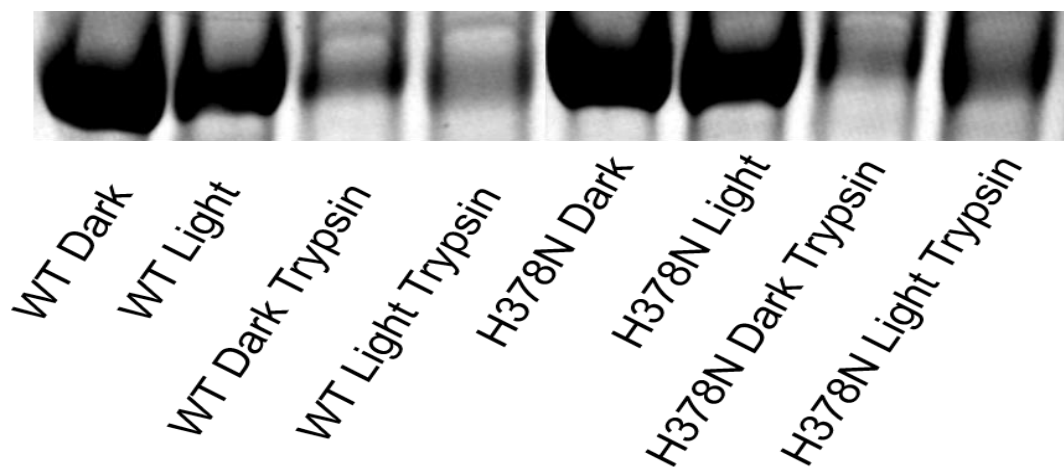
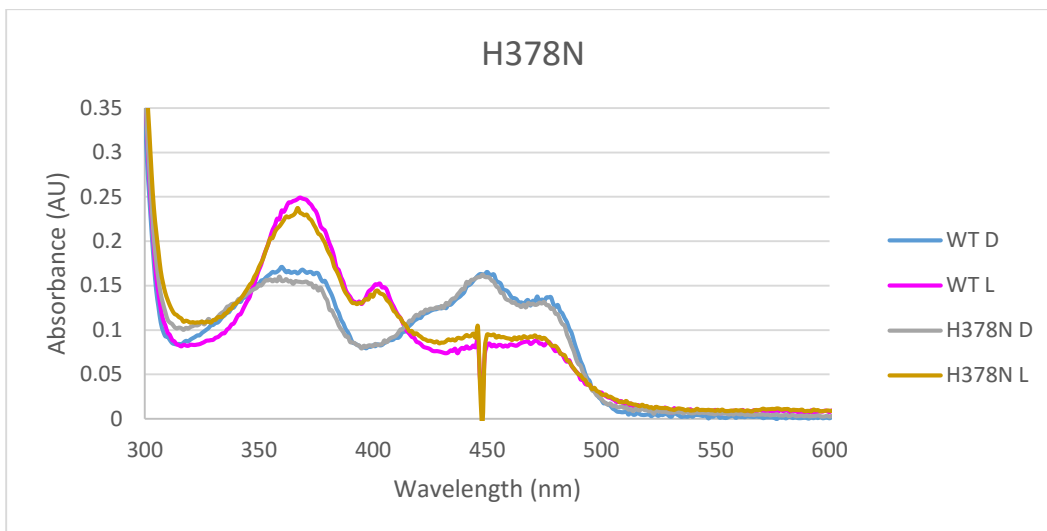
Although the effect of light on conformational changes and the path of electrons in reducing CRY's FAD has been studied to some extent, the mechanistic cause of these conformational changes is unclear. Since movement of the CTT of CRY has been shown to be linked with reduction of FAD and binding of TIM, this movement was chosen as our target for computational studies in an effort to determine how reduction of FAD induces a conformational change. The CTT contains a conserved FFW motif that is separated from the FAD by a conserved histidine-H378^{16,23,30}. In 6-4 PLs, the analogous His has been shown to protonate in response to changes in FAD redox state^{31,32}. To test the importance of H378 protonation on CTT movement, we performed molecular dynamics simulations and principal component analysis.

The results of the MD simulations showed that protonation of H378 in correlation with reduction of FAD to ASQ flavin caused the residue to leave the flavin pocket and drift towards the FFW motif (data not shown-personal correspondence Ganguly, A.). PCA of the FFW motif revealed the motions of the CTT as a result of this protonation and movement. When H378 was not protonated, no significant CTT movement was seen. However, upon single H378 protonation CTT movement was seen with an ASQ flavin, and with a doubly protonated H378, CTT movement was

seen both with an ASQ flavin and with an oxidized flavin (data not shown-personal correspondance Ganguly, A.). From this, it was concluded that protonation of H378 may be associated with movement of the CTT. However, experimental studies were needed to determine the exact role of protonation in CTT movement.

In order to determine the role of protonation in the movement of the CTT, reduction kinetics of CRY were determined using buffers of varying pH, from 7 to 9. It was found that WT CRY in buffer pH 7 reduced much more quickly than WT CRY at pH 9, with pH 7 CRY reducing in about 100s, while CRY at pH 9 took about 300 sec. CRY at pH 7.5, 8, and 8.5 had intermediate times associated with their respective pHs. This difference suggests that there is indeed a protonation event involved in the stable reduction of CRY's FAD cofactor at equilibrium (Fig. 8A).

In order to confirm it is the H378 is the residue that is undergoing protonation, we created an H378N mutant and investigated the results of this mutation. The spectra of H378N reduced fairly similarly to WT, with slightly quicker reduction kinetics (Fig. 7A,C). Partial trypsin digest, used to probe light dependent conformational changes, showed no large differences between WT and H378N, showing that making this mutation alone does not render the protein irresponsive to light (Fig. 7B).



	Reduction	Recovery			
	t(1/2) (sec)	t(1/2) (sec)	$\Delta 450\text{nm}$	$\Delta 365\text{nm}$	$\Delta 403\text{nm}$
WT	42	400	8.3E-02	-8.0E-02	-7.0E-02
H378N	22	300	6.5E-02	-7.7E-02	-5.8E-02

Fig. 7: (A) Spectra of WT and H378N mutant CRY in the dark and after light exposure. (B) SDS-PAGE gel showing bands for dCRY and H378N in the dark and after light exposure both with and without partial trypsin digest. (C) Reduction capability of H378N mutant CRY compared to WT.

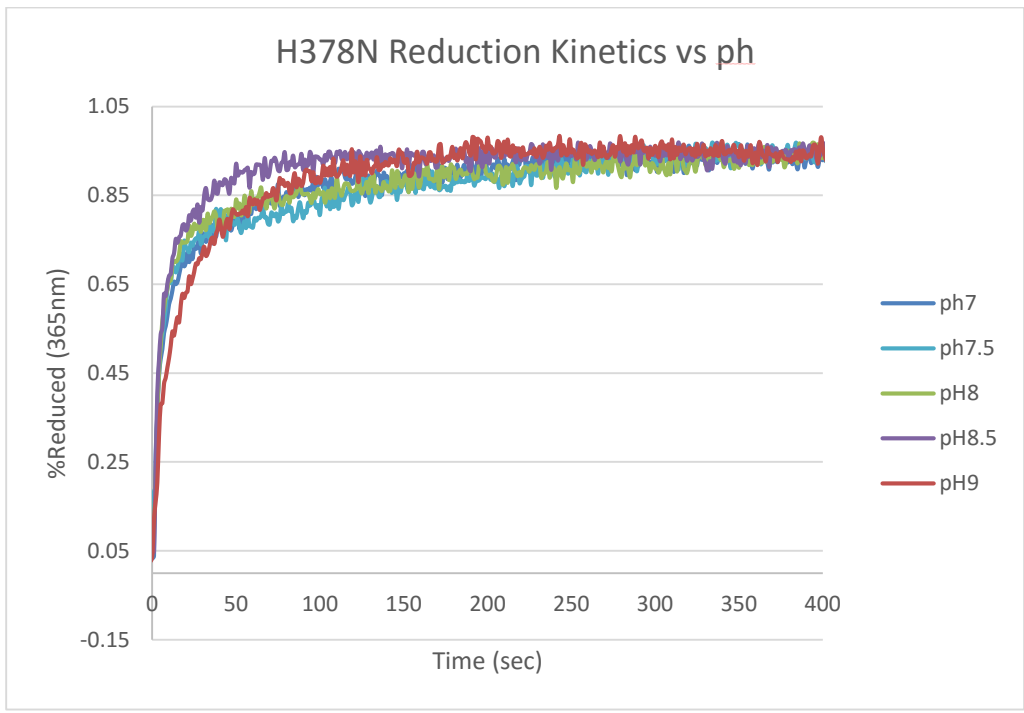
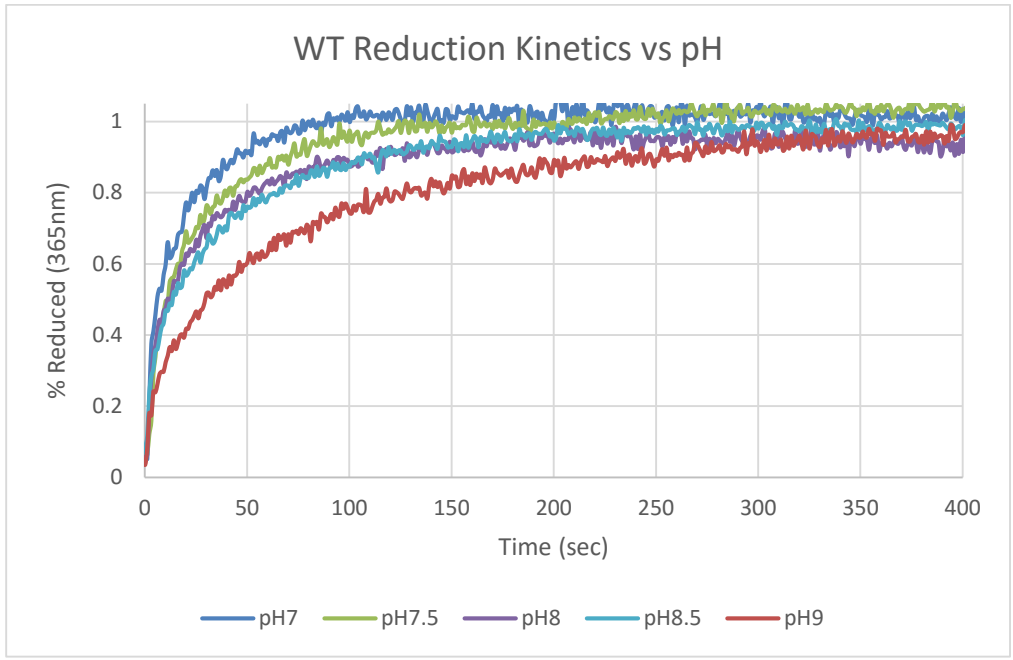


Fig. 8: Reduction of WT dCRY (A) and H378N mutant (B) during exposure to light vs pH. Absorbance at 365nm plotted vs time of light exposure with maximum normalized to 1 and minimum to 0.

pH dependence of H378N mutant dCRY was tested as well. Asparagine should have a much different pKa than histidine, and thus experience a different pH effect than WT CRY. Indeed, with H378N CRY we saw little to no pH dependence in the rate of FAD reduction (Fig. 8B). However, H378N CRY under all conditions reduced at a similar rate to WT CRY at pH 7, the pH with the fastest rate recorded in this study.

If protonation of H378 is needed to stabilize ASQ and produce conformational change in dCRY, we would expect that mutating this residue would slow down reduction kinetics or inhibit conformational change. The fact that we see a pH dependence on reduction kinetics with WT but not with H378N tells us that H378 is indeed protonated upon FAD reduction in dCRY, but the fact that dCRY continues to retain reduction and conformational change activity perhaps shows that other pathways for ASQ stabilization and conformational change are allowed.

Light Dependent Binding to TIM Peptide

In order to test that a conformational change is directly linked to the redox state of FAD, we attempted to show that reduction of CRY leads to binding of its partner TIM. TIM is a very large (1398a.a.) unstructured protein that has not been successfully purified in any form. However, upon investigating the sequence of TIM, it was discovered that it contains a FFW motif, similar to the FFW motif on the CTT of CRY that binds next to the FAD cofactor (Fig. 9A). Since it is known that FAD reduction results in a conformational change in the CTT, it was hypothesized that the FFW motif on TIM could take the place of the CTT upon light exposure.

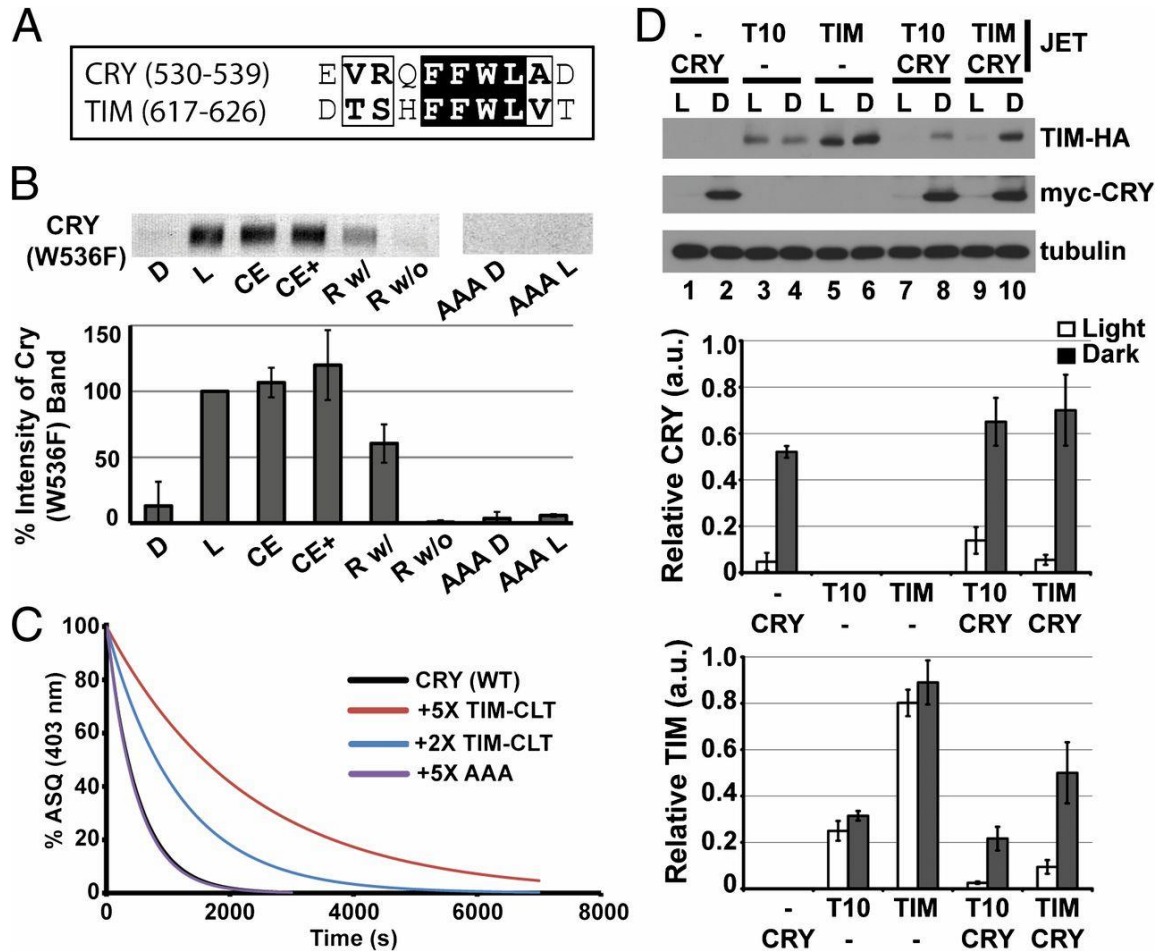


Fig. 9: Interaction of dCRY with the TIM-CTL. (A) dCRY CTT motif is conserved by TIM. (B) dCRY (W536F) was pulled down by a biotin-tagged peptide containing the TIM-CTL via streptavidin-conjugated agarose beads much more in the L than in the D and when dCRY is reduced. CE, dCRY treated with Cr:EDTA for 15 min; CE+, treatment for 2 h; R w/, dCRY 2 h recovery after light exposure with peptide; R w/o, dCRY 2 h recovery after light exposure without peptide; AAA, TIM-CTL with FFW mutated to AAA and incubated in either the D or the L. Quantification of dCRY band intensities from four independent experiments is shown. (C) ASQ recovery kinetics are slowed down by increasing concentrations of TIM-CTL but not by the AAA peptide. (D) Effect of TIM-CTL in dCRY-mediated TIM degradation. (Upper) Western blot analysis of TIM and dCRY expressed with JET in S2 cells under light or dark conditions. T10 represents TIM with the 10-residue CTL changed to poly-Ala; T10 and TIM both show dCRY-mediated degradation in the light. (Middle and Lower) Quantification of relative protein levels is shown below.

To test this hypothesis, a short peptide consisting of 23 residues surrounding the FFW motif on TIM with a biotin label called the TIM-c-terminal tail-like (TIM-

CTL) was used to pull down dCRY using streptavidin linked beads both with and without exposure to light. The result of this was that CRY is indeed pulled down by this peptide only in the presence of light. In addition, letting dCRY recover from light exposure before adding the peptide showed no binding, meaning that the conformational change induced by light exposure is reversible (Fig. 9B).

Letting dCRY recover in the presence TIM-CTL showed that some dCRY was still bound, suggesting that dCRY FAD recovery and/or conformational change recovery is slowed by the presence of TIM-CTL (Fig. 9B). This was confirmed by following recovery of ASQ CRY kinetically using UV-Vis spectroscopy. In the presence of TIM-CTL, both at 2X and 5X the concentration of dCRY, ASQ recovery was slowed significantly (Fig. 9C). This could be because TIM-CTL blocks access to the FAD cofactor, so it cannot be oxidized by oxygen, or because TIM-CTL locks dCRY into a conformation where the ASQ is more stable than the fully oxidized FAD. In addition, when 2X TIM-CTL was added to dCRY and the reduction kinetics were studied, an increase in reduction rate was seen with the presence of TIM-CTL, likely because of a slower rate of oxidation (Fig. 9C).

In order to test whether reduction of the FAD cofactor is sufficient to cause conformational change or if light, which would cause further excitation of the cofactor, is needed, we subjected dCRY to chemical reduction by Cr:EDTA before incubating with TIM-CTL. Our results showed that Cr: EDTA was able to reduce the FAD of dCRY to ASQ state, and that this reduction was sufficient to cause binding to TIM-CTL even without light (Fig. 9B).

To determine the importance of the FFW motif, a peptide was instead used where FFW had instead been mutated to AAA. When using this peptide dCRY was not pulled down in the dark or the light, and the recovery of ASQ to oxidized FAD was not slowed, showing that the FFW motif is needed for TIM-CTL binding to dCRY (Fig. 9B).

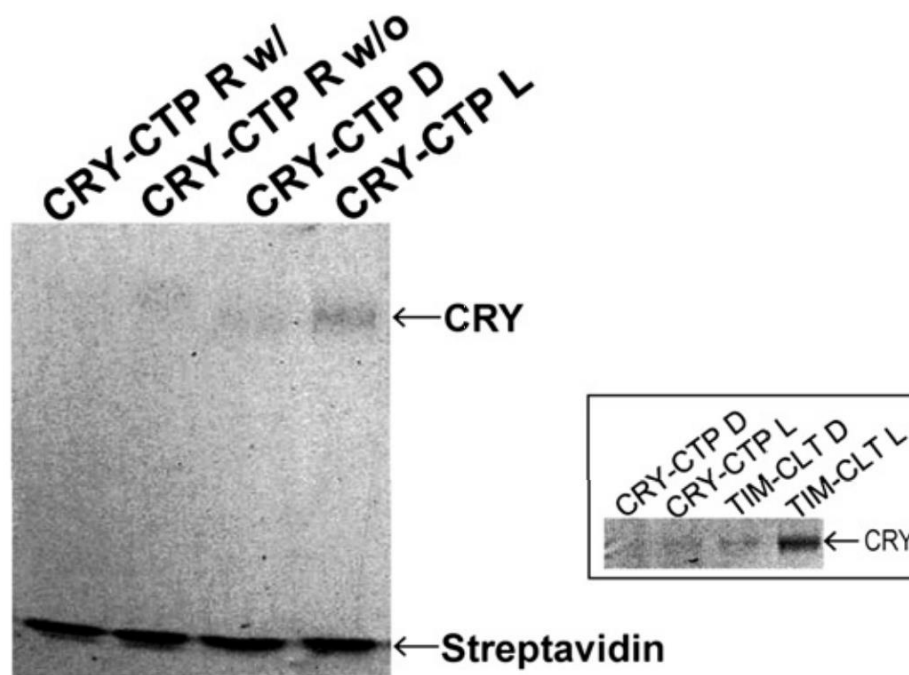


Fig. 10. Inability of dCRY-CTL peptide (CRY-CTP) to interact with dCRY. Pull-down assays of dCRY with a biotin-labeled CRY-CTP peptide are shown. (Inset) Peptide corresponding to the C-terminal tail (CTT) of dCRY, CRY-CTP, does not interact with dCRY as tightly as the TIM-CTL. Furthermore, the CRY-CTP, although present at a higher concentration than dCRY, does not compete effectively with the covalently attached CTT on recovery. This may indicate that the interactions of the CTT with the FAD pocket and/or CTT dynamics are influenced by other regions of dCRY that are unable to perform these functions with the free peptide. D, dark; L, light; R w/, recovery of the ASQ in the presence of CRY-CTP; R w/o, recovery in the absence of CRY-CTP.

One question was why dCRY would preferentially bind the FFW motif on TIM-CTL instead of the FFW motif on its own CTT. To confirm that this was the

case, and that it was not for some other reason such as concentration dependence, a peptide was created similar to the CTT of dCRY, called the CRY-CTP, and pull-downs were attempted with this peptide. However, pull-down with this peptide showed only a small amount of dCRY binding (Fig. 10). This suggests that while the FFW motif is needed for binding to dCRY by TIM-CTL, it is not sufficient, and other parts of the peptide are needed as well.

To test the importance of this CTL peptide of TIM *in vivo*, protein levels were investigated in S2 insect cells by performing western blots on samples with and without light. Overexpressed CRY showed light dependent degradation both with and without TIM overexpression, while WT TIM was only degraded in the light. TIM with the ten residues listed in Fig. A mutated to poly-alanine (T10) showed lower baseline levels, but still showed light dependent degradation (Fig. 9D). This shows that *in-vivo* other parts of TIM are able to counteract TIM-CTL mutation and still allow for light dependent binding and degradation of TIM by dCRY.

Discussion

Several other studies have attempted to study the importance of the TRP triad in dCRY by mutating these residues, so there are often similar experiments that we can compare our results with. However, these comparisons are complicated by the fact that there is no standard for conditions under which dCRY photoreduction is tested. dCRY concentration, reductant type, light intensity and wavelength are all variable between studies, and these can all cause significant differences in the ability of dCRY to photoreduce.

Our mutational studies of members of the TRP triad of CRY have shown that these residues are indeed all important for reduction of the FAD cofactor in response to light. All mutations impeded FAD reduction to some extent, with some mutations almost eliminating reduction and some allowing a fair amount. The role of these TRP triad residues in-vivo are still debated^{11,33}, but the fact that some reduction can be seen in all mutants may help explain why some light-dependent activity is still seen in-vivo with many TRP triad mutants.

Due to a recent report that an additional tryptophan may be needed to transport electrons in animal photolyase and cryptochromes, we also mutated W394 to phenylalanine and tyrosine and saw a significant reduction in reduction activity in the mutants. This agrees with data studying the *Xl(6-4)Photolyase*²⁵, and supports the theory that W394 may play a role as a fourth essential tryptophan in electron transport in dCRY.

Overall, our results suggest that tyrosine is the most effective substitute for tryptophan in the TRP triad, with both W342Y and W420Y showing significantly more reduction activity compared to their phenylalanine counterparts. Leucine mutants always had poor reduction activity, perhaps because they are sufficiently different from tryptophan as to introduce structural instability.

Of note is the fact that changing pH and the addition of reductants caused a large change in the ability of WT CRY and mutants to reduce FAD. This means that depending on the exact environment of CRY in vivo, its behavior may be greatly accelerated and/or reduced, perhaps explaining why in-vivo activity of CRY mutants does not always correlate with what is observed in vitro.

We have also shown the important of C416 in dCRY in determining the active state of FAD upon light exposure. All mutants studied showed full reduction activity, with C416A and C416S looking fairly similar to WT. Interestingly, C416N showed the production of NSQ upon light exposure, confirming that this residue can affect the most stable state of FAD upon light exposure. Further mutational studies will be conducted to investigate the possibility of changing dCRY to form fully reduced flavohydroquinone upon light exposure.

Studies on H378 show a possible mechanism for conformational change in dCRY. Histidine residues had been suggested as possible proton acceptors in cryptochromes previously³⁴, and a pH dependence on the rate of recovery had been found in aCRY³⁵. However, as far as we know, this is the first time that H378 has been investigated specifically. A pH dependence in WT that is not conserved in the H378N mutant supports this theory. However, full conformational change seen by trypsin digest and the fact that FAD reduction rate in H378N is still as fast as WT at low pH mean that an alternate mode for conformational change is occurring that needs to be further investigated.

Investigation of binding by TIM-CTL, show a possible region for binding by the dCRY pocket on TIM, and show that binding of this region occurs in a light dependent manner. By chemically reducing dCRY with Cr:EDTA, we have also shown that binding and conformational change is directly related to redox state of the FAD cofactor, and that further excitation is not needed for dCRY to function.

Importance of the TRP triad has been confirmed by seeing a decrease in light responsiveness from a series of mutants. Overall, our laser light was ~50-200X

stronger than previous studies on dCRY mutants. While likely not a physiologically relevant intensity, this light allows us to show that all mutants studied were capable of some light response. This could explain why WT-like function *in vivo*, where the environment is likely more amenable to FAD reduction, was seen by mutants which appeared unresponsive to light *in vitro*. Our mutational studies of W394 support the inclusion of it as a fourth member of the TRP triad. Investigation of H378 proposes a novel mechanism for conformational change in dCRY, though several questions still remain about its role. Peptide binding by a section of TIM advises on how dCRY conformational change leads to partner binding, and full activity after exposure to chemical reductants support to theory that FAD redox state is directly linked to conformational change. This study explains several discrepancies in previous studies and opens up several areas for experimentation in the future.

Methods

Expression and Purification-dCRY was cloned from constructs previously used to express in insect cells¹³ and inserted in pET-28 using NdeI and XhoI sites. This plasmid was expressed in C41 cells. The cells were grown till density at $A_{600} \sim .8$, induced with 4mM IPTG and supplemented with FAD, and grown overnight at room temperature (~25 degrees). Cells were harvested and frozen at -80 degrees.

For purification, cells were lysed by sonication in lysis buffer containing 150mM NaCl, 50mM HEPES pH 8, .5mM Triton-X, .5mM TCEP, and 5mM Imidazole. Insoluble cell debris was removed by centrifugation at 48384g for 35min. The clarified cell lysate was applied to a Nickel NTA Agarose Beads (Gold Biotechnology) equilibrated with lysis buffer and the protein was eluted with elution

buffer 150mM NaCl, 50mM HEPES pH8, 200mM Imidazole, .5mM TCEP, and 10% glycerol. Protein was further purified by anion exchange chromatography and Superdex200 gel filtration column with gel filtration buffer (GFB) 10% glycerol, 150mM NaCl, 50mM HEPES pH 8.0. Purified protein was flash frozen in liquid nitrogen and stored at -80 degrees. Point mutations were made as described previously³⁶ and checked by DNA sequencing.

Spectroscopy-Spectra were collected using a quartz cuvette with path length 1cm. All spectra were normalized by subtracting the absorbance at 700nm. Light spectra were collected after shining the sample with a 440nm laser (WSTech) for 20min.

Timeless C-Terminal Tail-Like Peptide Pull-Down-Timeless C-terminal tail-like (TIM-CTL) peptide Biotin-SNAKVPIDTSHFFWLVTYFLKKK (0.8 nmol; Biomatic) was added to 3 μ L of High Capacity Streptavidin Agarose Resin (Thermo Scientific) in 15 μ L of buffer 1 [50 mM Tris·HCl (pH 7.5), 150 mM NaCl, 10% glycerol] and incubated for 10 min. Beads were then washed with 1,000 μ L of GFB before adding 0.4 nmol of dCRY in GFB with 5 mM DTT, and they were incubated for 12 min either under high-intensity blue light or wrapped in tin foil (dark). Samples were then washed three times with 1 mL of GFB before being run on NuPAGE 4–12% Bis-Tris gel. For Cr:EDTA samples, dCRY was first anaerobically incubated in 15 mM Cr:EDTA for either 15 min or 2 h before addition to resin. For recovery samples, dCRY was allowed to recover in the dark at 4 °C for 2 h either after addition to beads or before addition to the resin before washing three times with 1 mL of GFB. In case of Cr:EDTA samples, the resin was washed with anaerobic buffer in the glove box.

For AAA mutants, 0.8 nmol of AAA peptide

BiotinSNAKVPIDTSHAAALVTYFLKKK (Biomatic) was substituted for peptide TIM-CTL. The gel was stained with coomassie blue per standard procedure, and gel bands were analyzed using the integrated density function in ImageJ. dCRY values were normalized to the intensity of streptavidin, and the band intensity of dCRY (light) was set to 100. Identical experiments were performed with a biotin labeled peptide that corresponds to the dCRY C-terminal tail: Biotin-SNEEEVRQFFWLADKK (Biomatic).

Trypsin digest assay-3uL of 100uM CRY was added to 3uL of 10uM trypsin and quenched after 30s with 3uL of 20uM trypsin inhibitor and 10uL of SDS loading buffer followed by 10min of heating at 90⁰ C. For the light samples, CRY was exposed to laser light of 440nm for 20min before addition of trypsin, and the sample was kept under light for the 30s digestion period. Samples were run by SDS-PAGE and visualized using coomassie blue staining.

Cell Culture Stability Assays. dCRY, Drosophila ls-TIM (dTIM, long and short allele), and Drosophila Jetlag (JET), or site-directed mutants thereof, were N-terminally tagged with three myc epitopes, C-terminally tagged with three HA epitopes, or C-terminally tagged with a FLAG epitope, respectively, and cloned into the pAc5.1/V5 vector (Invitrogen) using standard cloning protocols. S2 cells were grown in Schneider's medium supplemented with 10% FBS and penicillin/streptomycin. dCRY was cotransfected with either empty vector, dTIM plasmid, or dTIM + JET plasmid with effectene (Qiagen) using the manufacturer's protocols. Cell medium was refreshed after 24 h in the transfection mixture, and the

cells were divided into two populations. Twenty-four hours later, each population was lysed in a modified radioimmunoprecipitation assay under red light or after being exposed to white light for 1 h (~600 lux). Equal amounts of lysates were run on 6% SDS/PAGE gels and immunostained using myc (Sigma), HA (Roche), antiFLAG (Sigma), and tubulin (Sigma) antibodies. Transfections were performed in triplicate, and each triplicate was repeated at least twice with similar results.

Principal Component Analysis: We performed a PCA on the motions of the FFW motif residing in the dCRY CTT. Trajectories were aligned to remove rotational and translational motions by first calculating root mean squared fluctuations (RMSFs) of all residues from each independent MD trajectory after aligning the trajectory to the protein backbone of the crystal structure. The average RMSFs of each residue from all the MD trajectories were calculated, and each trajectory was re-aligned based on only those residues that had average RMSFs below a threshold of 1.3 Å. The coordinates of the atoms corresponding to the FFW motif were extracted from these various aligned trajectories and concatenated into a single trajectory on which the PCA was performed.

To explore correlated motions in dCRY we constructed dynamic cross-correlation matrixes (DCCMs) for all MD trajectories. The DCCM of a trajectory was generated by normalizing the covariance matrix of the entire trajectory according to

$$C_{ij}^{corr} = C_{ij} / \sqrt{C_{ii}C_{jj}}$$

The DCCMs were generated for coarse-grained trajectories where each residue from the atomistic MD trajectories was replaced with a particle at its center of mass. All

analysis related to PCA and DCCMs were performed using various GROMACS tools, namely `trjconv`, `g_covar`, and `g_anaeig`.

REFERENCES

1. Chaves, I. *et al.* The cryptochromes: blue light photoreceptors in plants and animals. *Annu Rev Plant Biol* **62**, 335–364 (2011).
2. Lin, C. & Todo, T. The cryptochromes. *Genome Biol* **6**, 220 (2005).
3. Conrad, K. S., Manahan, C. C. & Crane, B. R. Photochemistry of flavoprotein light sensors. *Nat. Chem. Biol.* **10**, 801–9 (2014).
4. Crane, B. R. & Young, M. W. Interactive Features of Proteins Composing Eukaryotic Circadian Clocks. *Annu. Rev. Biochem.* **83**, 191–219 (2014).
5. Partch, C. L., Green, C. B. & Takahashi, J. S. Molecular architecture of the mammalian circadian clock. *Trends Cell Biol.* **24**, 90–9 (2014).
6. Peschel, N. & Helfrich-Forster, C. Setting the clock--by nature: circadian rhythm in the fruitfly *Drosophila melanogaster*. *FEBS Lett* **585**, 1435–1442 (2011).
7. Naidoo, N., Song, W., Hunter-Ensor, M. & Sehgal, A. A role for the proteasome in the light response of the timeless clock protein. *Science (80-.)*. **285**, 1737–1741 (1999).
8. Busza, A., Emery-Le, M., Rosbash, M. & Emery, P. Roles of the two *Drosophila* CRYPTOCHROME structural domains in circadian photoreception. *Science (80-.)*. **304**, 1503–1506 (2004).
9. Koh, K., Zheng, X. Z. & Sehgal, A. JETLAG resets the *Drosophila* circadian clock by promoting light-induced degradation of TIMELESS. *Science (80-.)*. **312**, 1809–1812 (2006).
10. Peschel, N., Chen, K. F., Szabo, G. & Stanewsky, R. Light-dependent interactions between the *Drosophila* circadian clock factors cryptochrome, jetlag, and timeless. *Curr Biol* **19**, 241–247 (2009).
11. Ozturk Selby, C.P., Annayev, Y., Zhong, D., Sancar, A., N. Reaction Mechanism of *Drosophila* cryptochrome. *Proc Natl Acad Sci U S A* **108**, 516–521 (2011).
12. Ozturk, N., VanVickle-Chavez, S. J., Akileswaran, L., Van Gelderb, R. N. & Sancar, A. Ramshackle (Brwd3) promotes light-induced ubiquitylation of *Drosophila* Cryptochrome by DDB1-CUL4-ROC1 E3 ligase complex. *Proc. Natl. Acad. Sci. U. S. A.* **110**, 4980–4985 (2013).
13. Vaidya, A. T. *et al.* Flavin reduction activates *Drosophila* cryptochrome. *Proc*

- Natl Acad Sci U S A* **110**, 20455–20460 (2013).
14. Dissel, S. *et al.* A constitutively active cryptochrome in *Drosophila melanogaster*. *Nat Neurosci* **7**, 834–840 (2004).
 15. Yang, H. Q. *et al.* The C termini of Arabidopsis cryptochromes mediate a constitutive light response. *Cell* **103**, 815–827 (2000).
 16. Zoltowski, B. D. *et al.* Structure of full-length *Drosophila* cryptochrome. *Nature* **480**, 396–399 (2011).
 17. Liu, Z. Y. *et al.* Dynamic determination of the functional state in photolyase and the implication for cryptochrome. *Proc. Natl. Acad. Sci. U. S. A.* **110**, 12972–12977 (2013).
 18. Berndt, A. *et al.* A novel photoreaction mechanism for the circadian blue light photoreceptor *Drosophila* cryptochrome. *J Biol Chem* **282**, 13011–13021 (2007).
 19. Froy, O., Chang, D. C. & Reppert, S. M. Redox potential: differential roles in dCRY and mCRY1 functions. *Curr Biol* **12**, 147–152 (2002).
 20. Zeugner, A. *et al.* Light-induced Electron Transfer in Arabidopsis Cryptochrome-1 Correlates with in Vivo Function *. *J. Biol. Chem.* **280**, 19437–19440 (2005).
 21. Song, S.-H. *et al.* Formation and function of flavin anion radical in cryptochrome 1 blue-light photoreceptor of monarch butterfly. *J Biol Chem* **282**, 17608–17612 (2007).
 22. Ozturk, N., Song, S. H., Selby, C. P. & Sancar, A. Animal type 1 cryptochromes. Analysis of the redox state of the flavin cofactor by site-directed mutagenesis. *J Biol Chem* **283**, 3256–3263 (2008).
 23. Czarna, A. *et al.* Structures of *Drosophila* cryptochrome and mouse cryptochrome1 provide insight into circadian function. *Cell* **153**, 1394–1405 (2013).
 24. Li, X. *et al.* Arabidopsis cryptochrome 2 (CRY2) functions by the photoactivation mechanism distinct from the tryptophan (trp) triad-dependent photoreduction. *Proc Natl Acad Sci U S A* **108**, 20844–20849 (2011).
 25. Muller, P., Yamamoto, J., Martin, R., Iwai, S. & Brettel, K. Discovery and functional analysis of a 4th electron-transferring tryptophan conserved exclusively in animal cryptochromes and (6-4) photolyases. *Chem. Commun.* **51**, 15502–15505 (2015).

26. Hoang, N. *et al.* Human and *Drosophila* cryptochromes are light activated by flavin photoreduction in living cells. *PLoS Biol* **6**, (2008).
27. Ozturk, N., Selby, C. P., Zhong, D. & Sancar, A. Mechanism of photosignaling by *drosophila* cryptochrome ROLE of the REDOX status of the flavin chromophore. *J. Biol. Chem.* **289**, 4634–4642 (2014).
28. Liu, B., Liu, H., Zhong, D. & Lin, C. Searching for a photocycle of the cryptochrome photoreceptors. *Curr Opin Plant Biol* **13**, 578–586 (2010).
29. Paulus, B. *et al.* Spectroscopic Characterization of Radicals and Radical Pairs in Fruit Fly Cryptochrome: Protonated and Non-Protonated Flavin Radical-States. *FEBS J.* **282**, n/a–n/a (2015).
30. Levy, C. *et al.* Updated structure of *Drosophila* cryptochrome. *Nature* **495**, 3–4 (2013).
31. Schleicher, E. *et al.* Electron nuclear double resonance differentiates complementary roles for active site histidines in (6-4) photolyase. *J. Biol. Chem.* **282**, 4738–4747 (2007).
32. Hitomi, K. *et al.* Role of two histidines in the (6-4) photolyase reaction. *J. Biol. Chem.* **276**, 10103–9 (2001).
33. Vaidya, A. T. *et al.* Flavin reduction activates *Drosophila* cryptochrome. *Proc. Natl. Acad. Sci. U. S. A.* **110**, 20455–60 (2013).
34. Immeln, D., Weigel, A., Kottke, T. & Pérez Lustres, J. L. Primary events in the blue light sensor plant cryptochrome: Intraprotein electron and proton transfer revealed by femtosecond spectroscopy. *J. Am. Chem. Soc.* **134**, 12536–12546 (2012).
35. Spexard, M., Thöing, C., Beel, B., Mittag, M. & Kottke, T. Response of the sensory animal-like cryptochrome aCRY to blue and red light as revealed by infrared difference spectroscopy. *Biochemistry* **53**, 1041–1050 (2014).
36. Samanta, D., Borbat, P. P., Dzikovski, B., Freed, J. H. & Crane, B. R. Bacterial chemoreceptor dynamics correlate with activity state and are coupled over long distances. *Proc. Natl. Acad. Sci.* **2**, 2455–2460 (2015).

CHAPTER 4

CONCLUSIONS AND FUTURE STUDIES

***Drosophila* Cycle**

We have solved the crystal structure of the PAS B domain of the transcription factor Cycle (CYC) of *Drosophila melanogaster*. While the structure of the full length mammalian homolog mBMAL1 and its dimer mCLOCK have previously been solved, our structure showed a variety of structural changes that occur when the monomeric form binds to its partner. In the cell, CYC is much more abundant than dCLK¹, so we can expect the majority of the protein to be in monomeric or homodimer form, making this information useful.

A novel finding from the structure of dCYC PAS B is the fact that it binds glycerol in an internal pocket. This is the first evidence of ligand binding by any of the PAS domains involved in *Drosophila's* circadian clock, and a novel ligand for binding by any PAS domain. mBMAL1 has been implicated in glycerol metabolism and brown fat formation^{2,3}, so binding of glycerol could be a feedback mechanism. Although binding of glycerol did not appear to cause any major structural changes in our crystal structures, it is possible that ligand binding regulates CYC stability or ability to bind partners.

To validate the finding that CYC binds glycerol, it would be desirable to test mutants in-vivo. This has already been done with mBMAL1 to some extent, where BMAL1^{-/-} cells had lower levels of glycerol and no circadian control³, however the same studies have not been carried out in flies. Studies of BMAL1^{-/-} or CYC^{-/-} flies

would not differentiate between CYC binding of glycerol and CYC promotion of another gene that is involved in metabolism. To do this we would need to find mutants of CYC/BMAL1 that are unable to bind glycerol. Several mutants have been purified, however we have been unable to crystallize them as of yet. Therefore, we would need to utilize an assay which can measure glycerol binding-perhaps ITC. Once mutants are identified, in-vivo testing of glycerol circadian control could be carried out to determine if there is some feedback from glycerol levels to CYC/BMAL1.

In addition, it would be useful to validate glycerol binding in BMAL1. This could be done by purifying BMAL1 and testing binding by ITC, or by crystallizing a complex with mCLK as before but using glycerol as a cryoprotectant if possible. It would be desirable to test this binding both with and without mCLK to see if glycerol binding affects the interaction in any way. We have attempted to express and purify dCLK and its domains, but have had little success. Pure dCLK would allow us to carry out these assays with CYC, which we have largely already characterized.

***Drosophila* Cryptochrome**

We have studied a variety of dCRY tryptophan triad mutants and their ability to reduce FAD spectroscopically with a much brighter light than has been used previously, with the result being that all mutants inhibited, but did not eliminate, FAD reduction to ASQ in-vitro. This, in addition to our finding that buffer conditions can influence reduction ability greatly, could explain why many previous labs reported no FAD reduction in-vitro but still saw light-dependent activity in-vivo⁴⁻⁶. We have also tested a proposed fourth member of the TRP triad in dCRY, the first study of this

residue in *Drosophila*, and found that, like other members of the TRP triad, mutation of W394 severely inhibit FAD reduction by light in-vitro.

In order to validate these results, it would be desirable to test the ability of these mutants to undergo conformational change and partner binding both in-vitro and in-vivo. We have already stated performing partial trypsin digests in-vitro to look at conformational change and we have also carried out some binding assays using GST-JETLAG pulldowns. Further in-vivo studies would be useful to further corroborate our results.

In addition to TRP triad mutations, we have also studied the role of histidine 378 in dCRY conformational change, the first time this residue has been studied in *Drosophila*. Molecular Dynamics studies suggested that FAD reduction to ASQ would cause a shift of as much as 4 pH units in the local pH of H378, which is likely to cause a change in protonation. Additionally, principal component analysis showed that protonation along with FAD reduction is likely to cause a change in CTT conformation.

In order to test these results, we purified H378N dCRY and compared FAD reduction at a range of pH values to WT. The result was that WT dCRY reduction rate was correlated with pH, with low pH reducing faster than high pH, which would agree with the theory that protonation is involved in FAD reduction stability. In addition, H378N mutants did not see a similar change in rate with pH, suggesting that it is H378 that is protonated. Some unanswered questions remain, however. H378N reduction rate was as fast as the fastest reduction of WT dCRY, which we would not expect if H378 protonation was desirable to stabilize ASQ. One possible explanation for this is

that H378 does not reduce to the same extent as WT dCRY, at least when looking at abs. 450nm (Fig. 1). So if the maximum reduction is set to 1, that value is actually a different magnitude of absorbance change for WT vs H378N. So if H378N is reducing to a smaller extent than WT, it is possible that the Δ Absorbance is actually slower than that of WT. Unfortunately this is hard to test since the initial absorbances need to be exactly the same. However, it should be possible with multiple trials and time.

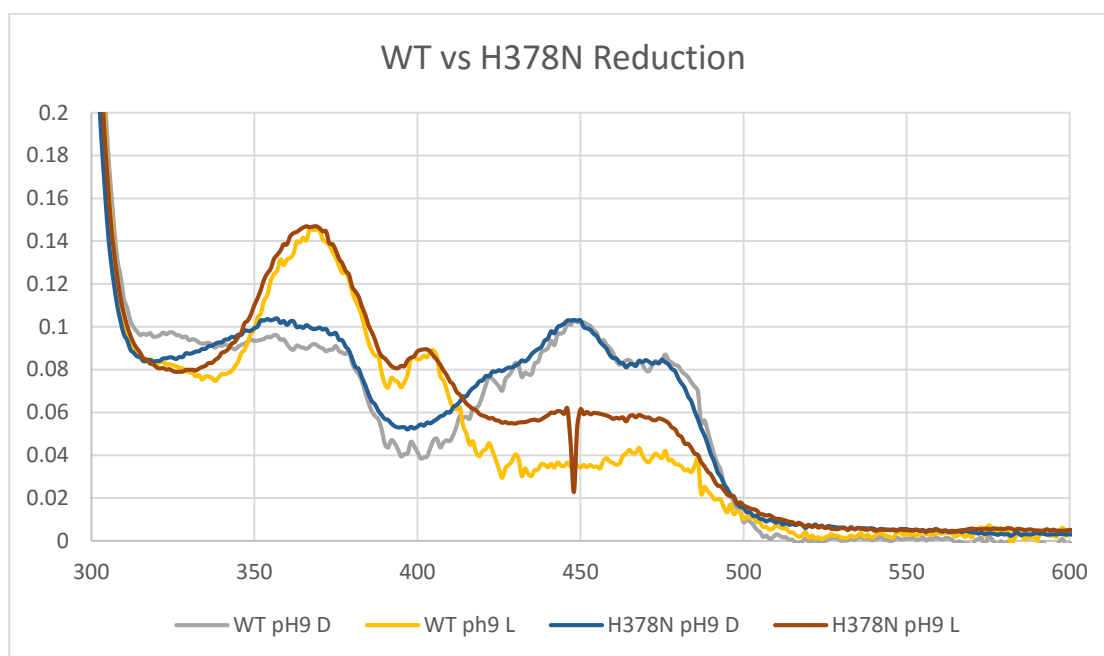


Fig. 1: Spectra of WT and H378N dCRY at pH 9 both before (D) and after (L) 20 min of light exposure.

Another test to look at the pH dependence of reduction would be to measure the midpoint potential to reduce the FAD. If a proton is indeed being taken up by H378, then we should see a difference in midpoint potential of $\sim 59\text{mV/pH}$ unit with WT, but not with H378N. We have put significant effort into measuring these potentials, but we have not yet reached the accuracy to confirm that this is the case.

Although a large variety of dCRY mutants have been tested for behavior both in-vitro and in-vivo, no TRP mutants have been crystallized. It has been suggested that reduced reduction activity in TRP mutants may be due to structural instability and not because of impaired electron transport capabilities⁷. We have had preliminary evidence that this may be the case for W342 mutants. In our hands, partial trypsin digest shows a broadening of the band of WT in the light. A similarly broad band was seen both in the dark and the light state W342Y mutant (Fig. 2), suggesting that W342Y is either stuck in a light state conformation or that it is unstable, so the CTT is accessible to trypsin in the dark when it is not in the WT. Solving a crystal structure of a TRP triad mutant may help confirm or deny this assertion.

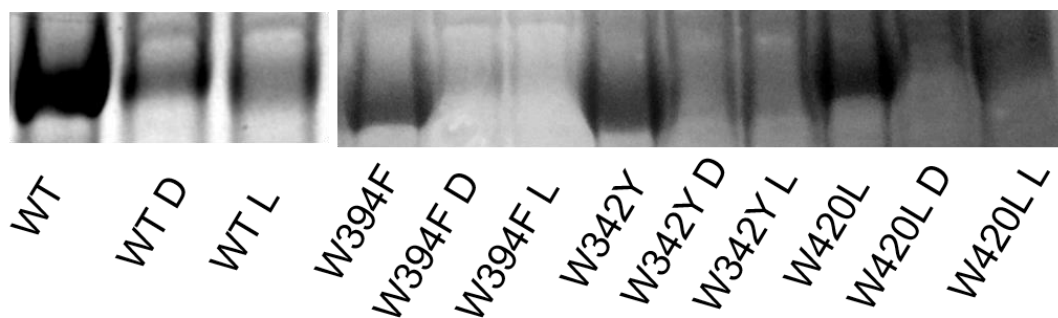


Fig. 2: Partial trypsin digest of WT and TRP Triad mutants of dCRY. SDS-PAGE bands of dCRY alone (no descriptor) or with partial trypsin digest in the dark (D) or the light (L).

Although we have made some intriguing discoveries as to the behavior of *Drosophila* Cycle and Cryptochrome, many of our conclusions remain to be validated, and the importance of our discoveries remain to be seen.

REFERENCES

1. Bae, K., Lee, C., Hardin, P. E. & Edery, I. dCLOCK is present in limiting amounts and likely mediates daily interactions between the dCLOCK-CYC transcription factor and the PER-TIM complex. *J. Neurosci.* **20**, 1746–1753 (2000).
2. Nam, D. *et al.* The adipocyte clock controls brown adipogenesis through the TGF- β and BMP signaling pathways. **16**, 1835–1847 (2015).
3. Shostak, A., Meyer-Kovac, J. & Oster, H. Circadian regulation of lipid mobilization in white adipose tissues. *Diabetes* **62**, 2195–2203 (2013).
4. Ozturk, N., Song, S. H., Selby, C. P. & Sancar, A. Animal type 1 cryptochromes. Analysis of the redox state of the flavin cofactor by site-directed mutagenesis. *J Biol Chem* **283**, 3256–3263 (2008).
5. Ozturk, N., Selby, C. P., Zhong, D. & Sancar, A. Mechanism of photosignaling by drosophila cryptochrome ROLE of the REDOX status of the flavin chromophore. *J. Biol. Chem.* **289**, 4634–4642 (2014).
6. Berndt, A. *et al.* Structures of Drosophila Cryptochrome and Mouse Cryptochrome1 Provide Insight into Circadian Function. *Cell* **153**, 1394–1405 (2013).
7. Li, X. *et al.* Arabidopsis cryptochrome 2 (CRY2) functions by the photoactivation mechanism distinct from the tryptophan (trp) triad-dependent photoreduction. *Proc Natl Acad Sci U S A* **108**, 20844–20849 (2011).

APPENDIX 1

SPECTRA OF CRYPTOCHROME MUTANTS

In order to determine the importance of TRP triad residues to the photoreduction of CRY's FAD cofactor, mutations were made to these residues and the spectra were recorded both before and after exposure to laser light of wavelength 440nm for 20min. All mutants studied experienced any reduction within the first 5 min, then laser light was kept on the sample for an additional 10min to make sure that the spectra were equilibrated.

Of interest is the fact that the addition of external reductants to the buffer significantly affected the ability of mutant CRYs to reduce FAD. For WT dCRY, full reduction was seen in all cases (Fig. 1), but for several variants, while significant reduction was seen even with no external reductants, the addition of 2mM TCEP caused a significant change, and the addition of 5mM DTT caused even more reduction. Some mutants had hardly any reduction with TCEP, but saw significant reduction in the presence of DTT, perhaps suggesting a different reduction mechanism than with TCEP, which can be seen with W342F (Fig. 4B). For this reason, unless stated otherwise, 2mM TCEP was used for all mutants. For all TRP Triad mutants, we attempted to mutate the residues of interest to phenylalanine, tyrosine, and leucine. The reason for this was that the different substitutions may have varying abilities to serve as an electron tunneling/hopping site in the absence of a tryptophan residue. Thus, if mutating a residue inhibited reduction, this range of substitutions would give us a better idea as to the importance of that residue.

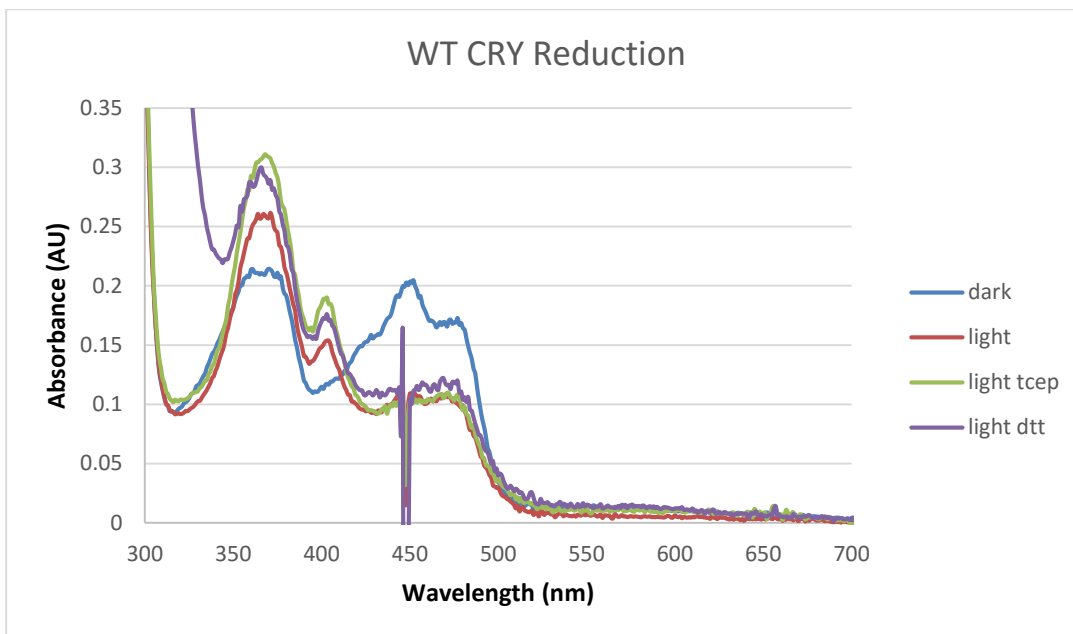


Fig. 1: Spectra of dCRY in the dark (blue) and after exposure to 440nm laser for 20 min in the presence of no reductants (orange), 2mM TCEP (gray), and 5mM DTT (yellow). The negative peak at ~440 nm is due to the laser light used.

Overall, we found that all mutations to any residues in the TRP triad/tetrad had an inhibitory effect on the ability of dCRY to reduce FAD, though the severity of that inhibition varied. All mutants studied appeared to retain at least a small amount of ability to reduce FAD.

Mutation of W420, the tryptophan closest to the FAD cofactor, seemed to have a large effect. Both W420F and W420L contained ~75% of the original FAD^{ox} levels at equilibrium, while W420Y had ~50%. In addition, W420R was purified, and while it appeared to contain some ligand (red coloration) the spectrum did not resemble an FAD redox state, and it was not changed by the addition of light. Interestingly, W420L seemed to shift the peak location of FAD ~3nm to the blue side, most likely by

changing the environment around the FAD cofactor. This change was not seen with W420Y and W420F (Fig. 2).

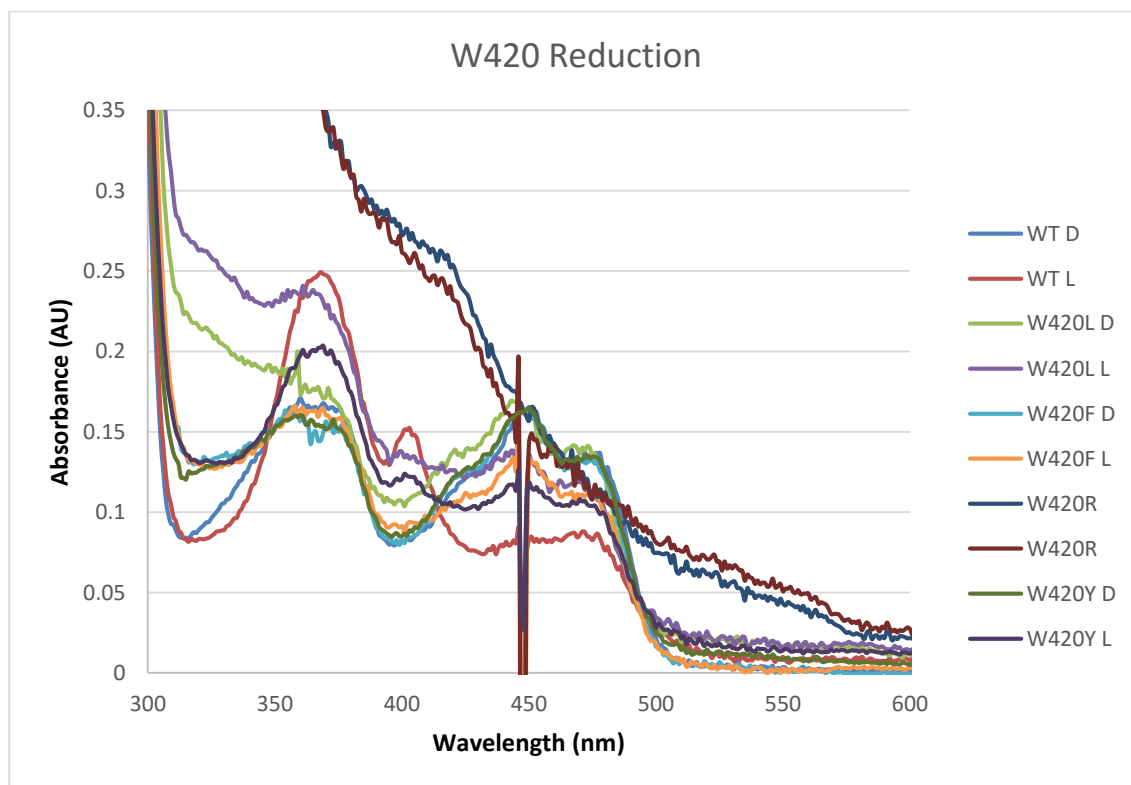


Fig. 2: Spectra of WT and W420 mutants both before (D) and after (L) 20min of light exposure.

Mutation of W397, the middle tryptophan in the canonical TRP triad, had a moderate effect on dCRY's ability to reduce FAD. W397L did not express/purify with sufficient yield to study, so only W397F and W397Y were compared to WT. Looking at both A_{450} and A_{403} , both W397F and W397Y retained a significant ability to reduce FAD, though both were stunted compared to WT. Unlike W420, the phenylalanine mutant W397F retained slightly more activity than the tyrosine mutant, W397Y (Fig. 3).

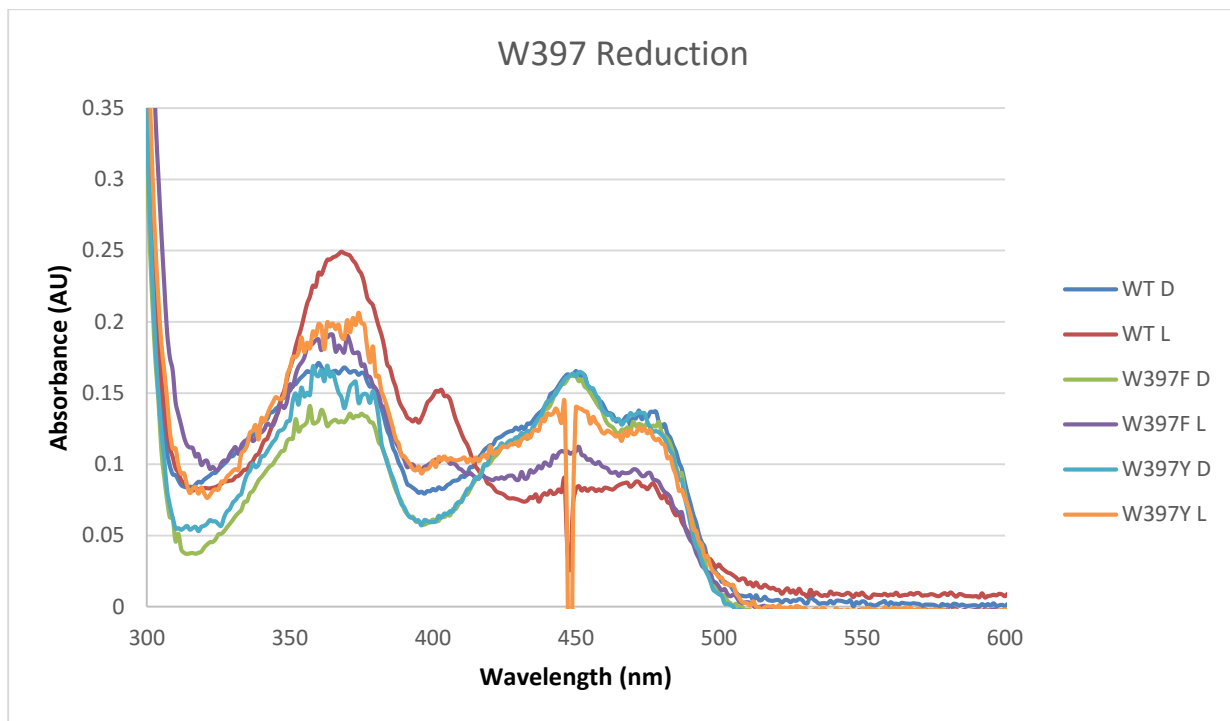


Fig. 3: Spectra of WT and W397 mutants both before (D) and after (L) 20min of light exposure.

Mutation of W342, originally thought to be the terminal electron donor in the tryptophan triad, produced a dramatic decrease in FAD reduction ability with all mutants. W342L and W342F showed almost no reduction after light exposure, while W342Y had a slight decrease in A_{450} peak height, though A_{365} and A_{403} did not increase much, perhaps suggesting that the change is only due to degradation and not FAD reduction. However, similar to W420, the tyrosine mutant seemed to have the most activity of the three mutations tested (Fig. 4).

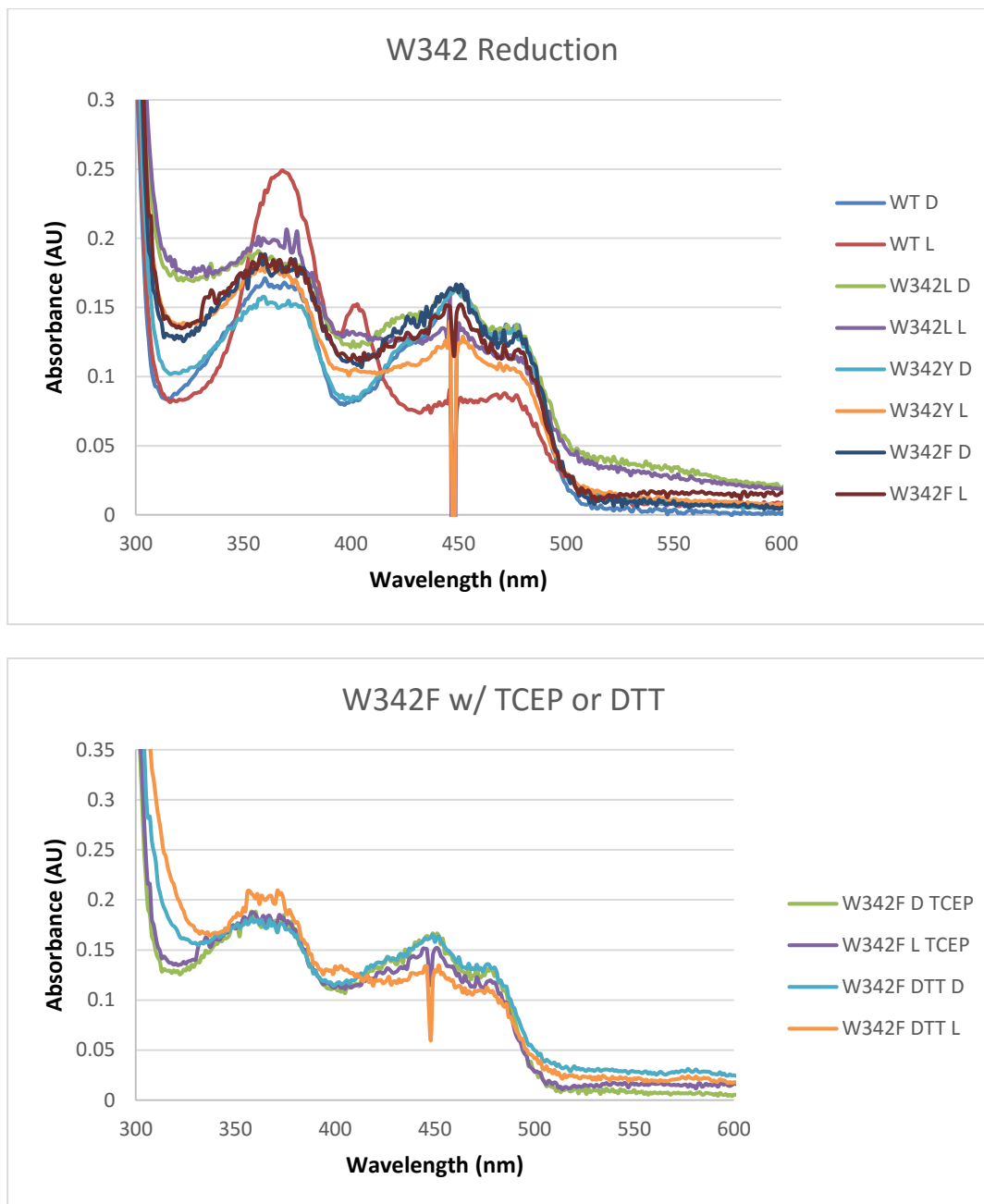


Fig. 4: (A) Spectra of WT and W342 mutants both before (D) and after (L) 20min of light exposure. (B) Spectra of W342F before and after 20min light either with 2mM TCEP or 5mM DTT.

A fourth tryptophan, W394, has been proposed as essential for FAD reduction in cryptochromes. Mutation of this residue caused a drastic decrease in the ability of dCRY to reduce FAD. W394Y did not express with a sufficient yield to enable

successful purification, so only W394F and W394L were compared. Both W394F and W394L showed only a slight ability to reduce FAD. Of note is the fact that the dark state spectrum of W394L had a much larger peak at ~425nm compared to WT, such that it was around the same absorbance as the peak at 450nm. This was attributed to contamination of the sample, since the residue mutated is sufficiently far away from the ligand binding pocket that altering binding in such a way seems unlikely (Fig. 5).

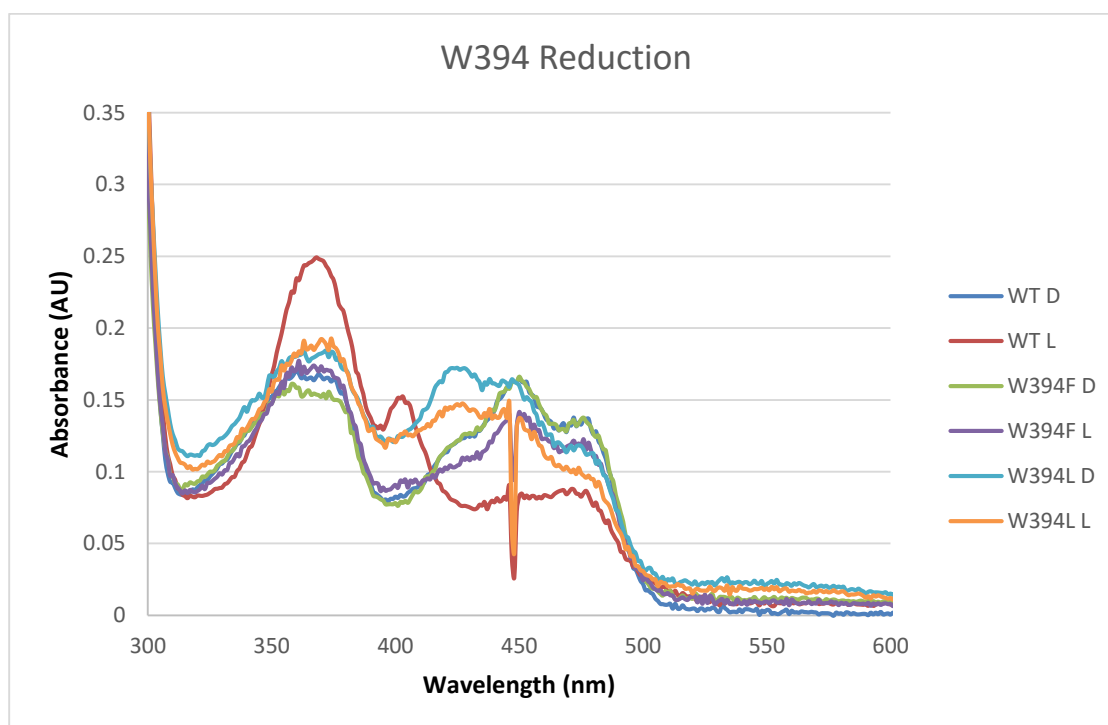


Fig. 5 Spectra of WT and W394 mutants both before (D) and after (L) 20min of light exposure.

One residue that has been shown to be important in cryptochromes is the amino acid located directly across from N5 of the FAD isoalloxazine ring. This nitrogen is thought to hold negative charge when FAD is reduced, and thus it is a prime location for reactions to occur. In some light sensing proteins such as Vivid in *Neurospora*, this takes the form of covalent bond formation with an adjacent cysteine.

In plant cryptochromes such as AtCRY1, this position is taken by an aspartic acid, D396, and it is thought that when FAD is reduced in AtCRY1, N5 deprotonates D396, which is why the FAD of AtCRY1 is reduced to the NSQ instead of the ASQ as in dCRY. In dCRY this position is taken by cysteine 416. In order to study the importance of this residue, we have mutated it to alanine, serine, and asparagine and investigated the results.

All C416 mutations appeared to retain full ability to reduce FAD. In accordance with previous studies¹, C416N saw the formation of some NSQ(Fig. 6A). Intriguingly, all mutations saw faster reduction kinetics than WT CRY as observed through the 365nm peak. C416N showed a quick rise in absorbance, and then a fall as ASQ was converted to NSQ (Fig. 6B). The overall rate of reduction is actually a combination of the forward rate and the reverse rate for FAD reduction, since ASQ is constantly being oxidized back to FAD^{ox}. By looking at the recovery rate, we can see whether an increase in reduction rate is because of a faster reduction or a slower recovery. Both C416S and C416A have a very similar rate of recovery as WT Cry (416S in Fig.7), suggesting that mutating C416 to an alanine or a serine is increasing the rate of reduction but not significantly changing the rate of oxidation of FAD. This may be due to a change in the midpoint potential for reduction of the FAD cofactor. Direct comparison of C416N to WT was not possible given the fact that it is reduced to NSQ by light. Similar to W420L, we see a shift in the peak position to the blue side from C416N and C416A, but not with C416S (Fig 6A).

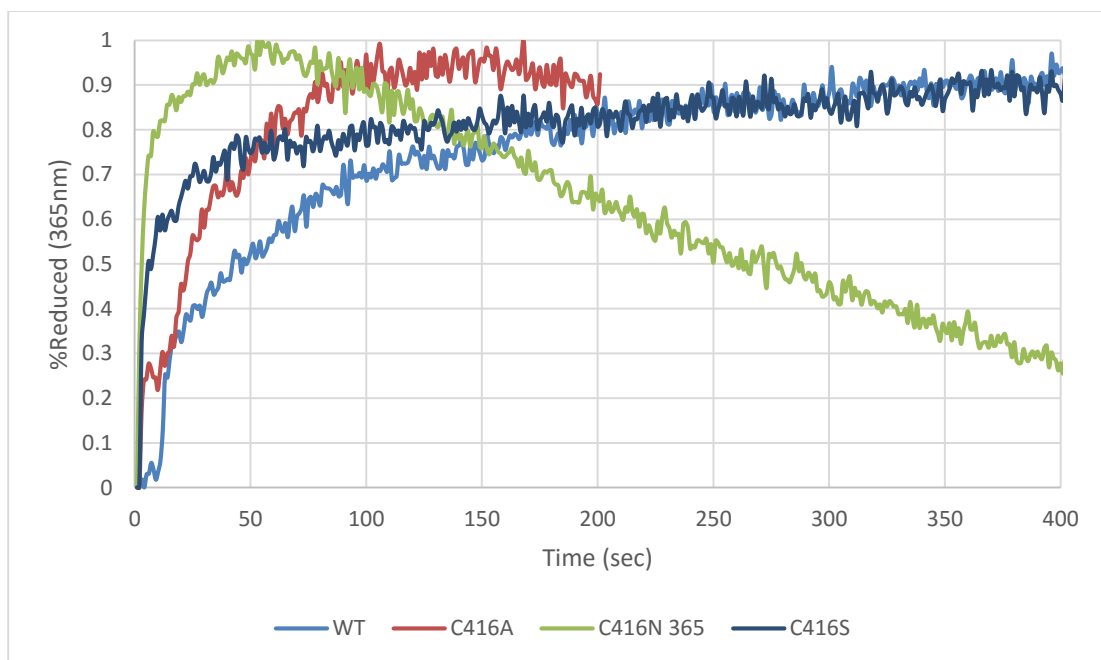
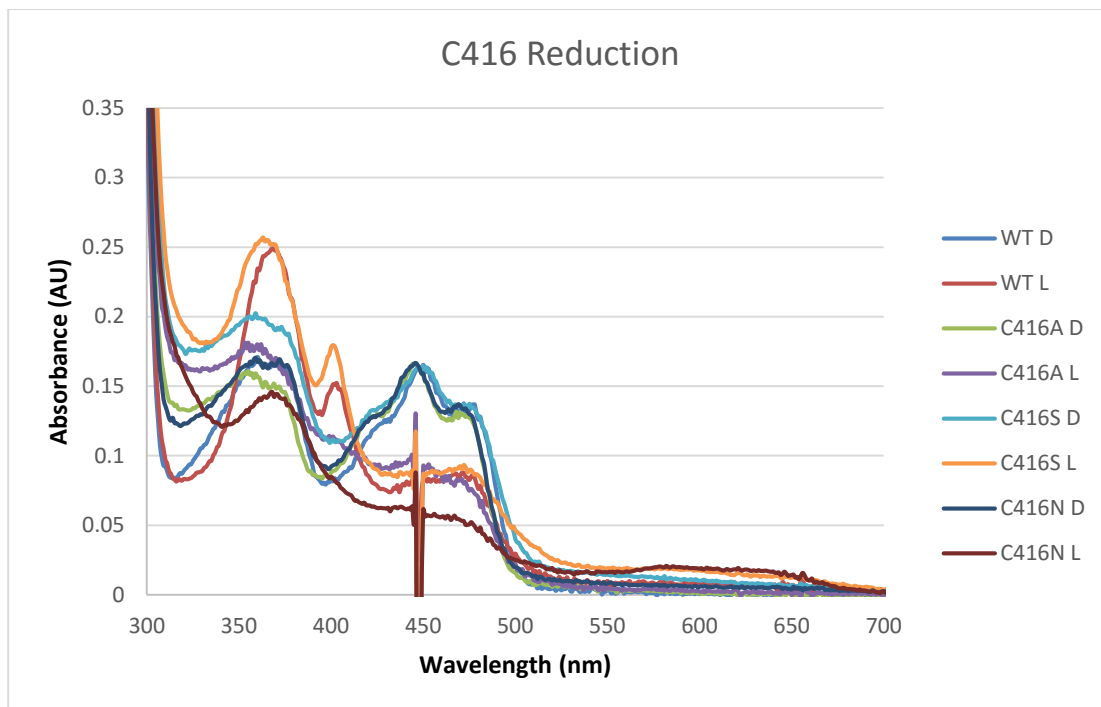


Fig. 6: (A) Spectra of WT and W394 mutants both before (D) and after (L) 20min of light exposure. (B) Change in absorbance at 365nm of WT and C416 mutants over time in the presence of light. Maximal absorbance has been normalized to 1 and minimum has been normalized to 0.

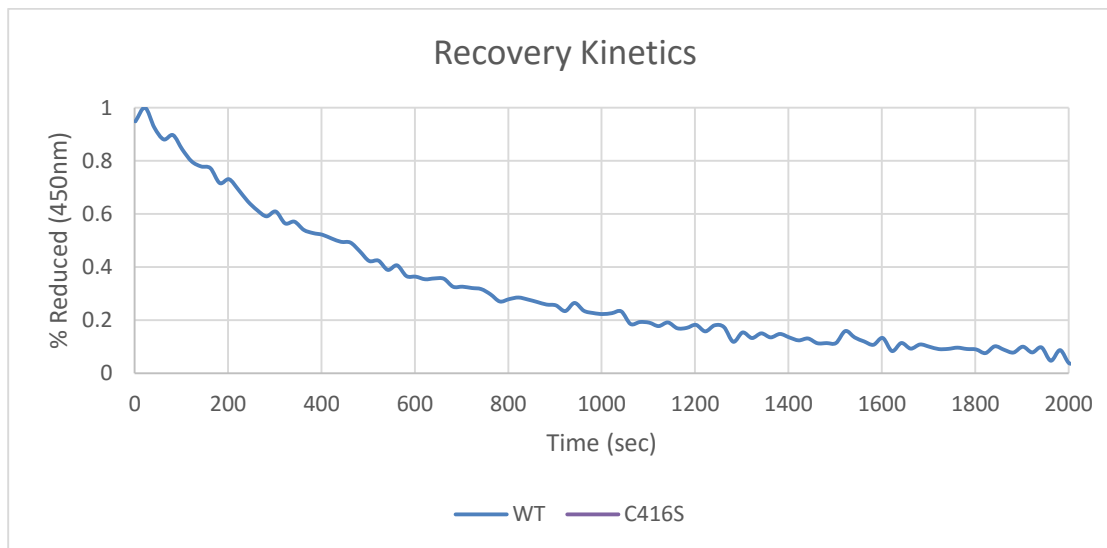


Fig. 7: Rate of recovery of WT and C416S dCRY. Absorbance at 450nm was plotted vs time with maximum set to 1 and minimum set to 0.

Discussion

Several other studies have attempted to study the importance of the TRP triad in dCRY by mutating these residues, so there are similar experiments for comparison with our results. However, these comparisons are complicated by the fact that there is no standard conditions for testing dCRY photoreduction. . Protein concentration, reductant type, light intensity and wavelength are all variable between studies, and, as we have shown, these can all cause significant differences in the ability of dCRY to be photoreduced.

The tryptophan in the TRP triad closest to the FAD, W420, has been mutated in several papers. Our experiments have shown that W420F and W420L severely ablated light responsiveness of CRY *in vitro*, while W420Y retained some activity. In 2002, Froy et al showed that W420A still had some light response *in vivo*, though less

than WT, which would agree with our data². Another study by Czarna et al showed that W420F had no reduction activity *in vitro* in the presence of 5mM BME³, whereas we saw a slight amount. Having not tested the effect of BME on dCRY reduction, we cannot refute their claim, though the fact that we used a different reductant, likely used a stronger light ($\sim 235 \text{ mW/cm}^2$ at 440nm vs 5 mW/cm^2 at 450nm)³, and exposed our samples for a longer time (30 seconds vs. up to 20 minutes) could explain the discrepancy. In 2014, Ozturk et al. showed that W420R did not bind FAD in the same way as WT, and that it was unresponsive to light both *in vitro* and *in vivo*⁴. Our data agrees with this.

The middle tryptophan in the TRP Triad, W397, has also been mutated in other studies. We found that both W397F and W397Y retained significant activity. In the same study by Froy et al. mentioned above, it was found that W397F and W397Y retained activity in S2 cells, which would agree with our data. However, contrary to our results, Ozturk and Czarna found no light-responsiveness of W397F *in vitro* via UV-Vis spectroscopy, though Ozturk et. al reported full conformational change by trypsin digest and light responsiveness *in vivo*⁴, while Czarna et al showed dampened, but still active, conformational change by partial trypsin digest⁵. Ozturk et. al used a lamp of 5 mW/cm^2 with an emission maxima at 366nm for 10min, which could explain the difference with our results. The fact that we saw some reduction of mutant W397F could explain why some light dependent activity of W397F mutants could be seen by partial trypsin digest and *in vivo* assays in other studies even though no reduction had been seen by UV-visible spectroscopy.

The original proximal tryptophan, W342, showed significant reduction in light-responsiveness when mutated to tyrosine or phenylalanine. Froy et al showed that both W342Y and W342F retained almost full light responsiveness in S2 cells, which perhaps suggests that in some cases even a small amount of light response by dCRY *in vitro* is sufficient to induce signaling *in vivo*, where a different environment is likely to make reduction more favorable². Once again, Ozturk et al. found that W342F showed to reduction *in vitro*, but retained activity *in vivo*⁶. However, a 366nm light at a rate of 1 mW/cm² was used for *in vivo* measurements, while a 1.2mW/cm² lamp at 450nm was used for *in vitro* spectroscopy, which could explain the discrepancy.

Based on a recent report that an additional tryptophan may be needed to transport electrons in animal photolyase and cryptochromes, we also mutated W394 to phenylalanine and tyrosine and saw a significant decrease in reduction activity. This agrees with data from a study on the XI(6-4)Photolyase⁷, and supports the theory that W394 may play a role as a fourth essential tryptophan in electron transport in dCRY.

Overall, our results suggest that tyrosine is the most effective substitute for tryptophan in the TRP triad, with both W342Y and W420Y showing significantly more reduction activity compared to their phenylalanine counterparts. Leucine mutants always had poor reduction activity, perhaps because they are sufficiently different from tryptophan as to introduce structural instability.

Of note is the fact that changing pH and the addition of chemical reductants caused a large change in the ability of WT CRY and mutants to reduce FAD. This means that depending on the exact environment of CRY *in vivo*, its reduction kinetics

may be significantly altered, perhaps explaining why *in vivo* activity of CRY mutants does not always correlate with *in vitro* observations. .

Our results with C416 mutants in general agree with previous studies. All mutants studied showed full reduction activity, however C416A and C416S showed faster reduction than WT with about the same recovery time. This is in contrast to Czarna et al, who showed similar photoreduction time but quicker recovery³. In agreement with several other studies, C416N showed the production of NSQ upon light exposure, though we saw a lower yield than some other studies^{1,6}.

REFERENCES

1. Paulus, B. *et al.* Spectroscopic Characterization of Radicals and Radical Pairs in Fruit Fly Cryptochrome: Protonated and Non-Protonated Flavin Radical-States. *FEBS J.* **282**, n/a–n/a (2015).
2. Froy, O., Chang, D. C. & Reppert, S. M. Redox potential: differential roles in dCRY and mCRY1 functions. *Curr Biol* **12**, 147–152 (2002).
3. Berndt, A. *et al.* Structures of Drosophila Cryptochrome and Mouse Cryptochrome1 Provide Insight into Circadian Function. *Cell* **153**, 1394–1405 (2013).
4. Ozturk, N., Selby, C. P., Zhong, D. & Sancar, A. Mechanism of Photosignaling by Drosophila Cryptochrome. *J. Biol. Chem.* **289**, 4634–4642 (2014).
5. Czarna, A. *et al.* Structures of Drosophila cryptochrome and mouse cryptochrome1 provide insight into circadian function. *Cell* **153**, 1394–1405 (2013).
6. Ozturk, N., Song, S. H., Selby, C. P. & Sancar, A. Animal type 1 cryptochromes. Analysis of the redox state of the flavin cofactor by site-directed mutagenesis. *J Biol Chem* **283**, 3256–3263 (2008).
7. Muller, P., Yamamoto, J., Martin, R., Iwai, S. & Brettel, K. Discovery and functional analysis of a 4th electron-transferring tryptophan conserved exclusively in animal cryptochromes and (6-4) photolyases. *Chem. Commun.* **51**, 15502–15505 (2015).